

**INVESTIGATION OF LONG-TERM VARIATIONS IN
STRATOSPHERIC OZONE THROUGH THE
COMBINATION OF DIFFERENT SATELLITE OZONE
DATA SETS**

A MASTER THESIS SUBMITTED TO THE INSTITUTE OF
ENVIRONMENTAL PHYSICS (IUP)

By

*Ebojie, Felix
(Mat. No. 2196990)*

IN PARTIAL FULFILLMENT OF THE REQUIREMENTS FOR THE
DEGREE OF

Master of Science

POSTGRADUATE PROGRAMME ENVIRONMENTAL PHYSICS (PEP)
UNIVERSITY OF BREMEN (FB1), BREMEN, GERMANY

August, 2009

SUPERVISOR: *PD Dr. Christian von Savigny*

REFEREE: 1. *PD Dr. Annette Ladstätter-Weißmayer*
2. *PD Dr. Christian von Savigny*

Declaration

I Ebojie, Felix herewith declare that I did the written work on my own and only with the means as indicated.

Date

Signature

Acknowledgements

My first thanks goes to every member of the department for their contributions in one way or another towards the completion of this programme. Among this great minds are Mr. Lars Jescke, the first name I got to know in this programme while back home in my country. Further thanks goes to Mrs. Anja Gatzka an intelligent and understanding secretary, Thiranan Sonkaew, a Phd student for helping me out at the earlier stage of this work, and my entire lecturers for their excellent and pragmatic teachings. My sincere appreciation goes to PD Dr. Christian von Savigny who was first my course mentor and later became my thesis supervisor and examiner, for his support in tougher times, teaching, patience, encouragement, guidance and understanding during this thesis work. Special thanks to my first examiner PD. Dr. Annette Ladstätter-Weißenmayer for her support and encouragement. I appreciate Prof Noltholt for his understanding and counsel when I was to choose my thesis topic. Many thanks also go to Prof. Dr. John Burrows in whose group I conducted this thesis. Thanks to my colleagues and a special thanks to my mum, brothers and sisters for their support, love and cares.

Finally, I am most thankful to the Almighty God for his love, favour, mercies and guidance toward the completion of this programme.

Abstract

The Monitoring of global ozone in the stratosphere is a necessary precondition to understanding atmospheric chemistry and the recovery of stratospheric ozone throughout the 21st century. This study is of great importance as changes in atmospheric ozone will have important consequence on humans, plants and animals. This master thesis is devoted to the investigation of long-term variations in stratospheric ozone (as a function of latitude and altitude) through the combination of data sets from the SCanning Imaging Absorption spectroMeter for Atmospheric CHartographY (SCIAMACHY), the Halogen Occultation and Gas Experiment (HALOE), and the Stratospheric Aerosol and Gas Experiment II (SAGE II). In the study, the Stratozone (version 2.2) algorithm developed to perform the routine retrieval of ozone vertical profiles was used to calculate long-term ozone variations in the stratosphere in order to determine whether stratospheric ozone amounts are consistently increasing or decreasing within some latitude/altitude bins over some period of time based on the availability of data from the different satellites under consideration: SCIAMACHY (08/2002 – date), HALOE (10/1991 – 11/2005), SAGE II (10/1984 – 08/2005). As the ozone amount varies on short-term, seasonal, inter-annual, and long-term time scales, it was considered important to calculate mainly the contribution of the seasonal variation on the total variability of the ozone time series in order to determine the trend of ozone. This was considered important as it is the most pronounced variation at the 35–45 km altitude. Finally, the information from each of the separate instruments was combined in order to compare the resulting ozone profile with that obtained from SCIAMACHY instrument. The three instruments showed quite a good agreement, with all the available data from 1984 to the late 1990s showing a decline of ozone near 40 km, by about 10% and after 1997, there was no noticeable decline. In fact ozone levels around 40 km seem to have increased since 2000, which is consistent with the beginning of the decline of stratospheric chlorine due to the enactment of the Montreal protocol in 1987.

Contents

1.0 Introduction	1
1.1 General	1
1.2 Motivation and objective	2
1.3 The discovery of ozone	2
1.4 The solar radiation	3
2.0 The atmosphere	5
2.1 Vertical structure of the earth's atmosphere	6
2.1.1 The temperature profile	6
2.1.1.1 The troposphere	7
2.1.1.2 The stratosphere	7
2.1.1.3 The mesosphere	8
2.1.1.4 The thermosphere	9
2.1.1.5 The exosphere	9
2.1.2 The pressure and density profile	9
3.0 Ozone chemistry	11
3.1 Stratospheric ozone	11
3.2 Ozone absorption theory	11
3.4 Ozone chemistry and the Chapman cycle	14
3.5 Incompleteness of the Chapman cycle	15
3.6 Chapman layers	17
3.7 The distribution of ozone in the stratosphere	19
3.8 History of the Chlorofluorocarbons (CFCs)	21
3.9 The Montreal protocol and its amendments	21
3.10 Ozone depletion	24
3.11 The ozone hole	24
3.12 The Arctic stratosphere	27
3.13 Chemicals responsible for ozone destruction	30
3.14 Polar stratospheric clouds	31
3.14.1 Type I Polar Stratospheric Clouds (PSCs)	31
3.14.2 Type II Polar Stratospheric Clouds (PSCs)	31
3.14.3 Heterogeneous reactions on the Polar Stratospheric Clouds (PSCs)	31

4.0 Past ozone study	34
4.1 Ground based measurement of atmospheric ozone	34
4.1.1 The Dobson spectrophotometer	34
4.1.2 The Umkehr measurements	36
4.1.3 UV LIDAR systems	36
4.1.4 Differential Optical Absorption Spectroscopy (DOAS) Measurement	36
4.2 Balloon and aircraft measurement of atmospheric ozone	37
4.3 Satellite measurement of atmospheric ozone	38
5.0 Instrument and theory	40
5.1 SCIAMACHY instrument	40
5.1.1 Measurement geometries of SCIAMACHY	41
5.1.1.1 Nadir measurements	42
5.1.1.2 Limb measurements	42
5.1.1.3 Occultation measurements	43
5.2 HALOE instrument	44
5.3 SAGE II instrument	44
5.3.1 Understanding the Antarctic ozone hole and PSCs with SAGE II measurements.	45
5.3.2 Monitoring the effect of the Mt. Pinatubo volcanic eruption and water vapor concentration using SAGE II measurements	46
6.0 Variations in stratospheric ozone	47
6.1 Short-Term Variability	47
6.1.1 Passage of the weather system	48
6.1.2 Diurnal variation	48
6.1.3 27 day solar rotation	49
6.1.4 Variation in temperature	49
6.1.5 Solar proton events	50
6.2 Seasonal variability	50
6.3 Inter-annual variability	51
6.3.1 Quasi-Biennial Oscillation (QBO)	51
6.3.2 The El Niño-Southern Oscillation (ENSO)	51

6.3.3	Volcanic eruptions	52
6.3.4	11-year suns spot cycle	52
6.4	Long-term variability	52
7.0	Results and discussion	54
7.1	Determination of the monthly means	54
7.2	Determination of ozone anomalies	57
7.2.1	Offset Corrected anomalies	62
7.3	Turn around event	64
7.4	Trend analysis	65
7.5	Summary	66

List of Figures

1.0	The Optical (UV-VIS-NIR) spectral range	4
2.0	Vertical temperature distribution	6
2.1	Vertical profile of pressure, density and mean free path for a standard atmosphere	10
3.0	The absorption cross section of ozone for different temperatures as measured with GOME FM [<i>Burrows et al. 1997</i>]	12
3.1	The ozone profile	13
3.2a	Increase in path length to the sun with increase in solar zenith angle	19
3.2b	Chapman weighting function	19
3.3	Brewer-Dobson circulation in the ozone layer	20
3.4	The effects of the Montreal protocol amendments and their	23
3.5	Actual and Projected Concentration of Stratospheric Cl versus time	24
3.6	Antarctic ozone hole	26-27
3.7	October zonal mean total ozone for the 1970s and early 1990s	27
3.8	Time series of monthly average column ozone poleward of 63° Arctic and Antarctic spring	29
3.9	Lowest value of ozone measured by TOMS each year in the ozone hole	29
3.10	Sources of stratospheric halogens; Chlorine compounds (A) Bromine compounds (B)	30
5.0b	SCIAMACHY in Nadir viewing geometry	41
5.0b	SCIAMACHY in Limb viewing geometry	41
5.0c	SCIAMACHY in Occultation-viewing geometry	41
7.0	The monthly mean ozone concentration averaged over different altitude and latitude bins	56
7.1	Ozone anomaly from the different instruments for different altitude and latitude bins	59
7.2	Ozone anomaly from all three instruments	60
7.3	Smoothed ozone anomalies from all three instruments	62
7.4	Combined and offset corrected anomalies with and without CCMVAL model simulations	62
7.5	Combined and offset corrected anomalies with the best fit trend to all instrument average before and after the 1997 (red line)	65

Chapter 1

1.0 Introduction

1.1 General

Ozone is one of the atmospheric trace constituents that have played a vital role in the evolution of life on earth. It protects biological organisms from harmful solar ultraviolet (UV) radiation by absorbing a portion of it that has the potential of damaging organic macromolecules essential for life [Cornu, 1879]. Evolution of life on earth is thought to have become possible only because of ozone formation caused by the release of molecular oxygen produced by cyanobacteria (blue-green algae) through oxygenic photosynthesis¹ [Warneck, 1988; Wayne, 1991]. Without ozone, life on earth would not have evolved in the way it has as the first stage of single cell organism development requires an oxygen-free environment which existed on earth over 3000 million years ago. As the primitive forms of plant life evolved and multiplied, they began to release minute amounts of oxygen through photosynthesis. This oxygen began to build up in the atmosphere and led to the formation of ozone layer in the upper atmosphere or stratosphere.

Most ozone is produced naturally in the upper atmosphere. While ozone can be found through the entire atmosphere, the greatest concentration occurs at altitudes between 20 and 40 km above the Earth's surface. This band of ozone-rich air is known as the "ozone layer". Ozone has great implications on the vertical structure of the Earth's atmosphere. The absorption of solar radiation by ozone, leading to its dissociation, causes a peak in the atmospheric temperature profile at about 50 km which defines the stratopause and leads to the stable stratification of the stratosphere. Ozone also occurs in very small amounts in the lowest few kilometers of the atmosphere, a region known as the troposphere where it is produced at ground level through photochemical reactions of volatile organic compounds (VOCs²) and nitrogen oxides (NO_x³), some of which are produced by human activities from power plants and automobiles [Haagen-Smit, et al., 1956]. Ground-level ozone is a component of urban smog and can be harmful to human health. Even though both the ozone in the stratosphere and troposphere contain the same molecules, their presence in different parts of the atmosphere have very different consequences. Stratospheric ozone blocks harmful solar radiation, thus making the earth a habitable place while the ground level ozone is one of the important greenhouse gases and a source of pollutant found in high concentrations in smog. Though it also absorbs UV radiation

¹The conversion of carbon dioxide (CO₂) to oxygen O₂

²carbon compounds that readily vaporize, found in solvents, degreasers and cleaning solutions e.g. benzene, toluene and vinyl chloride

³Nitric oxide (NO) + Nitrogen dioxide (NO₂)

and a low level of it is needed in the troposphere to form OH¹ radicals to clean the air of harmful chemicals, breathing it in high levels is unhealthy and even toxic. The high reactivity of ozone results in damage to the living tissue of plants and animals. This damage by heavy tropospheric ozone pollution is often manifested as eye, skin and lung irritation. The geographical and vertical distributions of ozone in the atmosphere are determined by a complex interaction of atmospheric dynamics and photochemistry.

1.2 Motivation and objective

The main goal of this master thesis is to statistically analyze the trend of stratospheric ozone by combining ozone profile measurements from SCIAMACHY^{2a}/Envisat^{2b}, HALOE^{3a}/UARS^{3b}, and SAGE II^{4a}/ERBS^{4b} and comparing SCIAMACHY ozone profiles with that of other instruments in order to search for the evidence of “recovery” or “stagnation of the decrease” of global ozone. This was born out of the weariness for the biological consequences of increase in solar UVB (280-320 nm) radiation that are associated with stratospheric ozone loss. Also, the observed evolution was compared with model simulations from the Chemistry Climate Model Validation initiative [*CCMVAL, Eyring et al., 2006, WMO, 2007*], in order to confirm if the three dimensional models reproduce the observations.

1.3 The discovery of ozone

Ozone is a triatomic molecule with three atoms of oxygen. It is one of the most extensively studied and best understood atmospheric trace constituents and has thus played an important role in the development of atmospheric chemistry. It was first noticed by Friedrich Schönbein following the observation of some atmospheric constituent with a peculiar odour⁵ [*Schönbein, 1840*] which was later assigned the chemical formula O₃ in 1865 by *Jacques-Louis Soret* and finally confirmed by *Schönbein in 1867* [*Rubin 2001*]. In 1881, a few years after the discovery of ozone, *W. N. Hartley* came up with the hypothesis that the observed spectrum at about 300 nm of UV light from the sun was influenced by the presence of ozone in the stratosphere. This spectrum was known as the "UV cutoff" because of its sharp attenuation in the ultraviolet range. Hartley's assumption was confirmed by Chappuis, who also discovered the absorption of

¹Hydroxyl

^{2a}Scanning Imaging Absorption Spectrometer for Atmospheric Cartography aboard ENVISAT-1, launched on March 1, 2002 [*Bovensmann et al., 1999*] ^{2b}European environmental satellite (<http://see.esa.int/>)

^{3a}Halogen Occultation Experiment aboard UARS (09/1991-11/2005) [*Russell et al., 1993*]

^{3b}Upper Atmosphere Research Satellite (<http://umpgal.gsfc.nasa.gov>)

^{4a}Stratospheric Aerosols and Gas Experiment II aboard ERBS (SAGE II, 10/84 -10/2005) [*Mauldin et al., 1985*]

^{4b}Earth Radiation Budget Satellite (<http://asd-www.larc.nasa.gov>)

⁵ozein (Greek) - smell

light by ozone in the visible range at about 500 and 700 nm (Chappuis band) of the spectrum. In the early 1920s *Dobson* began measuring the column amount of atmospheric ozone and created a time series, showing a continuous record of ozone column densities over Arosa (Switzerland) [e.g., *Dobson, 1968*] from 1926 to-date. A few years later the first photochemical model explaining the existence and shape of the stratospheric ozone layer was proposed by *Chapman in 1930*. With the advent of absorption spectrometers aboard Earth orbiting satellites (e.g SBUV¹ and TOMS²) scientists have been able to infer global maps of different minor constituents including ozone on a daily basis. This has broadened our knowledge in the global morphology of ozone, its dependence on latitude and season as well as its interaction with other chemical compounds, particularly the halones.

1.4 The solar radiation

The Sun produces radiation at many different wavelengths called the electromagnetic spectrum, ranging from very long wavelength radio waves to very short wavelength X and gamma rays. The human eye can detect wavelengths in the region of the spectrum from about 400 nm to 700 nm, known as visible region with the colour of light ranging from violet to red. Radiation with wavelengths shorter than those of violet light is called ultraviolet radiation (UV). The UV radiation can be subdivided into three different groups (Fig 1.0) based on the wavelength of the radiation (100-400 nm); these are referred to as vacuum UV (100-200 nm), UV-C (200-280 nm), UV-B (280-320 nm), and UV-A (320-400 nm). The oxygen molecules in the upper atmosphere and stratospheric ozone layer have large absorption cross-sections for solar ultraviolet radiation, depending on wavelength. The absorption by the stratospheric ozone is more effective for the shorter wavelengths and tends to reach its peak at 250 nm and drops rapidly with an increase in wavelength to even beyond 350 nm. Thus, the biologically harmful radiation below 200 nm (vacuum UV) is completely absorbed by oxygen molecule (O₂) and residual Nitrogen (N₂) while the ozone layer completely shields the radiation in the range (200-300 nm) with only a fraction of the UV-B and UV-A wavelength bands reaching the earth surface. The depletion of the protective ozone layer by certain atmospheric pollutants (Chlorofluorocarbons, halons and nitrogen oxides) that interact photochemically with ozone will promote the transmission of highly injurious ultraviolet radiation [*El-Hinnawi and Hashmi 1982*].

¹*Solar Backscatter Ultraviolet Spectrometer on Nimbus 7 (11/1978-1990), NOAA-9, NOAA-11, and NOAA-14 (1984-date) [Heath et al., 1975]*

²*Total Ozone Mapping Spectrometer on Nimbus 7 (11/1978-05/1993), Meteor 3 (08/1991-11/1994), and Earth-Probe (07/1996-date) [Heath et al., 1975]*

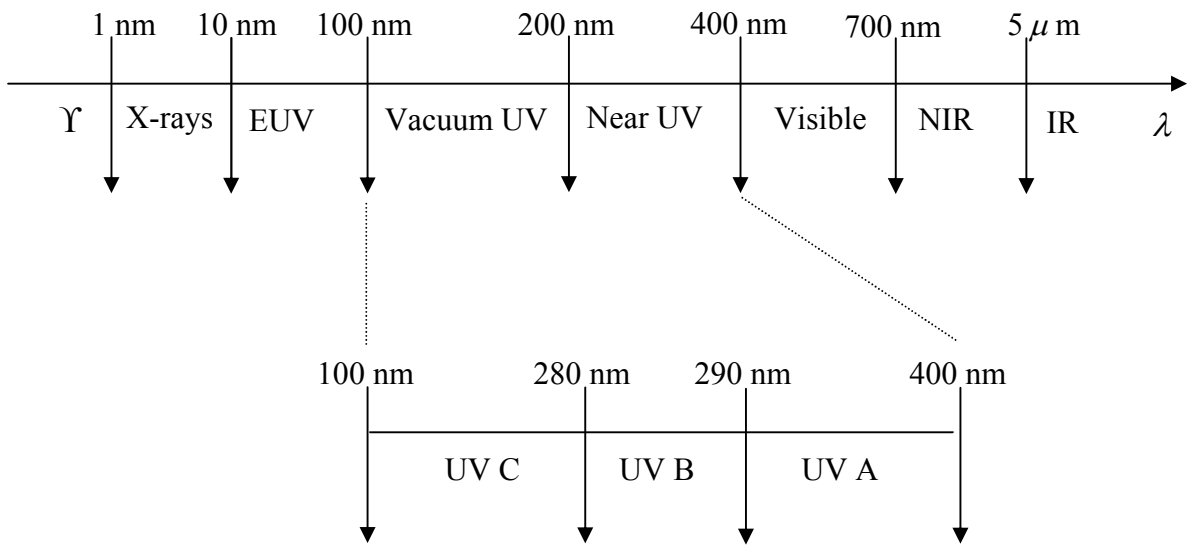


Fig 1.0: The Optical (UV-VIS-NIR) spectral range

Chapter 2

2.0 The atmosphere

The atmosphere is the gaseous envelope that surrounds the Earth and constitutes the transition between its surface and the vacuum of space. The early atmosphere is different from the atmosphere of today which had evolved in 3 stages; stage I (primordial atmosphere), evolved from the gravitational capture of the gases in the proto-planetary nebula of the sun consisting mainly of H₂ and He. Stage II (secondary atmosphere) results from the outgassing of the planet through volcanoes, geysers, cracks etc., consisting mainly of H₂O, CO₂, SO₂, H₂S, and CO leading to the formation of oceans with other gases from the influx of material from meteorites and comets, and sputtering of material of the planetary surface by cosmic rays and energetic particles. Stage III (the present atmosphere) is enriched in O₂ due to photosynthesis by plants leading to the presence of life. Since the presence of life, human activities have affected the composition of the atmosphere and presently, the atmosphere consists by volume of a mixture of gases composed primarily of nitrogen (78.08 %), oxygen (20.95 %), argon (0.93 %) and other noble gases (Ne, He, Xe) (<0.003 %), hydrogen (0.00005 %), and other gases in variable amount such as water vapour (0-4%), carbon dioxide (0.037 %), methane (1.7 ppm¹), nitrous oxide (0.3 ppm), ozone (0.0-0.07 ppm), particles (dust etc.) (< 0.15 ppm), chlorofluorocarbons (0.0002 ppm). It extends some 500 km above the surface of the Earth and the lower level (troposphere) constitutes the climate system that maintains the conditions suitable for life on the earth surface. The next atmospheric level, the stratosphere (12 to 50 km), contains the ozone layer that protects life on the planet by filtering harmful ultraviolet radiation from the Sun. The effect of man's activities through the burning of fossil fuels since the industrial revolution has altered the composition of the atmosphere, of greatest concern is the rising concentration of the greenhouse gases such as carbon dioxide, methane, nitrous oxide, and chlorofluorocarbons in the atmosphere as they trap heat energy emitted from the earth surface thereby increasing the global temperatures (global warming) [Hansen, 1989]. In addition, they also lead to photochemical smog and acid rain which are threats to survival on the earth surface.

¹Parts per million

2.1 Vertical structure of the earth's atmosphere

The vertical structure of the earth's atmosphere shows how changes in temperature with height can be used to classify the atmosphere into various levels. This change is not uniform, but instead behaves in different ways in different layers of the atmosphere due to the chemistry (thermodynamics, photo-chemistry, and dynamics), composition, and density of the atmosphere at the different levels best represented by the atmospheric vertical temperature profile, whose points of inflection are used to distinguish the levels into 5 regions (Fig. 2.0). As the altitude increases, atmospheric pressure decreases. Temperature, humidity and wind speed also change with altitude.

2.1.1 The temperature profile

The temperature changes in the atmosphere can be classified in terms of both small and large scale variations driven by the absorption of solar radiation. The temperature profile (Fig. 2.0) divides the atmosphere into 5 distinct layers: the troposphere, stratosphere, mesosphere, thermosphere, and the exosphere although not many scientific studies have been done on the exosphere. The altitude region from 0 to about 100 km is regarded as the homosphere because of the efficient mixing of the chemical constituents while the altitude region above 100 km is called the heterosphere and is characterized by diffusive separation of gases with different atomic weight.

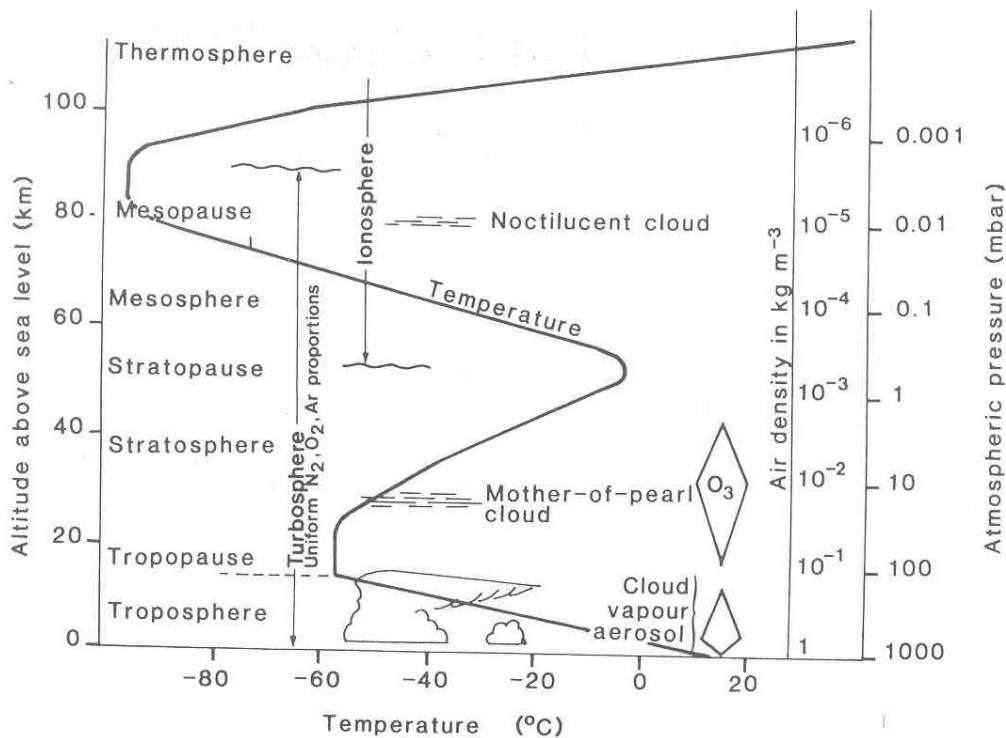


Fig. 2.0 Vertical temperature distribution
 (<http://envam1.env.uea.ac.uk/glossary.html>)

2.1.1.1 The troposphere

The troposphere begins at the ground and ranges in height to an average of 8-9 km at the poles to 17 km at the equator. It is heated from the ground, which absorbs solar radiation and releases heat back up in the infrared region. The temperature of the air in this region decreases linearly with altitude, at a lapse rate of 5 to 7 K/km due to adiabatic cooling; as the air rises the atmospheric pressure falls and so the air expands. For expansion to occur, work must be done to its surroundings which lead to a decrease in temperature due to conservation of energy. This is the most familiar region of the atmosphere, containing most of the clouds and weather phenomena. The air in this layer is turbulent and well mixed horizontally and vertically due to non uniform heating of the earth surface and the atmosphere. Most of the greenhouse gases including ozone are found in this region. The ozone in this region is regarded as bad ozone as it is a pollutant and a constituent of smog. The boundary between the troposphere and the stratosphere is the tropopause. This is the region of the atmosphere where the lapse rate changes from negative (in the troposphere) to positive (in the stratosphere). The tropopause is not a "hard" boundary as vigorous thunderstorms, for example in the tropical region can overshoot into the lower stratosphere and undergo a brief low-frequency vertical oscillation which can set up a low-frequency atmospheric wave train capable of affecting both atmospheric and oceanic currents in the region. The height of the tropopause varies with season due to changes in the atmospheric circulation.

2.1.1.2 The stratosphere

The stratosphere is situated between about 10 km and 50 km altitude above the earth surface at the lower latitudes and at about 8 km and 45 km at the poles. The temperature at the top of the stratosphere is as high as 270 K, about the same as the ground level temperature. This layer of the atmosphere is stratified in temperature with warmer layers higher up and cooler layers farther down because it is heated from above due to the absorption of ultraviolet radiation by the ozone layer. In fact it is this ozone layer that is basically responsible for the existence of the "stratosphere." The vertical stratification, with warmer layers above and cooler layers below, makes the stratosphere dynamically stable such that there is no regular convection and associated turbulence in this part of the atmosphere. This layer of the atmosphere is regarded as the region of intense interactions among radiative, dynamical, and chemical processes, in which horizontal mixing of gaseous components proceeds much more rapidly than vertical mixing. The stratosphere is mostly dry with the exception of the presence of winter Polar Stratospheric Clouds (PSCs) also known as nacreous clouds. One interesting feature of the

stratospheric circulation is the Quasi-Biennial Oscillation (QBO) in the tropical latitudes, which induces a secondary circulation responsible for the global stratospheric transport of tracers such as ozone and water vapour driven by gravity waves convectively generated in the troposphere. During winter, the contrast in temperature between orography and land and sea breezes lead to the generation of long Rossby waves in the troposphere which eventually lead to a sudden rise in temperature in the northern hemisphere of the stratosphere (sudden stratospheric warming). Stratospheric warming can also be observed in the southern hemisphere although not as frequent as those of the northern hemisphere. There are also situations of sudden drop in temperature during winter in both hemispheres, which leads to the formation of PSCs. In the stratosphere, ozone, though only a minor constituent with a mixing ratio of about 6-10 ppm strongly absorbs solar UV radiation similar to the absorption of visible light on the earth surfaces. The ozone absorption that is responsible for the temperature increase becomes negligible at higher altitudes creating a temperature peak at about 50 km that marks the next boundary: the stratopause, which is the boundary layer between the stratosphere and the mesosphere.

2.1.1.3 The mesosphere

The layer just above the stratopause is the mesosphere. It is located from about 50 km to 90-100 km altitude above the earth's surface depending on the latitude. Within this layer, temperature again decreases with increasing altitude due to decreasing solar heating and increasing cooling by CO₂ radiative emission. The main dynamical features in this region are atmospheric tides, internal atmospheric gravity waves and planetary waves which are mainly excited in the troposphere and lower stratosphere and propagate upward to the mesosphere. In this region of the atmosphere, the gravity-wave amplitudes can become so large that the waves become unstable and dissipate thereby creating momentum in the mesosphere which drives the mesospheric meridional circulation. The temperatures in the upper mesosphere can fall as low as 100 K varying according to latitude and season. Millions of meteors burn up daily in the mesosphere as a result of collisions with the gas particles contained there; this creates enough heat to vaporize almost all of the falling objects long before they reach the ground, thereby resulting in a high concentration of iron and other metal atoms in this region of the atmosphere. The minimum in temperature at the top of the mesosphere is called the mesopause, which is the coldest place in the atmosphere; it is the mesopause that separates the mesosphere from the thermosphere.

2.1.1.4 The thermosphere

This is the layer of the earth's atmosphere that extends from about 90-100 km to 400 km above the earth's surface. In this layer, the temperature increases with altitude due to the absorption of highly energetic solar radiation by nitrogen and residual oxygen which are partially converted into ions forming a layer called the ionosphere which begins from the upper mesosphere. The temperature in this region is as high as 2500 K during the day, although may not be felt as a thermometer in this region will read 0 K due to the large mean free path between the few atoms of gas which are supposed to transfer heat since it is close to vacuum. Atmospheric tides dominate the lower part of the thermosphere but dissipate towards the top as the concentration of the molecules is not high enough to support the motion needed for fluid flow. Aurorae are also formed in this layer of the atmosphere. The thermopause separates the thermosphere from the exosphere.

2.1.1.5 The exosphere

This is the outermost layer of the atmosphere ranging from about 500 km to 1000 km and may sometimes extend to about 10000 km above the earth surface due to the energy input of location, time of day, solar flux, season, and other atmospheric properties. The gases in this layer are the light gases such as hydrogen, helium, and atomic oxygen near the critical level (exobase) which may sometimes escape to space. It is this region of the atmosphere that many satellite orbit the earth.

2.1.2 The pressure and density profile

Pressure (P) and density (ρ) decrease nearly exponentially with height, according to the relation:

$$P(z) = P_0 e^{-z/H} \quad (2.0)$$

where P(z) is the pressure at height z, P_0 is the pressure at some reference level, which is usually taken as sea level ($z = 0$), and H (e-folding depth) referred to as the scale height is given by:

$$H = \frac{kT}{Mg} \quad (2.1)$$

where M is the molecular mass, g is the gravitational acceleration, k is Boltzmann's constant, and T is the absolute temperature. The drop in pressure by a factor e is the direct result of hydrostatic balance leading to the pressure gradient equation:

$$\nabla p = \rho g \quad (2.2)$$

CHAPTER 2. THE ATMOSPHERE

where p is the pressure, ρ is mass density, and g is the gravitational acceleration. The solution of the pressure gradient equation leads to a scale height ranging from 3 to 8 km throughout the lowest 100 km. This means that 90 % of the atmospheric mass is in the troposphere and only 10 % in the stratosphere. Therefore, dividing equation (2.0) by P_0 and taking the natural logarithm yields:

$$\ln \frac{p}{p_0} = -\frac{z}{H} \tag{2.3}$$

Equation (2.3) is useful for the estimation of the height of various pressure levels in the Earth’s atmosphere, because the pressure at a given height in the atmosphere is a measure of the mass that lies above the level and is sometimes used as vertical coordinate in lieu to height. Atmospheric pressure varies smoothly with height and there are no signs of any fine structure in the vertical pressure profile corresponding to those in the associated temperature profile and the horizontal pressure variations are very much smaller and smoothly distributed. As stated above, density also decreases with height in the same manner as pressure and the vertical variations in pressure and density are much larger than the corresponding horizontal and time variations. Fig. 2.1 shows a semi log plot of the vertical profile of pressure, density and mean free path for a standard atmosphere from 0 to about 160 km above the earth surface.

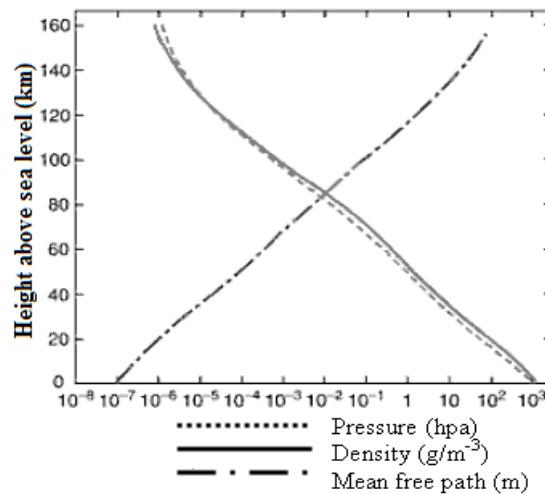


Fig. 2.1: Vertical profile of pressure, density and mean free path for a standard atmosphere

(see *Atmos. Phys.* by John Michael Wallace, Peter Victor Hobb)

Chapter 3

3.0 Ozone chemistry

3.1 Stratospheric ozone

Stratospheric Ozone, which is about 90 % of the ozone (O₃) in the earth atmosphere, is found in the region from about 10-50 km above the earth's surface where it forms a layer about 20 km thick (Fig. 3.1). The amount of ozone in this region of the atmosphere varies, depending mainly on latitude and season, where its presence causes stratospheric temperature inversion and a resulting temperature peak at the stratopause. *Fabry and Buisson [1921]*, who conducted the first detailed measurements of the atmospheric column of ozone, stated that ozone was responsible for the observed strong cut-off in solar UV spectra at about 300 nm towards shorter wavelengths. They also suggested that ozone is formed by solar UV radiation and that the ozone layer is situated at an altitude of about 50 km, which was equally confirmed by other scientists to be about 48-53 km [*Cabannes and Dufay, 1925; Lambert et al., 1926*]. In addition to its radiation properties, ozone reacts with many other trace species, some of which are anthropogenic in origin. It plays a vital role in the earth atmosphere by absorbing the biologically harmful UV radiation from the sun. Without ozone, the surface of the Earth would be bathed in UV radiation, which is harmful to the eyes and skin and could also result in damage to crops and marine phytoplankton¹ as well as being able to break DNA² molecular bonds. It has been observed that recent anthropogenic chemical additions to the atmosphere can destroy ozone [*Cicerone, 1974; Molina and Rowland, 1974*], also research has shown that stratospheric ozone concentrations have declined over the past three or four decades [*Wayne, 2000*]. However, there have been some recent speculations that the ozone loss rate is decreasing due to conformity with the Montreal Protocol³ adopted on September 16, 1987 [*Weatherhead et al., 2000; Newchurch et al., 2003*].

3.2 Ozone absorption theory

As mentioned earlier, ultraviolet radiation with a wavelength of less than 180 nm does not reach the stratosphere; from 180-240 nm it is absorbed primarily by O₂ to form O₃ and does not reach the lower stratosphere. From 240-290 nm it is absorbed by O₃ and does not reach the earth's surface; from 280-320 nm (UV-B) the radiation is partially absorbed by ozone and the portion that reaches the earth's surface is largely responsible for sunburn, skin cancer and other biological effects. From 320-400 nm (UV-A) the radiation is mostly transmitted to the ground and may be important in the formation of photo-chemical smog. The absorption spectrum of ozone in the UV to NIR¹ spectral regions is divided into four different absorption bands: The

¹near infrared

Hartley bands which extend from about 200 to approximately 310 nm, the Huggins bands that range from about 310 nm to 360 nm, the Chappuis bands that cover the visible region, ranging from between 400 and 650 nm and partly overlap with the Wulf bands which range from about 600 nm to 1100 nm. Fig 3.0 shows the ozone absorption cross section between 240 and 800 nm for temperatures ranging from 202 K to 293 K as measured in the laboratory with the GOME FM¹ [Burrows *et al.*, 1997]. The spectral resolution of the GOME FM is wavelength dependent and ranges from 0.3 nm to 0.4 nm. Interestingly, the Hartley as well as the Chappuis bands are rather insensitive to temperature, which makes it advantageous when ozone absorption structures in those bands are employed for remote sensing and absorption spectroscopy. On the other hand, The Huggins bands exhibit significant variation with changing temperatures, and the temperature sensitivity increases with increasing wavelength. Moreover, the Wulf bands are more temperature sensitive than the Chappuis bands. The molecular transitions associated with the absorption bands of ozone are still somewhat unclear, but according to Wayne [1987] the Hartley bands are probably caused by the ${}^1B_2 - X^1A_1$ transition. The Huggins bands may be due to the $2^1A_1 - X^1A_1$ transition. The Chappuis bands are probably caused by the ${}^1B_1 - X^1A_1$ and the Wulf bands seem to be caused by the ${}^3A_2 - X^1A_1$ and ${}^3B_1 - X^1A_1$ transitions (Fig 3.0).

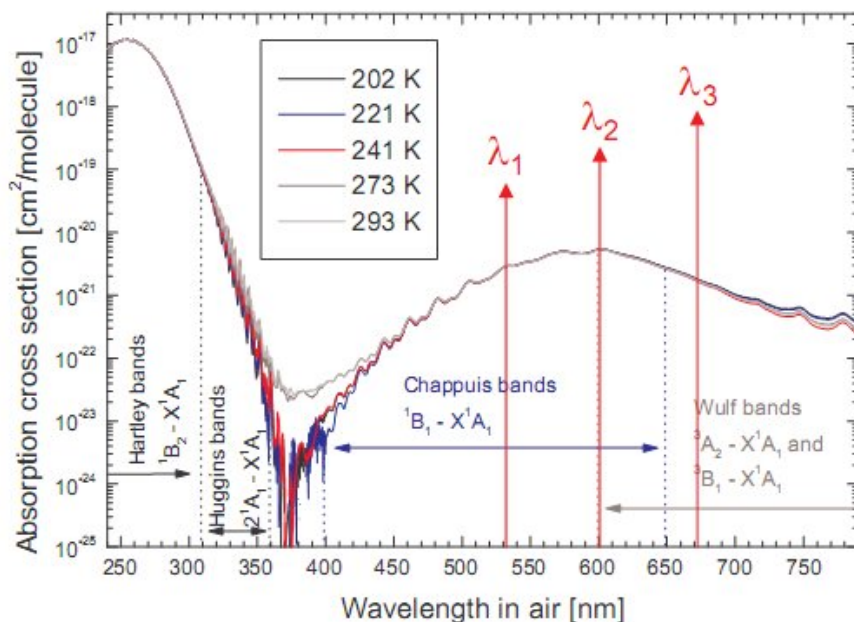


Fig 3.0: The absorption cross section of ozone for different temperatures as measured with GOME FM [Burrows *et al.* 1997]

¹Flight model

3.3 Ozone profile

Ozone profile¹ (Fig 3.1) measurements taken by balloon borne instruments known as ozonesondes, laser² instruments called lidar³, and profiling satellite instruments are usually reported in mixing ratio, number density, or partial pressure. Mixing ratio in ppmv⁴ corresponds to the fractional concentration of ozone as the number of ozone molecules per million air molecules. Number density refers to the absolute concentration as the number of ozone molecules per cubic centimeter. Partial pressure refers to the fraction of the atmospheric pressure at a given altitude for which ozone is responsible. Ozone profiles measured in each of these units appear somewhat different with only a close similarity between number density and partial pressure profiles because the partial pressure of ozone can be expressed as a function of the number density according to the relation

$$P = NkT \quad (3.0)$$

Where N is the number density, k is the Boltzmann's constant and T is the temperature in Kelvin.

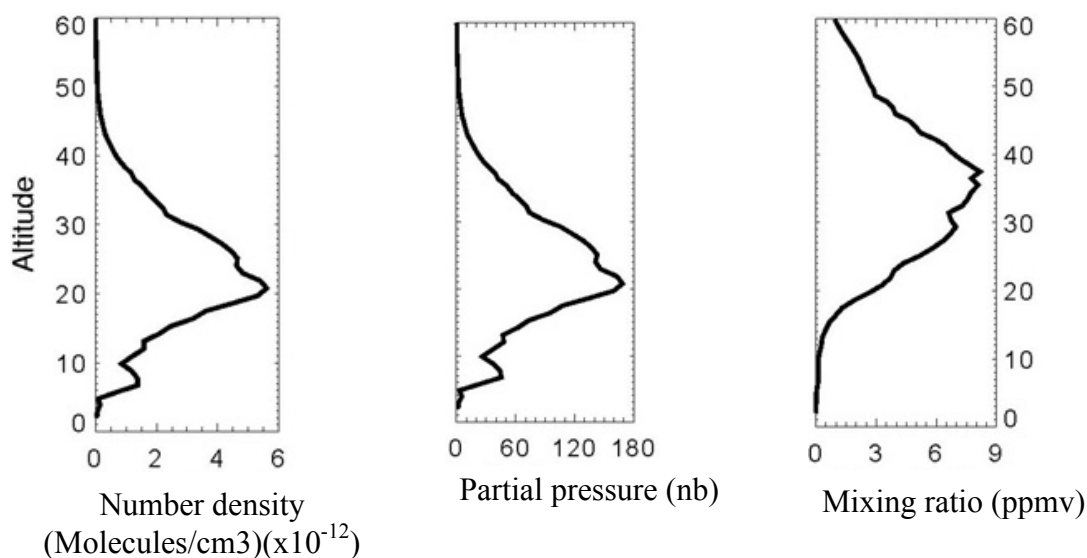


Fig. 3.1 The ozone profile
(see <http://www.ccpo.odu.edu/SEES/ozone/>)

Fig 3.1 shows the ozone profile in number density, partial pressure and mixing ratio, measured by SAGE II at 40°S on September 11, 1994. From the three profiles, it can be observed that the ozone layer peak occurs at altitudes between 20 and 40 km. In the case of the mixing ratio profile, the peak is significantly higher in altitude than for the number density and partial

¹ozone amount versus altitude

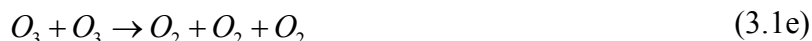
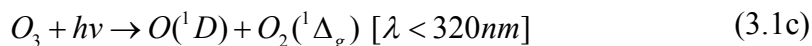
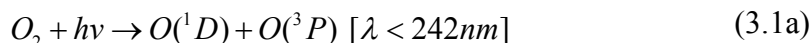
²light amplification by stimulated emission of radiation

³light detection and ranging; ⁴Parts per million by volume

pressure profiles. Also, there is a small peak between 8 and 10 km in the number density and partial pressure profiles and not well observable in the mixing ratios profile for such a linear scale because the mixing ratio only accounts for the fractional composition of the air molecules at this region of the atmosphere.

3.4 Ozone chemistry and the Chapman cycle

The first theoretical explanation of the ozone layer was proposed by Chapman (1930), who developed a steady-state photochemical model based on oxygen-only reactions. The combination of Chapman's reaction scheme and the insights from the past 78 years lead to the following reactions



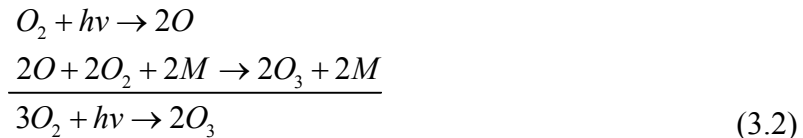
Where M (in 3.1b and 3.1f) is another molecule (typically N₂ or O₂) which carries away the extra energy of the three body reaction.

The reactions in (3.1) can be classified into three different groups namely:

1. Those that produce odd-oxygen (the combination of [O] and [O₃]), e.g., reaction (3.1a)
2. Those that balance the ratio of atomic oxygen (O) and O₃ concentrations, e.g., reactions (3.1b) and (3.1c)
3. Those that destroy odd oxygen, e.g., reactions (3.1d), (3.1e), and (3.1f).

Reactions (3.1a), (3.1b), and (3.1c) provide the mechanism for converting UV-light into heat with reactions (3.1b) and (3.1c) being very efficient at the inter-conversion of O and O₃, even at the top of the atmosphere where the pressure is low, thereby leading to the concept of odd oxygen which is produced only in reaction (3.1a) and lost in reactions (3.1d), (3.1e), and (3.1f). However, due to the low concentration of O in the stratosphere, reaction (3.1f) is too slow in comparison with reactions (3.1d) and (3.1e) and so can be neglected. At higher altitude, reaction (3.1b) slows down while reaction (3.1c) becomes faster, thus atomic oxygen is favoured at higher altitudes while O₃ is favoured at lower altitudes. At altitudes below 60 km, ozone is the dominant form of odd oxygen so it forms about 99 % of odd oxygen in the stratosphere and its rate of production can be equated with the rate of the O atom formation which is twice the rate of O₂ photolysis (3.1a). The dissociation of ozone leading to the

production of O and O₂ can also occur a little above 320 nm and by the absorption in the Chappuis band. According to the steady-state model, since most of the odd oxygen is in the form of ozone, it can be stated that stratospheric ozone concentrations are proportional to the square root of the rate of the photolysis of oxygen (3.1d) [Wayne, 1987]. Though the odd oxygen reactions provide a basic foundation for understanding the sources and sinks for odd oxygen, they do not give a proper detail of the processes involved. The production mechanism for O₃ can be described by the combination of reactions (3.1a) and (3.1b)



After sunset, reactions (3.1a) and (3.1c) stop while reaction (3.1b) and (3.1d) remain, thus allowing the concentration of the atomic oxygen to drop and ozone is no longer destroyed in (3.1d). Since the ratio of the concentration of O to that of O₃ is governed by the rapid photochemical reactions which interconvert O and O₃, at steady state, the rate of creation of ozone from three body collisions will be equal to the rate of photodissociation of ozone by sunlight. This can be expressed as:

$$K_{(o,o_2)}[O][O_2][M] = J_{o_3}[O_3] \quad (3.3)$$

where the brackets [] around a chemical symbol indicate the concentration of the chemical in molecules/cm³; $K_{(o,o_2)}$ is the reaction rate coefficient for the reaction of O with O₂ in cm⁶ molecule⁻² sec⁻¹, and J_{o_3} is the photodissociation coefficient for O₃ in molecule⁻¹ sec⁻¹. As the reaction rate of (3.1b) decreases with increasing altitude, the ratio of the concentration of ozone to that of atomic oxygen [O₃]/[O] decreases with increasing altitude as both [O₂] and [M] fall off exponentially. At 50 km, the daytime ratio of [O]/[O₃] is a little less than 0.1. Thus, ozone at 50 km will increase by about 10 % at night and then decrease again as sunlight returns.

$$[O]/[O_3] = J_{(o_3)} / K_{(o,o_2)}[O_2][M] \quad (3.4)$$

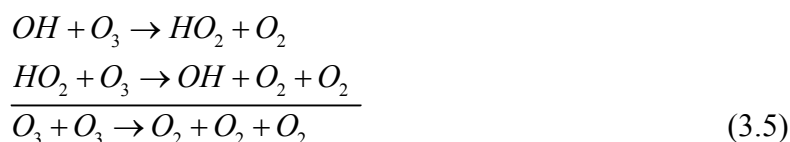
Also, the measured rate of reaction of (3.1d) is much smaller than that required by the oxygen only model.

3.5 Incompleteness of the Chapman cycle

Although the Chapman cycle was an important step towards a better understanding of the chemistry of stratospheric ozone, it was incomplete as it could not address some important issues such as:

1. The ozone column being very small at the tropics (where the solar zenith angle (SZAs) is small) and maximum at the temperate and high latitude.
2. The predictions of ozone densities are a factor of 2 higher than observed densities in the tropics
3. The predictions of the Chapman model being too low at the polar latitudes.

It has been found that these inconsistencies disappear if additional odd oxygen loss mechanisms, i.e. the ozone catalytic destruction cycles involving hydrogen, halogen and nitrogen compounds, as well as the Brewer-Dobson¹ circulation are considered. The work of *Bates and Nicolet [1950]* on the odd hydrogen reaction (HO_x i.e H, OH, HO_2), showed that the rate of reaction of (3.1e) can be increased by the presence of a catalyst as shown below:



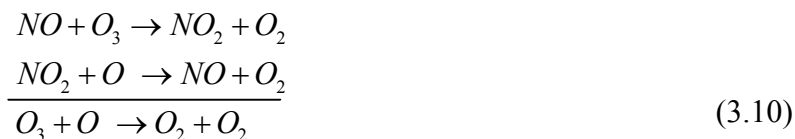
It was also observed that the rate of reaction of (3.1d) could also be increased catalytically by e.g.:



¹slow stratospheric equator-to-pole motion

CHAPTER 3. OZONE CHEMISTRY

Crutzen [1970] and Johnston [1971] investigated the impact of NO_x (NO and NO₂) on ozone which accounts for about 70 % of ozone loss at 30 km altitude (3.10).



As shown in above (3.6-3.10), the net effect of the reactions is the formation of 2 oxygen molecules from an ozone molecule and an oxygen atom while the NO-NO₂ and Cl-ClO are unaffected. At about 40 km altitude, these catalytic processes can destroy nearly 1000 ozone molecules before the catalyst (NO-NO₂ and Cl-ClO) becomes inactive and forms reservoir species such as Hydrochloric acid (HCl) or Chlorine nitrate (ClONO₂) where they last for a few days before they are photolyzed. During photolysis the Cl atom is released which then starts the ozone destruction process once again; eventually the Cl atom is carried out of the stratosphere. Therefore the amount of ozone in the stratosphere is due to a balance between the solar production and the loss by a number of these catalytic reactions. If it were possible to increase the solar ultraviolet output at wavelengths below 240 nm, ozone levels would rise. The loss of ozone in the natural form results from normal levels of gases such as methane, nitrous oxide, methyl bromide, and methyl chloride, so if there is an increase in these natural levels of chlorine, nitrogen, bromine or hydrogen in the stratosphere, or if new compounds are added to the stratosphere, the loss of ozone will increase, and the level of ozone will decrease, until a new equilibrium between production and loss is achieved.

3.6 Chapman layers

Due to the variation in optical density of the atmosphere, species such as ozone whose concentration depend on photochemical production, form layer-like structures called Chapman layers having a profile defined by the Chapman function. The shape of the Chapman layer can be explained by a simple model in which incident light travels downward from the top of the atmosphere. Although the solar intensity is higher at the top of the atmosphere, little amounts of atomic oxygen are produced due to the low concentration of O₂. As the light travels through the atmosphere, it interacts with the atmospheric medium and decreases in intensity such that at lower altitude the solar intensity has decreased to an extent that despite the abundance of O₂ not enough oxygen atoms can be produced. But somewhere in between there is a compromise that maximizes the production of O atoms due to photolysis and this is the region where the ozone layer is formed. Wayne [2000] described a simple derivation of the Chapman function starting with:

$$n = n_0 e^{-z/H} \quad (3.11)$$

Where n is the atmospheric number density, n_0 is the reference number density at a reference altitude z_0 , z is the altitude above the reference, and H is the scale height of the atmosphere. For a light beam with intensity I , the interaction of the photons with the medium leads to a decrease in the intensity of the beam. This is known as Beer-Lambert's law given as:

$$-dI = In\sigma dz \quad (3.12)$$

$$-dI = Id\tau \quad (3.13)$$

Where σ is the absorption cross section and τ is the optical depth of the medium given as:

$$\tau = \int_0^z n(z')\sigma dz' \quad (3.14)$$

Integration of equation (3.13), leads to

$$I(z) = I_0 e^{-\tau}, \quad (3.15)$$

where I_0 is the incident beam intensity. The absorber cross section varies with the wavelength λ and for a small cross section, the optical depth is small for the same path length and the atmosphere is more transparent at this wavelength. The decrease in photon intensity heats the atmosphere and equally provides some important observable features in the atmosphere. For a plane parallel atmosphere, with a small increase in altitude dz , the path length to the sun would increase by $\sec\theta dz$ where θ is the solar zenith angle (Fig 3.2a). Equation (3.13) can now be written as

$$-dI = In\sigma \sec\theta dz \quad (3.16)$$

Combining equations (3.11) and (3.16) and integrating over dz , yields;

$$I = I_\infty \exp(-n_0\sigma H \sec\theta e^{-z/H}) \quad (3.17)$$

where I_∞ is the incoming solar radiation at $z = \infty$. The rate, q , at which energy is removed from the incoming radiation per unit length, is given by:

$$\begin{aligned} q &= dI_z / (\sec\theta dz) = (dI / dz) \cos\theta \\ q &= I_\infty n_0 \sigma \cos\theta \exp(-\frac{z}{H} - n_0\sigma H \sec\theta e^{-z/H}) \end{aligned} \quad (3.18)$$

The peak of the Chapman layer corresponds to the maximum of the rate of equation (3.18). Equation (3.18) can be used to derive an arbitrary altitude sketch of the Chapman function (Fig

3.2b) showing an increase in the extinction rate from top to bottom until it reaches a maximum and then a quick drop to zero.

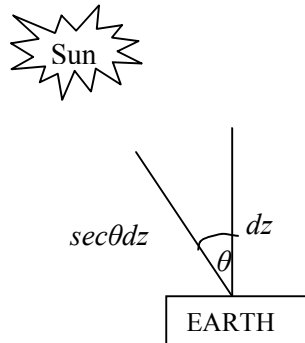


Fig. 3.2a: Increase in path length to the sun with increase in solar zenith angle

At the O_2 Herzberg band (around 220 nm), the peak of its photo-dissociation is in the stratosphere, accounting for the high concentration of odd oxygen and therefore, ozone in this region [Wayne, 2000]. Although Chapman layer chemistry explains the typical ozone profile that can be seen all over the globe it neglects the other processes (e.g., dynamics) responsible for the distribution of ozone throughout the atmosphere.

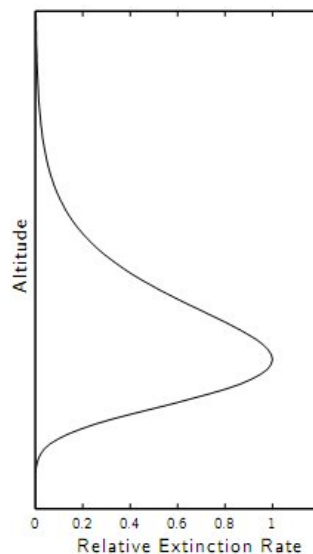


Fig 3.2b: Chapman weighting function
(www.bu.edu/cism/ScienceSeminar/Solomon/)

3.7 The distribution of ozone in the stratosphere

Since stratospheric ozone is produced following the photolysis of oxygen molecules by ultraviolet radiation, one would expect to find a higher level of ozone concentration near the equator and a lower level towards the poles and also a higher level during summer than during

winter. But the opposite is the case as a high level of ozone is found in the mid-to-high latitudes of the northern and southern hemisphere and during spring in the northern hemisphere. This latitudinal and seasonal dependence is due to the prevailing stratospheric wind patterns known as Brewer-Dobson circulation (Fig. 3.3) and solar intensity which is higher at the tropics and lower at the poles. The Brewer-Dobson circulation, first proposed by *Brewer (1949) and Dobson (1953)*, qualitatively corresponds to rising motion in the tropics, followed by poleward transport, leading to a reduction of ozone densities at low latitudes. At high latitudes, sinking motion lowers the altitude of the ozone peak and leads to an accumulation of ozone which is in agreement with higher total ozone columns at higher latitudes. The Brewer-Dobson circulation is most efficient in the winter hemisphere, whereas meridional transport in the summer stratosphere is partly weakened by stable and strong easterly winds [e.g., *Roedel, 1992*]. During winter, the ozone layer increases in depth, however, the overall column amounts are greater in the northern hemisphere high latitudes than in the southern hemisphere high latitudes. Also, while the highest amounts of column ozone over the Arctic are observed in the northern spring (March-April), the opposite is true over the Antarctic, where the lowest amounts of column ozone occur in the southern spring (September-October). In fact, while the highest amounts of column ozone anywhere in the world are found over the Arctic region during the northern spring period of March and April which later decreases during summer, the lowest amounts of column ozone anywhere in the world are found over the Antarctic in the southern spring period of September and October, owing to the ozone hole phenomenon.

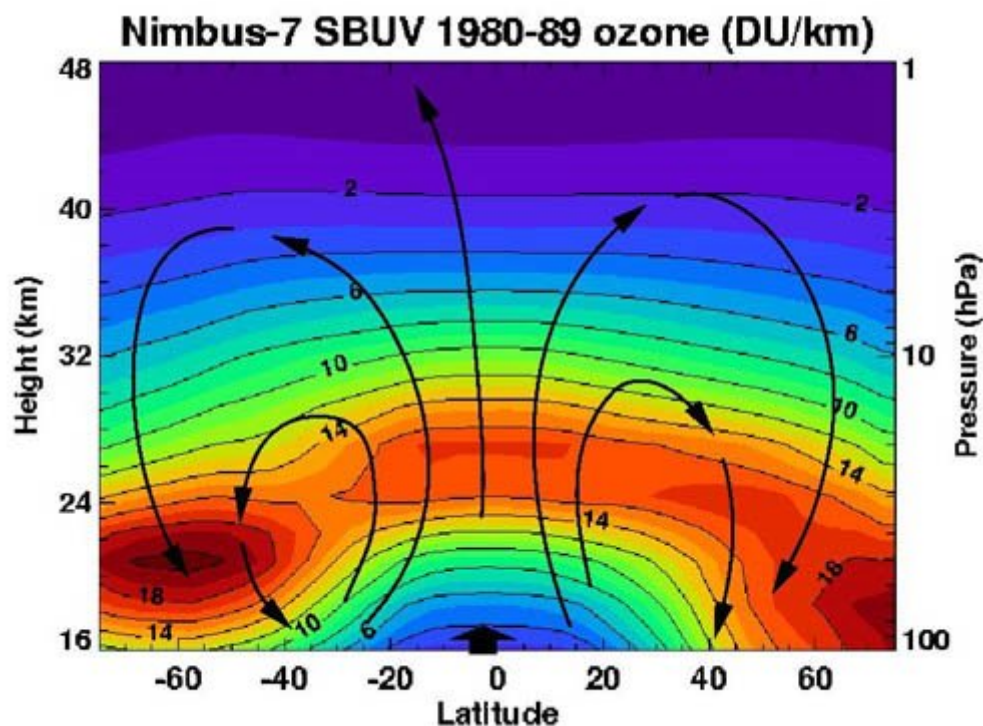
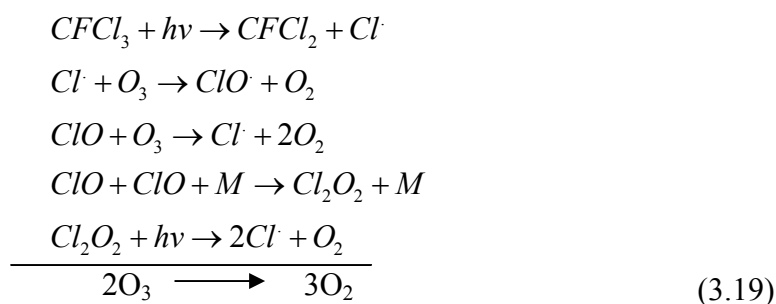


Fig. 3.3: Brewer-Dobson circulation in the ozone layer.
 (<http://www.atmosphere.mpg.de>)

3.8 History of the Chlorofluorocarbons (CFCs)

The Chlorofluorocarbons (CFCs), also called Freons, are a group of chemical compounds comprising carbon, fluorine, and chlorine. CFCs were invented in the early 1930s as propellants for aerosols, refrigeration coolants, and electronic circuit board cleaners. After it was shown by *Crutzen* [1970] that nitric oxide (NO) could catalyze the destruction of ozone, chemists *Frank Sherwood Rowland and Mario Molina* in 1973 began studying the impacts of CFCs in the earth's atmosphere. In 1974, *Stolarski and Cicerone* [1974] first demonstrated that chlorine can also catalyze the destruction of ozone. In the same year, *Rowland and Molina* found that CFC molecules were stable enough to remain in the atmosphere for about 50-200 years before they reached the middle of the stratosphere where they are finally broken down by ultraviolet radiation (3.19) thereby releasing chlorine atoms [Rowland et al. 1989, 1991]. They then proposed that these chlorine atoms might be expected to cause the breakdown of large amounts of ozone in the stratosphere. The *Rowland-Molina* hypothesis suffered a lot of setbacks mainly from the criticisms by the representatives of the aerosols and halocarbon industries but the scientific community was shocked when British Antarctic Survey scientists *Farman, Gardiner and Shanklin* [1985] published a journal paper showing a sharp decline in polar ozone over Antarctica in southern hemisphere spring. This led to some nations coming together to establish a framework for negotiating international regulations on ozone-depleting substances (ODS) and consequently *Crutzen, Molina and Rowland* were awarded a Nobel Prize for Chemistry in 1995 for their findings.



3.9 The Montreal protocol and its amendments

The Montreal protocol, an international treaty designed to protect the ozone layer by phasing out the production of ozone depleting substances such as the halogen compounds (chlorofluorocarbon (CFC) commonly called freons, and bromofluorocarbon compounds known as halons) and a number of chemical compounds (carbon tetrachloride and trichloroethane etc.), was opened by 24 nations for signature on September 16, 1987 and adopted on January 1, 1989 followed by a first meeting in Helsinki, May 1989 and has since

then undergone some amendments: in 1990 (London), 1991 (Nairobi), 1992 (Copenhagen), 1993 (Bangkok), 1995 (Vienna), 1997 (Montreal) and 1999 (Beijing) as shown in (Fig. 3.4), with over 190 countries currently joining the campaign while countries like Andorra, Iraq, San Marino, Timor-Leste and Vatican City were still yet to join as of September 2007. These amendments have resulted in a more rapid decline of ozone depleting substances [Showstack, 2003, Anderson, et al., 2000]. It is believed that if the international agreement is adhered to, the ozone layer is expected to recover by 2050. The countries ratifying the Montreal protocol committed themselves to reducing the production and consumption of 5 CFC compounds (CFCl_3 (CFC-11), CF_2Cl_2 (CFC-12), $\text{C}_2\text{F}_3\text{Cl}_3$ (CFC-113), $\text{C}_2\text{F}_4\text{Cl}_2$ (CFC-114), and $\text{C}_2\text{F}_5\text{Cl}$ (CFC-115)) and 3 halons (halon 1211, 1301, and 2402) (Fig. 3.5). According to the protocol, developed countries were required to phase out the production and consumption of the 5 regulated CFCs by January 1, 1996 and the production and consumption of the regulated halons by January 1, 1994 while for developing countries with a per capita consumption of the regulated substances below a certain threshold (0.3 kg per year) were given the deadline of about 2010. There are a few exceptions of the substances (e.g. the metered dose inhalers commonly used to treat asthma and other respiratory problems or halon fire suppression systems used in submarines and aircraft) that are still in essential use because no acceptable substitutes have been found. Based on this, several reports have been published by various institutions, governmental and non-governmental organizations to present alternatives to the ozone depleting substances, since these substances are still useful in various technical sectors such as agriculture, refrigerating, laboratory measurements and energy production. Recent research has shown that since the Montreal protocol came into effect, the atmospheric abundances of several regulated species have decreased in the lower atmosphere since mid of the 1990s (e.g. CFC-11) [Egorova, 2001]. It is also noted that the abundances of species with longer atmospheric lifetimes (e.g. CFC-12) do not increase anymore and are expected to decrease over the next few years. Although halon concentrations have been found to be increasing as halons presently stored in fire extinguishers are released but they are expected to decline by 2020. Also the concentration of Hydrochlorofluorocarbons (HCFCs) has increased drastically because they were used to replace CFCs in solvents or refrigerating agents. The HCFCs and Hydrofluorocarbons (HFCs) have been found to have a larger greenhouse gas potential (on a per molecule basis), but the total effect is still significantly smaller than that of the anthropogenic CO_2 . At the moment, the Montreal protocol has placed a restriction on HCFCs by 2030 but non on HFCs. The substitution of HFCs for CFCs is currently not showing any significant increase in global warming but there is the likelihood that over time, a steady

increase in their use could lead to enhanced global warming, also worrisome is the case of smuggling of CFCs from undeveloped to developed countries. Interestingly satellite measurements at the end of 1990s showed that the stratospheric chlorine load does not increase anymore, but decreases slowly [WMO 2007]. Although, this has not yet resulted in a significant reduction in the size of the ozone hole [Newman *et al.* 2006]. However, in the altitude range of 40 km, where the first papers [Crutzen 1974, Cicerone *et al.*, 1974] already predicted the greatest effects of chlorine on ozone destruction, there are possible signs of the beginning of ozone recovery [Newchurch *et al.*, 2003, Steinbrecht *et al.*, 2009, Zanis *et al.*, 2006, Jones *et al.*, 2009]. In fact, the Montreal protocol has often been called the most successful international environment agreement to date.

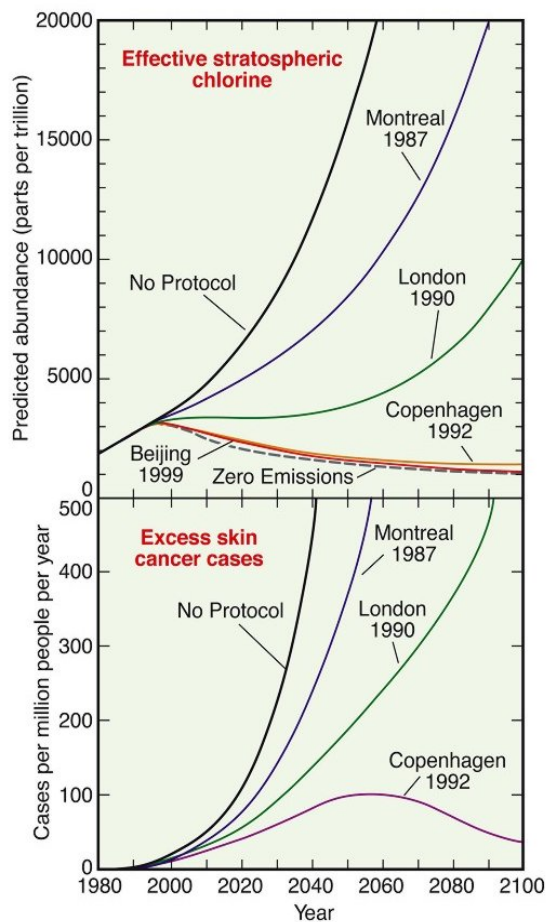


Fig. 3.4: The effects of the Montreal protocol amendments and their phase-out schedules (see <http://www.epa.gov/ozone/intpol/history.html>)

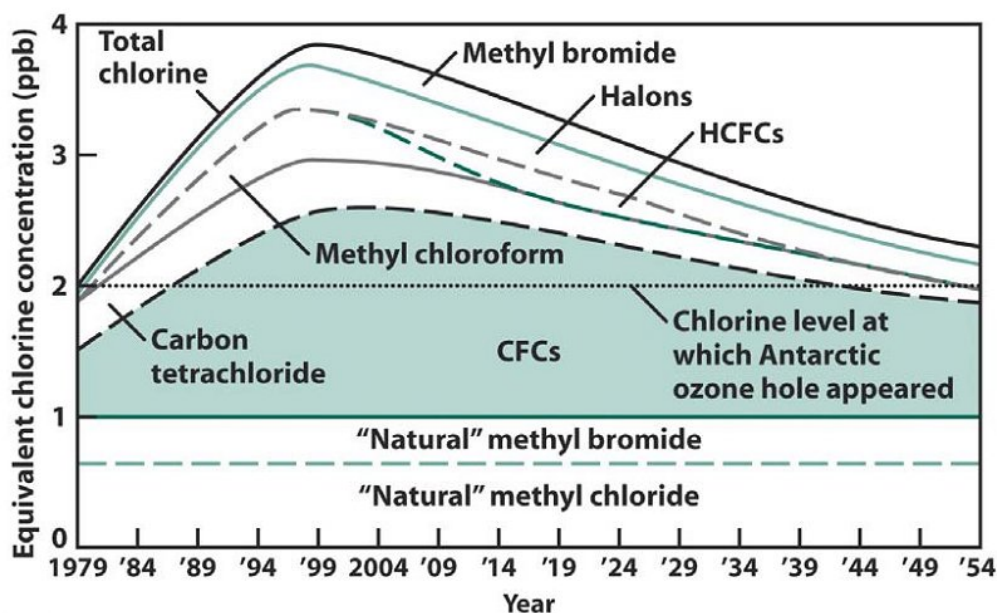


Fig. 3.5: Actual and Projected Concentration of Stratospheric Cl versus time
(Adapted from *Environmental Chemistry*, Third edition ©2005 W.H. Freeman and company)

3.10 Ozone depletion

There are basically two mechanisms by which total amounts of stratospheric ozone are depleted, namely:

1. Slow, steady decline of about 4 % in the total volume of ozone during the past 2 decades
2. Fast, but seasonal decrease during polar spring mainly in the southern hemisphere.

3.11 The ozone hole

The ozone hole is a depression of the ozone layer during which all the ozone between about 15 and 19 km is destroyed whereas the ozone higher up is less affected, thus causing the over-all amount of ozone in the atmosphere to decline. In the lower stratosphere the ozone hole is most usually measured not in terms of ozone concentrations but by the reduction in the total column ozone above a point on the earth's surface and expressed in Dobson units (DU). The mechanism by which the polar ozone hole forms is different from that for the mid-latitude thinning, but the proximate cause of both trends is due to the catalytic destruction of ozone by atomic chlorine and bromine which are initially formed during the photolysis of chlorofluorocarbon (CFC) compounds (freons) and bromofluorocarbon compounds (halons) in the stratosphere. In the mid-latitudes, it is preferable to speak of ozone depletion rather than holes as the ozone loss is much less and slower – only a few percentages per year compared to the sudden and near total loss of ozone over Antarctica at certain altitudes. The tropics do not share much on ozone depletion as there are no significant trends. The observed reduction in

CHAPTER 3. OZONE CHEMISTRY

stratospheric temperatures can also be explained by the ozone depletion. Since the stratosphere is mainly warmed by the absorption of UV radiation by ozone, a reduction in ozone amount would result in the cooling of the stratosphere, although some stratospheric cooling is predicted from increase in greenhouse gases such as CO₂, ozone induced cooling is found to be probably dominant.

The Antarctic ozone hole discovered in the early 80s by *Farman et al.* [1985] and later confirmed by other scientists [see *Hofmann et al.*, 1987, 1997; *Iwasaka and Kondoh*, 1987], is the region of the Antarctic stratosphere where the ozone level was noticed to have dropped to about 33 % of their pre-1975 values during southern spring. The Antarctic ozone hole (Fig. 3.6) occurs during the Antarctic spring (September to early December) after the formation of an atmospheric container called the polar vortex by strong westerly winds that circulate around the continent. Observations taken in the Antarctic region from aircraft, the ground, and satellites have demonstrated that the ozone hole results from the increased amounts of chlorine and bromine in the stratosphere, combined with the peculiar meteorology of the southern hemisphere, cold temperature during polar winter, ice cloud formation and polar sunrise during spring that produces the energy necessary for the catalytic reactions. Ground based measurements of ozone started first in 1956, at Halley Bay in Antarctica while satellite measurements of ozone started in the early 70s, with the first comprehensive worldwide measurements in 1978 with the Nimbus-7 satellite. In the early 1990s, when the Total Ozone Mapping Spectrometer (TOMS) was used to measure the ozone column amount, they showed a noticeable decrease in column ozone (less than 220 DU) in the Antarctic spring and early summer when the obtained results were compared to that obtained in the early 1970s (about 300-350 DU) (Fig 3.7). It was observed that the hole was first larger than the Antarctic continent in 1987 and became more alarming on September 03, 2000 when the hole was noticed by groups of British Antarctic survey and NASA¹ to have covered 28.4×10^6 km² and 30.3×10^6 km² respectively. An increase in the ozone depletion area was later noticed on September 5, 2006 and was recorded to cover about 29.5×10^6 km² by NASA and 28.0×10^6 km² by ESA². Currently, measurements by NASA on September 12, 2008, have also shown a decrease in the ozone amount when compared to that of September 15, 2007 and was classified as the fifth largest Antarctic ozone hole covering about 27×10^6 km². Some theories which were proposed to account for the existence of the "hole" include the dynamical theory, the nitrogen oxide theory, and the heterogeneous chemistry theory. The dynamical theory (*Tung et al.*, 1986) proposed that the atmospheric circulation over Antarctica had changed in such a way

¹National Aeronautics and Space Administration established on July 29, 1958

²European Space Agency established in 1975

CHAPTER 3. OZONE CHEMISTRY

that air from the troposphere, where there is little ozone, was being carried into the polar lower stratosphere, and hence led to the observed reductions. The nitrogen oxide theory (*Callis and Natarajan, 1986*) proposed that increased levels of NO_x produced by the photochemical effects of a sunspot peak period in 1979 were responsible for destroying more ozone. The heterogeneous chemistry theory (*Solomon et al., 1986, Crutzen and Arnold, 1986, Toon et al., 1986*) proposed that reactions were occurring on the surfaces of tiny cloud particles (polar stratospheric clouds) that form in the extremely cold conditions and that these reactions alter the polar stratospheric chemistry. Measurements over Antarctica have shown that the heterogeneous chemistry theory is correct. Antarctic ozone loss is caused by the heterogeneous reactions of chlorine and bromine compounds on the surfaces of polar stratospheric clouds. Although bromine and even fluorine is more effective in ozone removal than chlorine, these species are much less abundant in the stratosphere compared to chlorine. Once the chlorine is freed by these heterogeneous reactions, the weak levels of sunlight initiate and maintain the catalytic ozone loss photochemistry (eqns. 3.5-3.10).

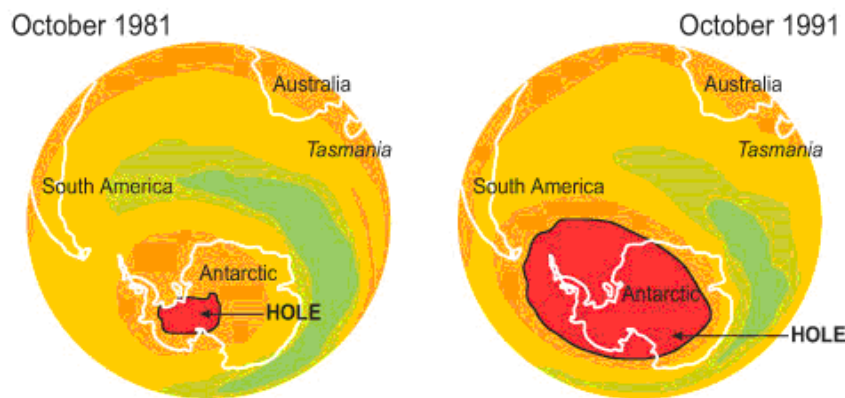


Fig 3.6a: Total average ozone column for Oct 1981 & 1991
(See <http://www.theozonehole.com/ozoneholehistory.htm>)

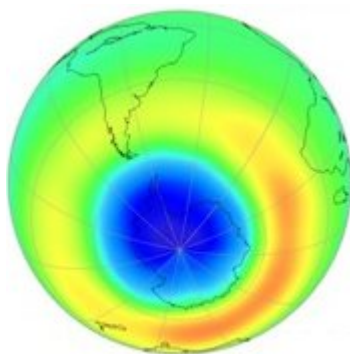
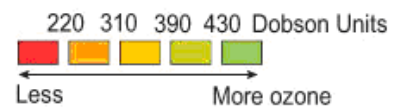


Fig 3.6b: second largest Antarctic ozone hole (September, 2000)

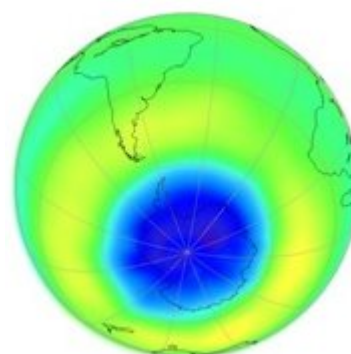


Fig 3.6c: Largest Antarctic ozone hole (September 21-30, 2006)

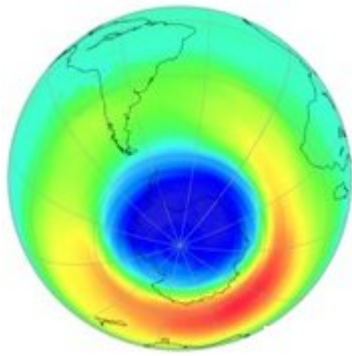


Fig 3.6d: Antarctic ozone hole (September 13, 2007)

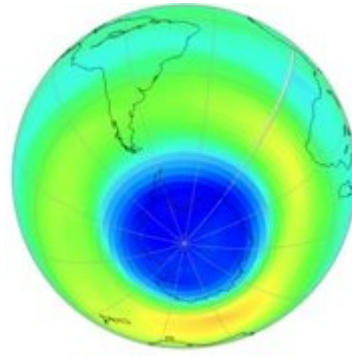
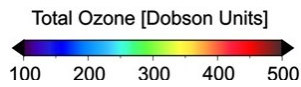


Fig 3.6e: fifth largest Antarctic ozone hole (September 12, 2008)



See <http://www.theozonehole.com/ozoneholehistory.htm>

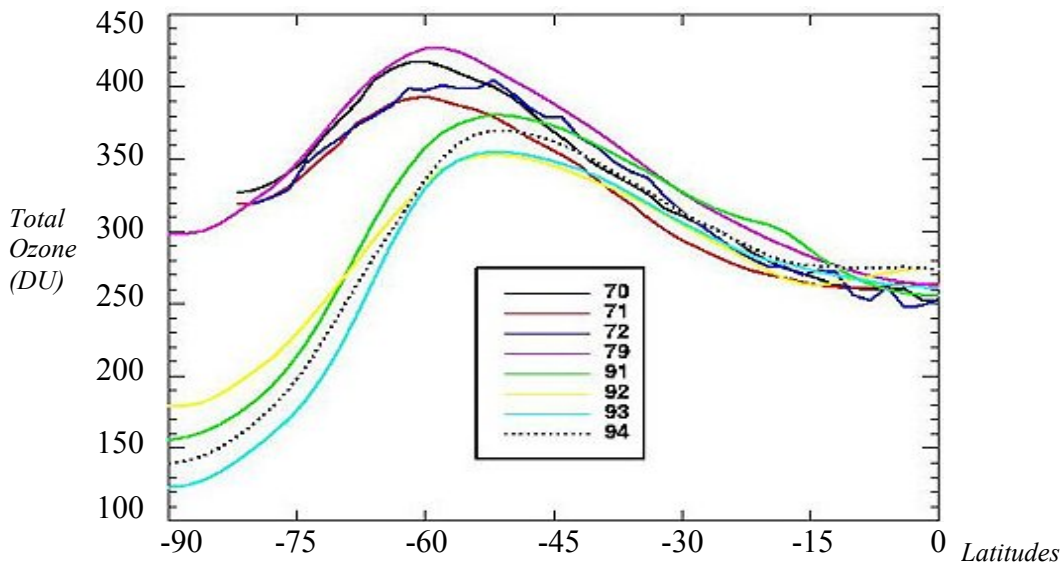


Fig 3.7: October zonal mean total ozone for the 1970s and early 1990s (see <http://www.theozonehole.com/ozoneholehistory.htm>)

3.12 The Arctic stratosphere

Over the last two decades, some very low ozone levels were equally observed over the Arctic during the late winter and early spring. These low values led to the curiosity that human activity may also be seriously impacting the Arctic stratosphere and that the ozone layer may not recover in the next few decades. The Arctic stratosphere is in a way different from the Antarctic stratosphere because, firstly, natural ozone levels in the Arctic spring are much higher than in the Antarctic spring, and secondly, Arctic spring stratospheric temperatures are

higher than those in the Antarctic stratosphere. As a result of the higher Arctic stratospheric temperatures, polar stratospheric clouds are much less common in the Arctic and its polar vortex is warmer and much more variable than the Antarctic vortex leading to a stronger inter-annual variability in both chemical loss of ozone and in dynamical supply of ozone-rich air to high latitudes. Therefore compared to the Antarctic, Arctic ozone trends are much more variable and higher due to the structure of the Northern Hemisphere (Fig. 3.8). However, the Arctic winter time shares some resemblance with that of the Antarctic, in that it also exhibits a cold polar vortex that separates the air enclosed in it from the mid-latitude air, and there is also the transport of air from the upper stratosphere and partly from the mesosphere to the lower stratosphere by strong adiabatic descent throughout winter period [Tuck, 1989]. Indeed, signs of a perturbed chlorine chemistry showing that the Arctic was primed for chemical ozone depletion were reported in the late 80s [e.g. Solomon et al., 1988; Schiller et al., 1990; Brune et al., 1990]. Although measurements with the Total Ozone Mapping Spectrometer (TOMS) (Fig 3.9) in the spring of 1995, 1996, 1997 and 1998 detected ozone losses for the first time in the Arctic that were commensurate to that observed in Antarctica a decade earlier, observations and modeling over the last two decades have shown that conditions for severe ozone loss are directly related to the severity and persistence of the Arctic winter. The persistence of cold temperatures leads to the formation of extensive polar stratospheric clouds which in turn activate chlorine and lead to large ozone losses. It has been suggested that temperature and wind changes induced by increased concentration of greenhouse gases would alter the propagation of planetary waves such that it would no longer be able to break the polar vortex as often, thereby reducing the warming of the stratosphere (Shindell et al. 1998). It was estimated that due to this effect the ozone loss over the Arctic by the year 2020 will be doubled what it would be without greenhouse gas increase, and that recovery from Arctic ozone depletion will be delayed by some 10-15 years. This explains that the Arctic vortex would be more stable and produce significantly lower stratospheric temperatures, leading to more extensive PSC formation which will further add to the greenhouse cooling of the stratosphere, thus resulting in greater ozone loss. Based on this, there is the likelihood that the ozone layer recovery may not track the slow decline of industrial halogen compounds in the atmosphere in response to the Montreal protocol. The detection of the Arctic ozone hole has led to several campaigns, such as from the US Airborne Arctic Stratospheric Expedition (AASE I and AASE II), the European Arctic Stratospheric Ozone Experiment (EASOE) (1991-1992), the Second European Stratospheric Arctic and Mid-latitude Experiment (SESAME) (1994-1995), and the Third European Stratospheric Experiment on Ozone (THESEO) (1997-2000). In order to overcome the

problems imposed by the strong meteorological variability shown by ozone column amounts, measurements of ozone and other atmospheric gases and particles using satellites, aircraft, small, large and long duration balloons, and ground-based instruments throughout the Arctic were carried out. Ozone losses of over 30 % were observed in the Arctic stratosphere at 17-25 km altitude during the 1994-1995 winter, which is regarded as one of the coldest stratospheric winters on record. These losses were a direct result of the activation of chlorine and bromine species on the surfaces of PSCs [e.g., Tilmes et al., 2004]. The three European campaigns are noteworthy and gave a better effectiveness in the estimation of ozone loss than would have been possible through individual national research.

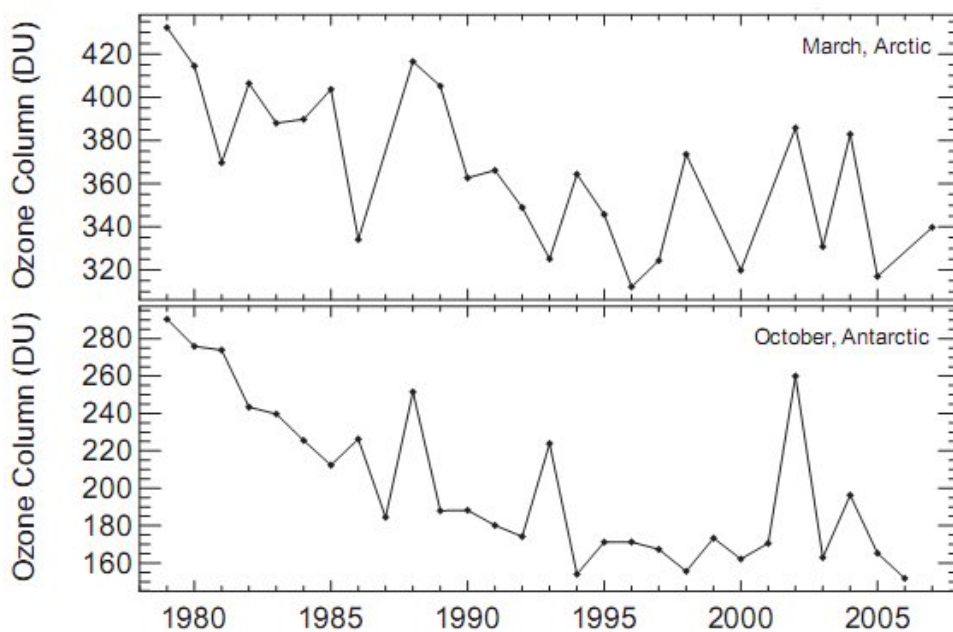


Fig. 3.8 Time series of monthly average column ozone poleward of 63° Arctic and Antarctic spring. (Adapted from Muller et al., 2008)

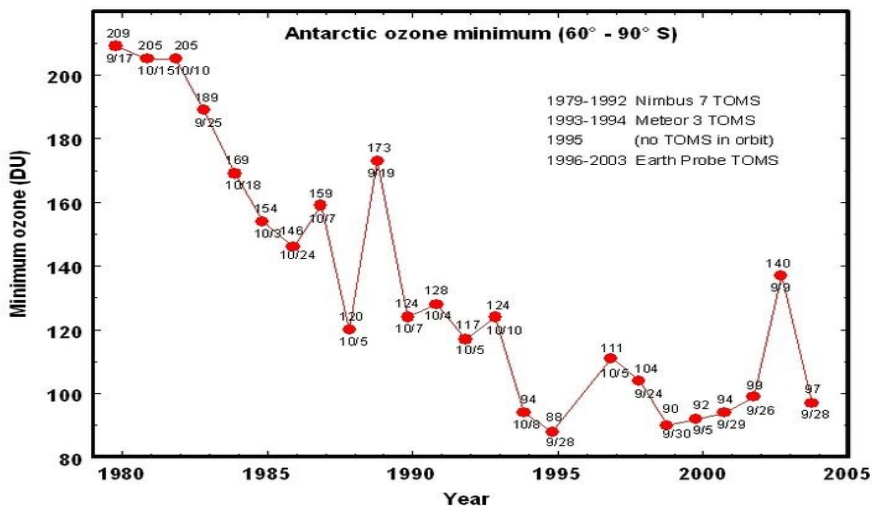


Fig. 3.9: Lowest value of ozone measured by TOMS each year in the ozone hole
See <http://www.nasaimages.org/luna/servlet/>

3.13 Chemicals responsible for ozone destruction

The main free radical catalysts that can destroy the ozone layer are the hydroxyl radical (OH.), the nitric oxide radical (NO.), atomic chlorine (Cl.) and atomic bromine (Br.) which have both natural and anthropogenic sources. Presently most of the OH and NO in the stratosphere is of natural origin while human activities have dramatically increased the atmospheric amounts of CFCs and halons (Fig. 3.10) which later find their way into the stratosphere where they are photolyzed to yield chlorine and bromine atoms respectively, which catalytically destroy ozone molecules (eqns. 3.6 & 3.7).

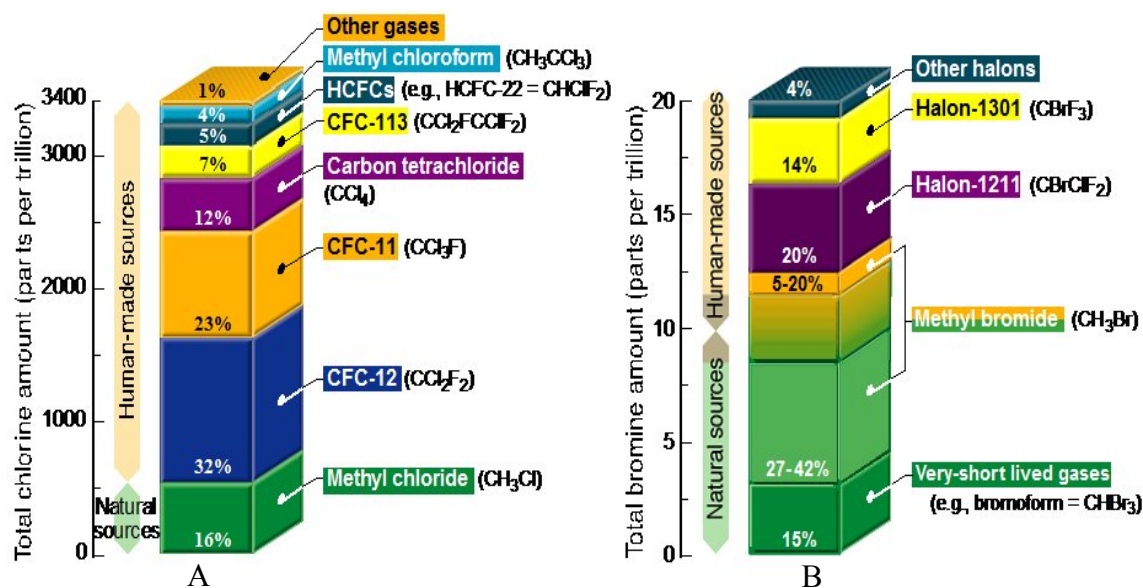


Fig. 3.10: Sources of stratospheric halogens; Chlorine compounds (A), Bromine compounds (B)
(See <http://www.unep.org/ozone/faq.shtml>)

From Fig. 3.10, only methyl chloride has a large natural source; it is produced biologically in the oceans and chemically from biomass burning. The CFCs and CCl_4 are nearly inert in the troposphere, and have lifetimes of 50-200 years. Due to their long life-time, they can travel to the stratosphere where they are photolyzed by UV radiation of wavelength less than 230 nm [Rowland 1989, 1991]. The hydrogen-containing halocarbons are more reactive, and are removed in the troposphere by reactions with OH radicals. This process is slow, however, and they live long enough (1-20 years) for a substantial fraction to reach the stratosphere. It has also been shown that very large volcanic eruptions can inject hydrogen chloride (HCl) directly into the stratosphere, but direct measurements have shown that their contribution is very small compared to that of chlorine from CFCs. Natural sources of chlorine in the stratosphere constitute less than 20 % while those from CFCs constitute about 80 % of the chlorine in the stratosphere. The halons, although being very reactive and constituting to mass destruction of

ozone, occur only in small quantities in the stratosphere (Fig 3.10). The Montreal protocol has played a major role in enhancing the reduction of these compounds in the stratosphere (Fig 3.5).

3.14 Polar Stratospheric Clouds

Polar Stratospheric Clouds (PSCs) also known as the nacreous clouds are clouds that form in the extremely cold and dry conditions ($< -80^{\circ}\text{C}$), that exist in the polar night regions of the stratosphere. PSCs are responsible for the Antarctic ozone hole in that they provide the surfaces on which the heterogeneous reactions necessary for ozone destruction occur. PSCs are divided into two classes, Type I and Type II, both of which are formed only under extremely cold conditions that are found typically in the winter polar vortex region of the Arctic and Antarctic stratosphere. They tend to form much more frequently in the more isolated, colder Antarctic vortex, hence the existence of the ozone hole over there and not over the Arctic. The temperature at which they form is referred to as the frostpoint.

3.14.1 Type I Polar Stratospheric Clouds (PSCs)

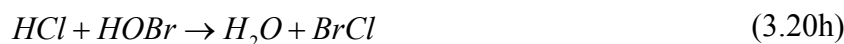
Type I PSCs are composed of a super-cooled liquid ternary solution of nitric acid, sulfuric acid, and water ice ($\text{HNO}_3\text{-H}_2\text{SO}_4\text{-H}_2\text{O}$), as well as frozen Nitric Acid Trihydrates (NAT), ($\text{HNO}_3\cdot\text{H}_2\text{O}$). The frostpoint for Type I PSCs is (-78°C), and they are much smaller than Type II PSCs, with particle diameter of $< 1\ \mu\text{m}$ and a sedimentation rate of the order of 0.01 km per day.

3.14.2 Type II Polar Stratospheric Clouds (PSCs)

Type II PSCs are water ice particles that form when the temperature falls below (-85°C). They are relatively large, with a diameter of $< 10\ \mu\text{m}$, having a sedimentation rate of 1.5 km per day.

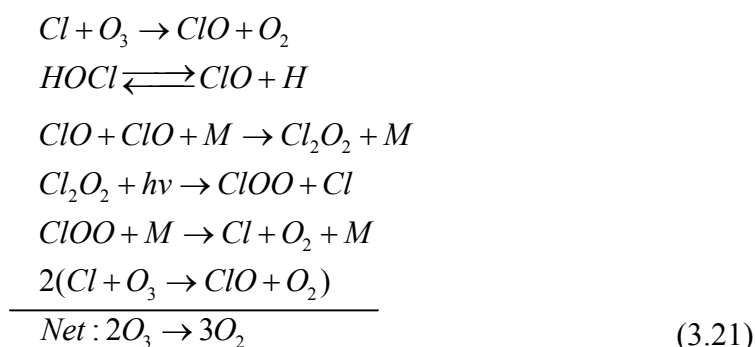
3.14.3 Heterogeneous reactions on the Polar Stratospheric Clouds (PSCs)

Heterogeneous reactions which refer to chemical reactions occurring in multiple states (gas, liquid, and solid), are extremely important in the discussion of Antarctic ozone hole, since they not only free chlorine and bromine from reservoir species into reactive forms but also help in the removal of reactive nitrogen species (NO_x) from the atmosphere by converting it to nitric acid (HNO_3), which prevents the newly formed ClO from being converted back into ClONO_2 . Today, a variety of heterogeneous reactions of importance to stratospheric chemistry are known with the most basic ones shown in reactions 3.20a-3.20h



The reaction rates of the above reactions depend on the particle type, particle surface area, and temperature. During cold winter, reactions (3.20) increase dramatically, giving a better understanding of the ozone budget of the polar stratosphere. Reaction 3.20a, proposed by *Solomon et al.*, [1986], converts the relatively stable chlorine reservoir species HCl and ClONO₂ into Cl₂, thereby perturbing gas phase chlorine partitioning. Equally of importance is (3.20e) [*Molina et al.*, 1987], which is responsible for the activation of HCl and thus for a complete activation of the stratospheric chlorine reservoir. Heterogeneous reactions on the noncrystalline stratospheric sulfate aerosol were known to be important for mid-latitude chemistry [*e.g.*, *Hofmann and Solomon*, 1989], but were not thought to be of great relevance for polar chlorine activation. Current studies have shown reaction probabilities of stratospheric species on a variety of solid and liquid aerosol particles. These reaction probabilities are frequently strongly temperature dependent being relevant only at low temperatures with the exception of (3.20d), which is important at all temperature occurring in the stratosphere. Reaction (3.20d) can take place whenever there is a particle in the stratosphere (*e.g.* after volcanic eruption). It plays an important role in the explanation of nitrogen chemistry of the middle latitude stratosphere. Molecules such as ClONO₂ and HCl in reaction (3.20a) become highly reactive with one another when dissolved in sulfuric acid-water but are non reactive in their gaseous state, thus acting as chlorine reservoir species. The absorption of HCl and ClONO₂ on a liquid sulfate aerosol particle in the stratosphere results in the release of Cl₂ and the retention of a nitric acid (HNO₃) molecule within the aerosol particle. The nonreactive HNO₃ formed remains in a solid (frozen) state on the surfaces of the PSCs. As the PSCs undergo sedimentation, the HNO₃ is carried out of the stratosphere. This process leads to the removal of nitrogen from the stratosphere and is called denitrification. Since HNO₃ photolysis results in the formation of reactive NO₂, which in turn reacts with ClO to form the reservoir ClONO₂ species, the removal of nitrogen from the stratosphere means that there is more reactive, ozone destroying ClO. The chlorine species Cl₂ and HOCl created in reactions

(3.20a), (3.20b), and (3.20d) are short lived so they are quickly photolyzed by sunlight even at visible wavelengths. The Cl_2 molecules are photolyzed into two chlorine atoms, which then participate in the Cl_x catalytic cycles (eg. 3.6). The HOCl photolysis liberates ClO , another Cl_x species which then recombines and finally generates Cl which then begins the ozone destruction processes (3.21). It was suggested that heterogeneous decomposition of CFCs on the surface of PSC particles by dissociative electron attachment (DEA) would constitute a new pathway to the contribution of the formation of the ozone hole [Lu and Sanche, 2001; Wang et al., 2008]. However, there have been a number of arguments backed up with both model simulations and observations that heterogeneous reactions of CFCs on PSCs cannot be of substantial importance to polar ozone chemistry [Harris et al., 2002; Müller, 2003, 2008]. Recently an issue of current scientific research is the findings of Katja Drdla, stating that PSCs are not necessary for polar chlorine activation, but instead liquid binary $\text{H}_2\text{SO}_4/\text{H}_2\text{O}$ sulphate aerosol particles dominate the activation. [See Tilmes et al., 2007, 2008a; Feck et al., 2008].



Chapter 4

4.0 Past ozone study

Since the discovery of the importance of atmospheric ozone, several measurements have been carried out around the globe in order to understand the behaviour of the ozone layer and more recently its depletion. The first set of measurements was ground based and later the balloon, aircraft, rocket, and satellite borne instruments were used.

4.1 Ground based measurement of atmospheric ozone

During the study of meteors by *Lindemann and Dobson in [1923]* at Oxford University they discovered that the temperature of the stratosphere increases with altitude, so they concluded that the governing process in the stratosphere must be radiative and the temperature inversion was due to UV radiation being converted into heat through ozone absorption which is in line with Hartley's prediction in 1881 [*see Khrgian, 1975*]. This discovery led to an increase in ground based research into atmospheric ozone. Although the spectrograph designed by Fabry and Buisson in 1921 was the first set of ground based instrument used to measure total ozone column, it was soon superseded by that designed by Dobson in 1924, which was cheaper, easier to build and allowed regular measurements to be made over extended time periods. Other ground based instruments earlier used and some of which are still currently in use include the M-83 ozone-meter and the M-124 filter ozone-meter, Umkehr's, and the Brewer spectrophotometer. These instruments serve as the basis for validating satellite based ozone measurements.

4.1.1 The Dobson spectrophotometer

The Dobson spectrophotometer is a double monochromator that measures the relative intensities of pair wavelengths in the Huggins and Chappuis ozone band at wavelength ranges of (300-350 nm) and (440-1180 nm) respectively, with a long-term ozone measurement precision of 1% (for the 2 sigma level). The wavelength is chosen such that one is significantly absorbed by ozone while the other is attenuated in the instrument by a calibrated optical wedge. The wedge position is adjusted until equal signals for the two beams are obtained. Measurements are made for two separate pairs of wavelengths to allow cancellation of errors due to aerosols in the atmosphere [*Dobson, 1957*]. Daily measurements have been made using a Dobson instrument at the station in Arosa, Switzerland, from 1926 to the present. Since 1957, a network of more than 30 stations has been making measurements of the total ozone column. This network is spread over much of the world but is heavily concentrated in the Northern

Hemisphere. The network of instruments is calibrated relative to a single world standard instrument, which is itself calibrated each summer at Mauna Loa. The calibration is then transferred to the rest of the instruments through secondary standard [Komhyr, 1989].

The standard unit for total atmospheric column of ozone is expressed in Dobson unit (DU), which describes the thickness of a layer of pure ozone if the total amount of ozone in the atmosphere were brought to standard conditions (293.15K and 1013hPa). For example, an atmospheric ozone column of 300 DU brought down to the surface of the earth at 0°C would occupy a 3mm thick layer of pure ozone. One DU is 2.69×10^{16} ozone molecules/cm² or 2.69×10^{20} ozone molecules/m². Although the instrument is primarily designed to measure ozone total column it can also be used to find the vertical distribution of ozone. This technique involves measurements at two wavelengths in the UV region at which ozone absorbs strongly at one wavelength and weakly at the other wavelength. This can be explained by Lambert-Beer's law which defines the direct spectral irradiance $I_o(\lambda)$ reaching the Earth's surface at wavelength λ after attenuation by column amounts in the atmosphere with absorption cross section $\sigma_i(\lambda)$ by a particular atmospheric constituents having density n

$$I(\lambda) = I_o(\lambda) \exp\left(-\int \sigma_\lambda n(x) dx\right) \quad (4.0)$$

Therefore the general relation for the calculation of total ozone from direct solar observation can be determined from:

$$\frac{I(\lambda)}{I(\lambda')} = \frac{I_o(\lambda)}{I_o(\lambda')} \exp\left(-\int \sigma_\lambda n(x) dx + \int \sigma_{\lambda'} n(x) dx\right) \quad (4.1)$$

Taking the natural logarithm, we have

$$\ln \frac{I(\lambda)}{I(\lambda')} = \ln \frac{I_o(\lambda)}{I_o(\lambda')} - (\sigma_\lambda - \sigma_{\lambda'}) \int n(x) dx \quad (4.2)$$

where $I_o(\lambda)/I_o(\lambda')$ is known from measurement of solar radiation and $\int n(x) dx$ is the absorber column amount along the effective light path, which is same as the slant column density. Direct solar measurements are limited to daylight hours when the direct solar beam is not obscured by clouds or other obstacles for a period of at least 2 min (Dobson) or 5 min (Brewer). The solar zenith angles suitable for measurement for the different spectrophotometer differ and do not exceed 72° for the Dobson and M-124 filter instruments, and 75° for the Brewer Spectrophotometer due to the different wavelengths and temperature dependence for the atmospheric constituent absorption coefficients. While the Dobson spectrometer measures relative ratios of spectral irradiance at three wavelength pairs (A: 305.5/325.4; C: 311.5/332.4;

D: 317.6/339.8nm), the Brewer spectrophotometer measure spectral irradiance at five operational wavelengths (306.3, 310.1, 313.5, 316.8 and 320.1nm), and the M-124 filter instrument measures at 302 and 326nm with the spectral band pass of 20 nm.

4.1.2 The Umkehr measurements

The Umkehr measurements are a sequence of special ozone measurements done from sunrise to sunset using a spectrophotometer under clear skies and they provide atmospheric ozone profiles at nine levels (0-49 km) with a systematic uncertainty or bias of about 15% to 20%, which is based on the assumption that there are no ozone variations within each layer. Currently a technique has been developed that enables 15 levels to be extracted from the data. The Umkehr technique is based on the ratio of zenith sky radiances of two wavelengths in the ultraviolet with one strongly and the other weakly absorbed by ozone, which increases with increasing solar zenith angles but suddenly decreases at zenith angles close to 90°. This form of measurements allow the deduction of a low-resolution vertical ozone profile [e.g., *Paetzold and Regener, 1957; Dutsch and Staehelin, 1992*].

4.1.3 UV LIDAR systems

UV LIDAR systems developed in the 1980s as well as the microwave instrument operated from the laboratory can be used to carry out measurements on and off the zenith sky through a roof hatch or dome. LIDAR instruments must be located in such a way as to avoid interference from other UV sources and can in some instances take measurements in other directions by pointing the laser beam and detector to the direction of interest, but it is usually limited to operating at night and when there is not an appreciable amount of cloud cover. This technique which is similar to that employed by the Dobson spectrometer also involves measurements at two wavelengths in the UV region at which ozone absorbs strongly at one wavelength and weakly at the other wavelength.

4.1.4 Differential Optical Absorption Spectroscopy (DOAS) Measurement

The DOAS technique is a remote sensing method that is based on absorption spectroscopy in the UV and visible wavelength range performed at moderate spectral resolution to identify and separate different species. Long light paths can be obtained from the atmosphere by using either sun or moon as the light source and even a longer light path can be realized at twilight from scattered light. The scattered light observations can be taken at all weather conditions

without significant loss in accuracy for stratospheric measurements. The intensity measured by the instrument which is weakened by absorption, Rayleigh and Mie scattering along the light path is given by:

$$I(\lambda, \theta) = a(\lambda, \theta)I_0(\lambda) \exp\left(-\int \left(\sum_{j=1}^N \sigma_j(\lambda)\rho_j(s) + \sigma_{Mie}(\lambda)\rho_{Mie}(s) + \sigma_{Ray}(\lambda)\rho_{Ray}(s)\right) ds\right) \quad (4.3)$$

where $a(\lambda, \theta)$ is the scattering efficiency, $I_0(\lambda)$ is the unattenuated intensity, $\rho_j(s)$ is the concentration of trace gas j and $\rho_{Mie}(s)$ and $\rho_{Ray}(s)$ are concentrations of Mie and Rayleigh scatterers, respectively. If the absorption cross-section does not vary along the light path s , then the equation is simplified using the slant column¹ (SC) given by:

$$SC_j = \int \rho_j(s) ds \quad (4.4)$$

inserting 4.4 into 4.3 yields

$$I(\lambda, \theta) = a(\lambda, \theta)I_0(\lambda) \exp\left(-\sum_{j=1}^N \sigma_j(\lambda)SC_j + \sigma_{Mie}(\lambda)SC_{Mie} + \sigma_{Ray}(\lambda)SC_{Ray}\right) \quad (4.5)$$

Since Rayleigh and Mie scattering efficiency vary smoothly with wavelength, they can be approximated by low order polynomials.

4.2 Balloon and aircraft measurement of atmospheric ozone

The first attempt to directly measure the vertical profile of the atmospheric ozone concentration was made by James Glaisher and Henry Tracey Coxwell on a manned balloon in Wolverhampton, England on September 5, 1862. In the experiment, they used the Schönbein method during which the balloon reached an altitude of 11 km but could only measure ozone up to an altitude of 4.8 km before it lost consciousness at greater altitudes [Hoinka, 1997]. On July 31, 1934 in Stuttgart, Regener and Regener (1934) carried out the first successful balloon-borne measurements of the vertical distribution of ozone just after the first Umkehr measurements. They recorded the solar UV spectrum in the stratosphere and deduced an ozone profile from these measurements; with the data obtained from the measurement confirming the first Umkehr observations. Balloon borne ozone sondes measure height-resolved profiles of atmospheric ozone from the surface up to the 30-35 km range in the middle stratosphere and can be operated in all climatic regions and under severe weather conditions. The sonde has a reaction chamber where ozone molecules react with the chemical solution, an air pump, a power supply, and an electronic interface that converts the raw current signal and transfers it to the radiosonde. These components are mounted in a Styrofoam box in order to protect it from

¹the total amount of the absorber per unit area integrated along the light path through the atmosphere

low temperature effects and some mechanical impact. To transfer the ozone signal to the ground receiver, the ozonesonde has to be connected to a suitable meteorological radiosonde which transfers the ozone signal, along with meteorological parameters, to the ground station, where all signals are decoded and recorded. The instrument is accurate because of its direct measurement of atmospheric ozone. Also in the early fifties, *Paetzold (1950)* developed a method for determining the vertical profile of ozone during lunar eclipses up to altitudes that cannot be reached by balloons (about 45 km).

This method involves the determination of ozone profile from the ozone absorption in the Chappius band measured at the edge of the Earth's shadow on the moon [*Paetzold, 1951*]. The first in situ measurement of an ozone profile above balloon altitudes was made on October 10, 1946 by a UV spectrograph mounted in a tail fin of an A4 rocket [*Johnson et al., 1951*]. Remote sensing observations with MW radiometers, DOAS spectrometers [*Bruns et al., 2001*] and in-situ in photometers sampling the air in the troposphere and lower stratosphere measurement [*Wang et al., 2002*] can also be performed from aircraft. The secondary ozone maximum at about 90 km, which is an important feature of the vertical ozone profile was discovered both in ozone measurements from rocket payloads and in ozone concentrations in the upper atmosphere deduced from stellar occultation measurements made from a satellite [*Miller and Ryder, 1973; Hays and Roble, 1973*]. In fact rocket measurements have been a very important scientific tool in ozone measurement [e.g., *Miller and Ryder, 1973; Vaughan, 1982, 1984; Gernandt et al., 1989*].

4.3 Satellite measurement of atmospheric ozone

The first satellite measurements of the vertical distribution of ozone in the stratosphere and mesosphere were made using the same technique similar to that of the lunar eclipse, but by replacing the moon as a reflector by an artificial satellite [*Venkateswaran et al., 1961*]. Today, several ways of measuring ozone from a satellite platform have been discovered, with each method having its advantages and disadvantages. Many past studies on middle atmospheric ozone employed satellite-based measurements in nadir-viewing geometry with e.g. the Global Ozone Monitoring Experiment (GOME), the Total Ozone Mapping Spectrometer (TOMS) and the Solar Backscatter Ultra Violet Instrument (SBUV), where each measurement displays a little variation from the other. The measurements from GOME gave total ozone columns and some other trace gases as well as vertical concentration profile of ozone with a low vertical resolution (7-10 km) [*Burrows et al., 1999*]. This low vertical resolution does not provide enough information for many scientific applications and the understanding of the stratospheric

chemistry and dynamics can mainly be achieved from observations with better altitude resolution. Equally, measurements from SBUV [Heath *et al.*, 1975] were capable of producing global maps of the total ozone column with high spatial resolution, but the retrieved ozone profiles have limited vertical resolution [*e.g.*, Bhartia *et al.*, 1996]. In this study, satellite-based measurements done in limb and occultation viewing geometry were investigated. The limb-viewing geometry gives a better altitude resolution with the line of sight (LOS) of a limb-viewing detector being a tangential path through the atmosphere. The limb is scanned vertically, and spectra are measured at different tangent altitudes, thus leading to a good vertical resolution (2-4 km). Also in the limb-viewing geometry, the stratospheric optical depth of the LOS is longer than in the nadir-viewing geometry, thus enabling greater sensitivity to small amounts of stratospheric absorbers. The occultation viewing-geometry of satellite based measurements is self calibrating and involves simple retrieval techniques, thereby providing ozone density profiles with high vertical resolution, but suffers from poor geographical coverage. In this study, the trend of stratospheric ozone was investigated with satellite observations in the limb viewing geometry with the SCanning Imaging Absorption spectroMeter for Atmospheric CHartography (SCIAMACHY) (08/2002 – date) and in the solar occultation viewing-geometry with the Stratospheric Aerosol and Gas Experiment II (SAGE II) (10/1984 – 10/2005) and the Halogen Occultation Experiment (HALOE) (09/1991 – 11/2005) represented schematically in Fig. 5.0

Chapter 5

5.0 Instrument and theory

5.1 SCIAMACHY instrument

The SCanning Imaging Absorption spectroMeter for Atmospheric CHartographY (SCIAMACHY) [Bovensmann *et al.*, 1999] was launched on March 1, 2002 onboard the European Environmental Satellite (Envisat-1) from Kourou, French Guiana. It makes nadir, limb-scatter and occultation observations (Fig. 5.0). Envisat operates in a near-circular sun-synchronous polar orbit having a mean altitude of about 800 km at an angle of inclination of 98° with a period of 100 min (about 14 orbits per day), moving with an orbital velocity of approximately 7.45 km/s over ground crossing the equator on the descending node at about 10:00 local time. It always moves slightly against the rotation of the Earth and passes close to the poles, having a repeated orbital cycle of 35 days with respect to the position of the Earth's surface and allows daily near-global measurements of the atmospheric composition from space with a vertical resolution of 3-4 km [von Savigny *et al.*, 2005b; Rozanov *et al.*, 2005]. The SCIAMACHY instrument was proposed in 1988 by the SCIAMACHY team [Burrows *et al.*, 1988] and funded by Germany, The Netherlands and Belgium. It is a UV, visible and shortwave infrared, passive and moderate-resolution imaging remote sensing spectrometer comprising 8 spectral channels covering a wide spectral range from 240-2400 nm and has a spectral resolution between 0.24 nm and 1.5 nm, with each spectral channel having a grating spectrometer with a 1024 element diode array as a detector. It achieves a full global coverage in 6 days which results in a large amount of measured data requiring the operational retrieval algorithms to be numerically efficient. Due to its well established measurement geometries, high resolution and wide wavelength range, SCIAMACHY is able to observe many different trace gases despite their low concentrations (The mixing ratios of most constituents are of the order of ppm or less). The large wavelength range is also ideally suited for the detection of clouds and aerosols. The data obtained from SCIAMACHY can be applied in the area of Global Monitoring for Environment and Security (GMES) which includes "Atmospheric Monitoring", Kyoto and Montreal Protocol verification as well as "Chemical Weather" applications.

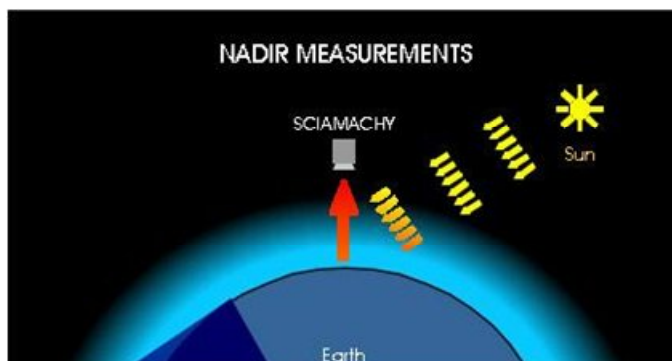


Fig. 5.0a: SCIAMACHY in nadir viewing geometry
(graphics by S. Noel)

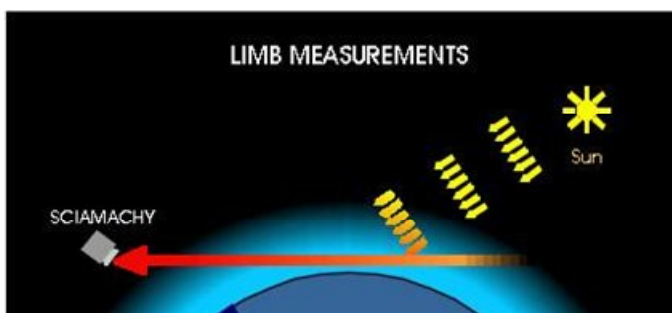


Fig. 5.0b: SCIAMACHY in Limb viewing geometry
(graphics by S. Noel)

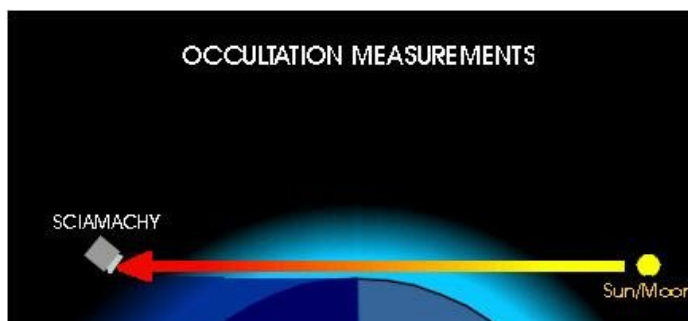


Fig. 5.0c: SCIAMACHY in Occultation-viewing geometry
(graphics by S. Noel)

5.1.1 Measurement geometries of SCIAMACHY

The multi-observational mode of SCIAMACHY has given it a good capability to obtaining a wide range of atmospheric information on trace gases, cloud and aerosol types. With the aid of the three different viewing geometries (Fig. 5.0) the total column values as well as distribution profiles for trace gases and aerosols in the stratosphere/mesosphere and in some cases the troposphere can be computed.

5.1.1.1 Nadir measurements

In this geometry, the instrument looks straightly downward in order to measure the radiance from underneath the satellite, thus recording solar radiation that has been scattered in the atmosphere or reflected from the surface. This observational mode has been successfully applied to other space borne instruments such as TOMS, BUV, SBUV SBUV/2, OMI¹ and GOME [Burrows *et al.*, 1999]. In the nadir mode, the mirror scans across-track, but the satellite moves by about 30 km within the 4.0 s followed by a fast 1.0 s back scan. The scanning procedure is repeated several times for a total duration of approximately 65 s or 80 s depending on the orbital region, with each scan covering an area on the ground of approximately 30 km along track (North-South) and 960 km across track (East-West). Therefore, the spatial resolution along track, determined by the number of readouts per scan, which is obtained from the scan speed of the mirror, the integration time of the detector, and the number of onboard coadditions of successive integration periods, is 30 km. This measurement geometry is advantageous in that, it provides accurate measurements, long time series, and good horizontal resolution. It is disadvantageous in that it cannot be used at night or over the winter poles as it requires sunlight. It also has poor vertical resolution below the ozone peak (~ 10 km), due to multiple scattering and reduced sensitivity to the profile shape. The major constituents measured typically by SCIAMACHY in nadir mode, have ground pixels sizes of 30 km x 60 km [Noël *et al.*, 2000] and the scientific data products derived from SCIAMACHY nadir spectroscopy [Bovensmann *et al.*, 1999] include O₃, N₂O, H₂O, CO₂, CO, CH₄, H₂CO, NO₂, BrO, SO₂, aerosols, and clouds (A typical nadir scan is shown in Fig. 5.0a).

5.1.1.2 Limb measurements

In the limb viewing geometry, the SCIAMACHY instrument observes the atmosphere tangentially to the Earth's surface starting at about 3 km below the horizon [Bovensmann *et al.*, 1999] (Fig. 5.0b) i.e., when the earth surface is still within the field of view of the instrument, and then scanning vertically up to the top of the atmosphere (about 100 km tangent height). At each tangent height a horizontal scan of the duration of 1.5 s is performed followed by an elevation step of about 3.3 km. No measurements are performed during the vertical repositioning. Thus, the limb observation sequence is performed with a vertical sampling of 3.3km. Although the horizontal instantaneous field of view of the instrument is about 110 km at the tangent point, the cross-track horizontal resolution is mainly determined by the integration time during the azimuthal (i.e., horizontal cross-track) scan, reaching typically

¹Ozone Monitoring Instrument launched onboard Aura on July 15, 2004 (<http://envisat.esa.int/object/>)

about 240 km. However, in this study all spectra measured during the azimuthal scans will be averaged to increase the quality of the input data, so as to achieve a cross-track resolution of about 960 km. Other instruments that use this technique for measurement of atmospheric trace elements are SME¹, SOLSE², and OSIRIS³. In this geometry, excellent spatial coverage, good vertical resolution and continuous measurement of data can be achieved. It is only hindered by its complex viewing geometry and poor horizontal resolution.

5.1.1.3 Occultation measurements

SCIAMACHY performs occultation measurements by using the elevation and the azimuth scan mirrors similar to that of the limb mode. In this mode, the instrument tracks the sun or moon during its rise or set behind the earth, thereby recording transmitted solar (or lunar) radiation for different tangent altitudes (Fig. 5.0c). The main disadvantage of the occultation measurements in general, is the limited spatial coverage, since the measurements in each orbit are only performed during sunrise or sunset. Some other space borne instruments that have been successfully used to measure trace gases as well as temperature and aerosol concentrations in the Earth's atmosphere using the solar occultation technique include the Stratospheric Aerosol Measurement (SAM-II) [McCormick *et al.*, 1979], the Stratospheric Aerosol and Gas Experiments (SAGE I, II and III) [Chu and McCormick, 1979; Chu *et al.*, 1989; McCormick *et al.*, 2002], the Halogen Occultation Experiment (HALOE) [Russell *et al.*, 1993a, 1993b], the Atmospheric Trace Molecule Spectroscopy (ATOMS) experiment [Gunson, 1992], and the Polar Ozone and Aerosol Measurement (POAM II and III) [Glaccum *et al.*, 1996]. The occultation measurements are well suited for monitoring long-term trends in atmospheric composition, because the measurement is self calibrating and relatively immune to long-term instrument degradation. It also has high photon count rates due to the brightness of the source (solar occultation), thus making it possible to achieve high signal-to-noise ratios with a relatively small instrument field of view (FOV), which allows for a high vertical resolution.

¹Solar Mesosphere Explorer (explorer 64) launched onboard Delta 2914 on October 6, 1981(Thomas *et al.*) (http://lasp.colorado.edu/mission_history/)

²Shuttle Ozone Limb Sounding Experiment launched onboard STS-87 on November 19, 1997 (<http://en.allexperts.com/e/s/st/>)

³Optical spectrograph and Infrared Imager System launched onboard Odin on February 20, 2001(Llewellyn *et al.*, 2003) (<http://www.iac.es/project/OSIRIS/>)

5.2 HALOE instrument

The Halogen Occultation Experiment (HALOE) was launched on September 12, 1991 onboard the Upper Atmosphere Research Satellite (UARS) spacecraft at an inclination angle of 57° , having an orbital period of 95.9 minutes. It started its science observations on October 11, 1991 after a period of outgassing. The HALOE instrument, being an occultation instrument is self calibrating, highly stable, very sensitive with a vertical resolution of about 1.8 km and can obtain 15 measurements during each sunrise/sunset by comparing the cold space spectra to the obtained spectra. Its temporal coverage is similar to that of the SAGE missions. It measures the vertical profiles of O_3 , HCl, HF, CH_4 , H_2O , NO, NO_2 , aerosol extinction at 4 infrared wavelengths, and temperature versus pressure with an instantaneous vertical field of view of 1.6 km at the Earth's limb. It has a global coverage of approximately 6 weeks, covering the latitude range of 80° S to 80° N, making extensive observations of the Antarctic region during southern spring. The altitude range of the measurements extends from about 15 km to 60-130 km, depending on the species, for example nitric oxide measurements extend through the lower thermosphere. Ozone is derived from absorption bands in the thermal infrared region between $9.22 \mu\text{m}$ and $10.42 \mu\text{m}$ [Russell III et al., 1993]. Examples of pressure versus latitude cross sections and a global orthographic projection for the September 21 to October 15, 1992, period show the utility of CH_4 , HF, and H_2O as tracers, the occurrence of desiccation throughout the southern hemisphere, the presence of the water vapor hygropause in the tropics, evidence of Antarctic air in the tropics, the influence of Hadley tropical upwelling, and the first global distribution of HCl, HF, and NO throughout the stratosphere. Data used in this analysis are from the HALOE V19 obtained from <http://haloe.gats-inc.com/download/index.php>. The overall goal of HALOE is to provide global-scale data on temperature, ozone and other key trace gases needed to study and to better understand the chemistry, dynamics and radiative processes of the middle atmosphere and also to study the impact of CFCs on ozone using hydrogen fluoride observations, in combination with other HALOE data.

5.3 SAGE II instrument

The Stratospheric Aerosol and Gas Experiment II (SAGE II) instrument was launched into a 57° inclination orbit on October 5, 1984 aboard the Earth Radiation Budget Satellite (ERBS) [Mauldin et al., 1985]. It orbits around the earth in a non-sun-synchronous mode at about 650 km with a nodal period of 96.8 minutes. It was initially planned to be in orbit for 2 years but was actually powered off on August 26, 2005, having measured for about 11 years. It was later succeeded by SAGE III, which was launched on December 10, 2001 onboard a Meteor-3M

spacecraft. SAGE II is aimed at providing data on the chemistry and dynamic motions of the Earth's upper troposphere and stratosphere (10-40 km). It uses the solar occultation technique to measure attenuated solar radiation throughout the 14 orbits per day (*McCormick et al., 1989, 1992*), in the Earth's limb utilizing seven channels centered at wavelengths ranging from 385 to 1020 nm, thereby observing in the Chappuis band centered at 600 nm for ozone. The exo-atmospheric solar irradiance that is used in determining limb transmittances can also be measured in each channel during each event. The measured sunlight, containing absorption signatures by trace gases and aerosols, is converted into vertical profiles of ozone, water vapor, nitrogen dioxide and aerosol extinction. The SAGE II instrument vertically scans the limb of the atmosphere during spacecraft sunsets and sunrises (about 15 sunsets and 15 sunrises each day). It was preceded by SAM II (Stratospheric Aerosol Measurement II), which has been measuring 1.0 μm aerosol extinction in the polar regions since 1978, and SAGE I, which provided near global measurements of aerosol extinction (at 0.45 and 1.0 μm), ozone, and nitrogen dioxide from 1979-1981. Since the solar occultation technique is inherently self-calibrating, accurate estimates can be made of long-term trends in the retrieved atmospheric constituents to aid in assessing their role in global change. Both SAGE I and II satellites had a low temporal and spatial coverage, tracking between typically 60° S and 60° N and obtaining a global coverage within a month. The derived profile for each measured species is typically of 1 km vertical resolution with an altitude uncertainty of $\sim 0.2\text{--}0.25$ km from the surface to 70 km (*Chu et al., 1989*).

5.3.1 Understanding the Antarctic ozone hole and PSCs with SAGE II measurements.

One of the important roles of measuring with SAGE II is in understanding the causes and effects of the Antarctic Ozone Hole. SAGE II has been used to measure the decline in the amount of stratospheric ozone over Antarctica since satellite measurements of the ozone hole began in the early 1980s. With the help of the high resolution SAGE II measurements, scientists were able to study the vertical structure of ozone in the Antarctic and, more importantly, the correlations between various trace gases. In the past studies, SAGE II measurements showed that the loss of water vapor in the region of depleted ozone was due to the formation of Polar Stratospheric Clouds (PSCs). PSCs were first noted by a team of NASA Langley scientists using another Langley satellite data set, Stratospheric Aerosol Measurement II (SAM II). SAGE II measurements showed that PSCs were also present unusually far south of the Arctic region during certain meteorological conditions, indicating that ozone destruction similar to that over the Antarctic was possible at lower latitudes. A study of the SAGE I and

SAGE II data sets showed a decrease in ozone amount in the upper stratosphere over the high latitudes of both hemispheres and in the lower stratosphere over most of the globe (Randal et al., 1999). SAGE II has been the only occultation instrument that was able to show ozone loss below 20 km globally.

5.3.2 Monitoring the effect of the Mt. Pinatubo volcanic eruption and water vapor concentration using SAGE II measurements

SAGE II aerosol data have also been used to study the large-scale motions of the stratosphere. After the volcanic eruption of Mt. Pinatubo in 1991, SAGE II measurements showed the transport of volcanic aerosols across the entire tropical stratosphere and into the middle and high latitudes in the months following the eruption [Trepte et al., 1993]. SAGE II aerosol measurements have also been used to study cirrus clouds in the tropics which are important for the understanding of cloud effects on global climate [Jensen et al., 1996]. Equally of great importance is the study of water vapor in the atmosphere with SAGE II measurements [Thomason, et al., 2004]. It is well established that atmospheric water vapor plays an important part in the Earth's radiation balance, in many chemical cycles, and it can also be used to trace the exchange of material between the upper and lower atmosphere [Schaefer et al., 2009] SAGE II has provided chemical and climate modelers with several years of high resolution water vapor measurements, which helps in better understanding of both the chemistry and motion of the atmosphere. Studies are still continuing on how varying water vapor concentrations can affect the global climate. By studying SAGE II water vapor profiles, we can determine the long- and short-term effects of variable water vapor concentrations on the temperature of the atmosphere.

Chapter 6

6.0 Variations in stratospheric ozone

During the measurement of ozone by *Dobson* in the 1920s, he observed that there was variability in the ozone column amount both on a daily and seasonal basis. He noted that the daily variability correlated with the passage of weather systems over the site of his measurements. To investigate this variation, he distributed his instruments to a number of places in order to carry out simultaneous measurements on a daily basis. In the analysis, he discovered that there was a regular variation of the total column amount of ozone with the weather systems. That is, the ozone amount anti-correlated with the air pressure, showing an increase when the air pressure falls and a decrease when the air pressure rises. The interaction of processes such as ozone production, loss, and transport that governs ozone variability observed on different time scales helps to determine both the amount of ozone in the stratosphere as well as its distribution with latitude, longitude and altitude [*WMO, 1995, 1999*]. The variations in the ozone amount based on short-term, seasonal, inter-annual and long-term time scales are due to continuous motion in the atmosphere. In the lower atmosphere (troposphere and lower stratosphere), ozone variability is chiefly due to the dynamical (transport) process [*WMO, 2003, Chipperfield, 2003*] where ozone acts as a tracer of atmospheric motion while in the upper stratosphere, the variability is mainly due to the photochemical processes, which involves the creation and destruction of ozone [*e.g. Garcia and Solomon, 1983; Randall et al., 1995*]. Ozone in the lower atmosphere has a longer lifetime than ozone higher up because of the screening out of the ultraviolet radiation that drives ozone photochemistry by the ozone higher up in the stratosphere.

6.1 Short-term variability

Short-term variability is used to describe the day-to-day and week-to-week variation in the column amount of ozone due to the effect of the passage of the weather systems as in the lower atmosphere or due to photochemical processes as in the upper stratosphere which could lead to different effects such as diurnal variations, variations in solar ultraviolet radiation, temperature driven variations, and particle precipitation events that originate from electromagnetic storms on the sun.

6.1.1 Passage of the weather system

The transport of ozone in the lower atmosphere (troposphere and lower stratosphere) is associated with the dynamics of motion in this part of the atmosphere. In the stratosphere, the direction of flow of wind in the mid-latitudes is westerly during winter and easterly during summer with the passage of a winter weather systems equivalent to the superposition of a secondary air flow on top of the overall westerly flow. In addition to the overall flow of air, the motion of individual air masses (advection) can be followed if we know the particular temperature, moisture content, and amounts of the trace gases (e.g., ozone) in different air masses. The motion of air in the troposphere and stratosphere is driven by pressure gradients. In a high pressure region, the air in the tropospheric column sinks downward thereby resulting in the compression and heating of the air but above the tropospheric high pressure system, the air rises and settles in the stratospheric column near the bottom of the stratosphere and is later removed from the column at higher altitudes [Narayana *et al.*, 2003]. Since the ozone mixing ratio in the lower stratosphere increases with increasing altitude, the air brought into this column has less ozone than the air being removed, thereby leading to a decrease in the amount of ozone in the column, thus accounting for the decrease in ozone amount within the high pressure region. The opposite is the case with a low pressure region where the ozone amounts are increased. These variations only lead to temporary redistributions of ozone with no net gain or loss. The slowness of the photochemical reaction in the lower stratosphere is the reason why transport processes are responsible for most of the observed variations in lower stratospheric ozone with a decrease in a high pressure region balanced by an increase in surrounding regions.

6.1.2 Diurnal variation

The daily variation in the amount of ozone in the upper stratosphere (above 40 km) is due to the reduction in the photochemical replacement time (PRT) as a result of low amount of ozone in the region [Tuck, 1977, Herman, 1979, Groves and Tuck, 1980 Pallister *et al.*, 1983]. During the day, UV radiation of wavelength less than 240 nm splits apart oxygen molecules to form atomic oxygen, which then rapidly reacts with another O₂ molecule to form ozone. After sunset, the photolysis of O₂ is shut off, and all the available O atoms are converted to ozone molecules in three body reactions that occur at a very fast rate. As the Sun rises, some of the ozone molecules are broken down by UV radiation at wavelengths less than 320 nm and some also react with O atoms to reform oxygen molecules (3.1d). Both the photolysis of O₂ (3.1a) and the reaction of O with O₃ (3.1d) are relatively slow processes compared to O₃ photolysis

(3.1c) and the reaction of O with O₂ molecules (3.1b). At altitude of 40 km, there is not much daily variation in the amount of ozone during the day as there is a balance between production and loss in ozone but when the sun sets, both production and loss are turned off.

6.1.3 27 day solar rotation

The sun rotates with a 27-28-day period, so the ultraviolet radiation from the sun is modulated by this rotational period. Occasionally, two active sunspot regions occur on opposite sides of the sun thereby leading to a 13-day modulation of ultraviolet radiation which directly affect ozone photochemistry and even the ozone column amount [DeLand and Cebula, 1998]. The photolysis of O₂ and O₃ leads to the production of atomic oxygen which can either react directly with O₃ or with any of the oxides of hydrogen, nitrogen, chlorine, and bromine (3.5-3.10). Thus, the photochemical reaction at the upper stratosphere leads to variations in the photolysis rate of O₂ and O₃.

6.1.4 Variation in temperature

Although the upper stratosphere is dominated by photochemical production and loss processes, dynamical variations also produce short-term variations. Planetary waves propagating upward from the lower atmosphere grow in magnitude as altitude increases thereby leading to variations in temperature which then affect the photochemical reaction rates, because the reaction rate coefficients that determine photochemical loss rates are temperature dependent. As mentioned above, the effect of temperature on ozone photochemistry is not only restricted to pure oxygen reaction but also has effect on catalytic reactions involving various oxides of nitrogen, hydrogen, chlorine, and bromine (3.5-3.10). The nitrogen oxide catalytic cycle has a similarly strong dependence on temperature as the pure oxygen case while the hydrogen, chlorine, and bromine oxide catalytic cycles each have much weaker temperature dependence. The temperature dependence on ozone photochemistry is such that the loss rate increases with increasing temperature. This means that ozone amounts will decrease when temperatures increase and are thus anti-correlated with temperature. This effect becomes strongest during winter when wave activity propagating into the stratosphere is strongest [Singleton *et al.*, 2005].

6.1.5 Solar proton events

Solar storms lead to ejection of large amounts of high energy protons that can penetrate the Earth's magnetic field near the poles [Mewaldt *et al.*, 2005]. These protons penetrate into the atmosphere, typically up to the 40 to 80 km layer, causing ionization of air molecules. As the ionized constituents recombine, they produce nitrogen and hydrogen oxides which can affect ozone through the NO_x [Garcia and Solomon, 1994, Crutzen, 1970, 1971] and HO_x [Bates and Nicolet, 1950] catalytic cycles. For the HO_x catalytic cycle, the effects are short lived because the hydrogen oxides which cause the primary ozone loss recombine within hours whereas the effects of nitrogen oxides can persist for several months.

6.2 Seasonal variability

In the upper stratosphere, the seasonal variability of ozone concentrations is driven by the seasonal variation of solar UV intensity, where during the late summer months ozone maxima occur due to an enhanced photochemical production [Brasseur and Solomon, 1984], but in the lower stratosphere, photochemistry is much slower, owing to reduced UV flux, so transport of ozone by large-scale atmospheric motions becomes important [Newman *et al.*, 2001]. The mid-latitude total column ozone exhibits a strong seasonal variation which is at its maximum in late winter or early spring and at minimum in late fall [Rood *et al.*, 2000]. The primary driver of the springtime maximum in total ozone is the transport of ozone rich air from the tropics towards the poles during winter when the photochemical time constant for ozone is long because of effective shielding of ozone in the lower stratosphere by ozone above and also because the solar angle becomes low at high latitudes during winter. But the question now is why is ozone transported to the poles during winter? This is because the primary circulation of the lower stratosphere driven by the dissipation of wave disturbances propagated upward from the troposphere is upward in the tropics and downward/poleward at the mid and high latitudes [Cooper *et al.*, 2005]. This large-scale wave (Rossby waves) disturbance with a spectrum of spatial and temporal scales generated in the troposphere by flow over mountain ranges and across the temperature contrast of land-sea interfaces is filtered in the stratosphere with only the larger scale waves propagating westerly into the stratosphere during winter. But as summer approaches the solar angle increases and also the large-scale waves stop propagating into the stratosphere as the direction of the wind in the stratosphere becomes easterly thereby leading to a decrease in the ozone concentration which gets to a minimum during late fall and picks up again when winter returns.

6.3 Inter-annual variability

Inter-annual variability corresponds to the variation in the annual distribution of the ozone amount which could be regular such as the Quasi Biennial Oscillation (QBO) or irregular such as in The El Niño-Southern Oscillation (ENSO), the 11-year solar cycle and volcanic eruption.

6.3.1 Quasi-Biennial Oscillation (QBO)

The Quasi-Biennial Oscillation is a reversal of the regular west-east winds in the tropical stratosphere that occurs approximately every 26 to 30 months [Baldwin *et al.*, 2001], due to the vertical propagation of waves from the tropical troposphere into the lower stratosphere. The QBO does not only change the circulation in the tropics, it also indirectly causes changes at the middle and high latitudes [Fleming *et al.*, 2002]. This variation in the propagation speeds of the extra-tropical waves also strengthens the Brewer-Dobson circulation. During the late winter months, when the Brewer-Dobson circulation is at its strongest, air from the tropics is transported towards the winter pole, which accounts for the large ozone concentration increments in the middle and lower stratosphere [Hasebe, 1980; Bowman, 1989].

6.3.2 The El Niño-Southern Oscillation (ENSO)

ENSO is a global event that arises from large-scale interaction between the ocean and the atmosphere, leading to large variations in equatorial Pacific Ocean surface temperatures within a period of 4-7 years between episodes. Normally, the waters of the Eastern Pacific Ocean near South America are quite cool as a result of upwelling ocean currents due to east to west transverse of the tropospheric trade wind in this region. However, in an El Niño period, the trade winds weaken, allowing the warmer waters of the Western Pacific to migrate eastward. This change in sea surface water temperature causes large-scale shifts in the global circulation patterns in the troposphere and lower stratosphere which equally affects the transport of ozone in these regions. There is a strong relationship between ENSO and variability in the southern hemisphere general circulation features [Shiotani, 1992, Zerefos *et al.*, 1992]. During La Nina the polar vortex is stronger and displaced more off the pole, the ozone croissant¹ (OC) becomes very strong between 40-60°S, and there are more PSCs and lower temperatures in the polar vortex above 16 km while during El Nino the polar vortex becomes weaker, more centered on the pole, midlatitude ozone is arranged in rings, and there are fewer PSCs and warmer temperatures in the polar vortex above 16 km [Collimore *et al.*, 2003]. This interannual variability is in contrasts with the strong longitudinally-focussed outflow from Indonesia during La Nina with the more longitudinally-extensive outflow events during El Nino.

¹Ozone contour shape of monthly mean ozone around 50°S between May and November

6.3.3 Volcanic eruptions

Explosive volcanic eruptions [Altorio *et al.*, 1992, Beig *et al.*, 2002, Stenchikov *et al.*, 2002] can inject large amounts of material such as chlorine, sulfur dioxide (SO₂) and some other compounds directly into the lower stratosphere which affect the content of ozone in the stratosphere. The ejected chlorine, although in minor proportion, enhances the catalytic destruction of ozone, while the SO₂ is converted to sulfate aerosol which provides the catalytic surface on which nitrogen and chlorine are converted from reservoir species to active form that begins the ozone destruction process.

6.3.4 11-year suns spot cycle

The output of solar ultraviolet radiation is influenced by magnetically active regions on the sun that occur intermittently in sunspots (cooler regions on the sun) during which the UV output increases as the sunspot activity increases. The sunspots occur in a quasi-regular 11-year cycle and the period of the greatest sunspot activity during the 11-year cycle is called the solar maximum at which certain wavelengths of UV radiation are enhanced due to the occurrence of numerous active regions, while the period when sunspot activity is at its least is a solar minimum at which the active region and the 27 day cycle disappears and the solar UV radiation comes to a minimum [Angel, 1989, Hood and McCormack, 1999]. The effect of sunspots on solar ultraviolet radiation output depends strongly on the particular wavelength of ultraviolet radiation [Dessler *et al.*, 1998] and it occurs in clusters on one side of the sun during solar maxima.

6.4 Long-term variability

This is the variations with time scales typically on the order of decades which are due to a trend or gradual build-up in the amount of ozone-destroying substances in the stratosphere. The most important influence on the long-term variability of stratospheric ozone is the introduction of significant amounts of chlorine into the stratosphere from anthropogenic chlorofluorocarbons (CFCs) (*see page 21*). In order to determine any long-term ozone trend we need to remove the cyclic variations in ozone and check whether or not the data set is long enough to determine the difference between real and cyclic variations with periods longer than the data set since some unknown factors that can contribute to a variation with a period longer than the period of our record might cause us to conclude erroneously about the existence of a long-term trend in the data [Newchurch *et al.*, 2003, Steinbrecht *et al.*, 2003, 2006]. To be

CHAPTER 6. VARIATIONS IN STRATOSPHERIC OZONE

certain that there are no major unresolved long-term variations such as the solar activity we need to understand all of the observed variations and attribute them to physical processes.

CHAPTER 7.

7.0 Results and discussion

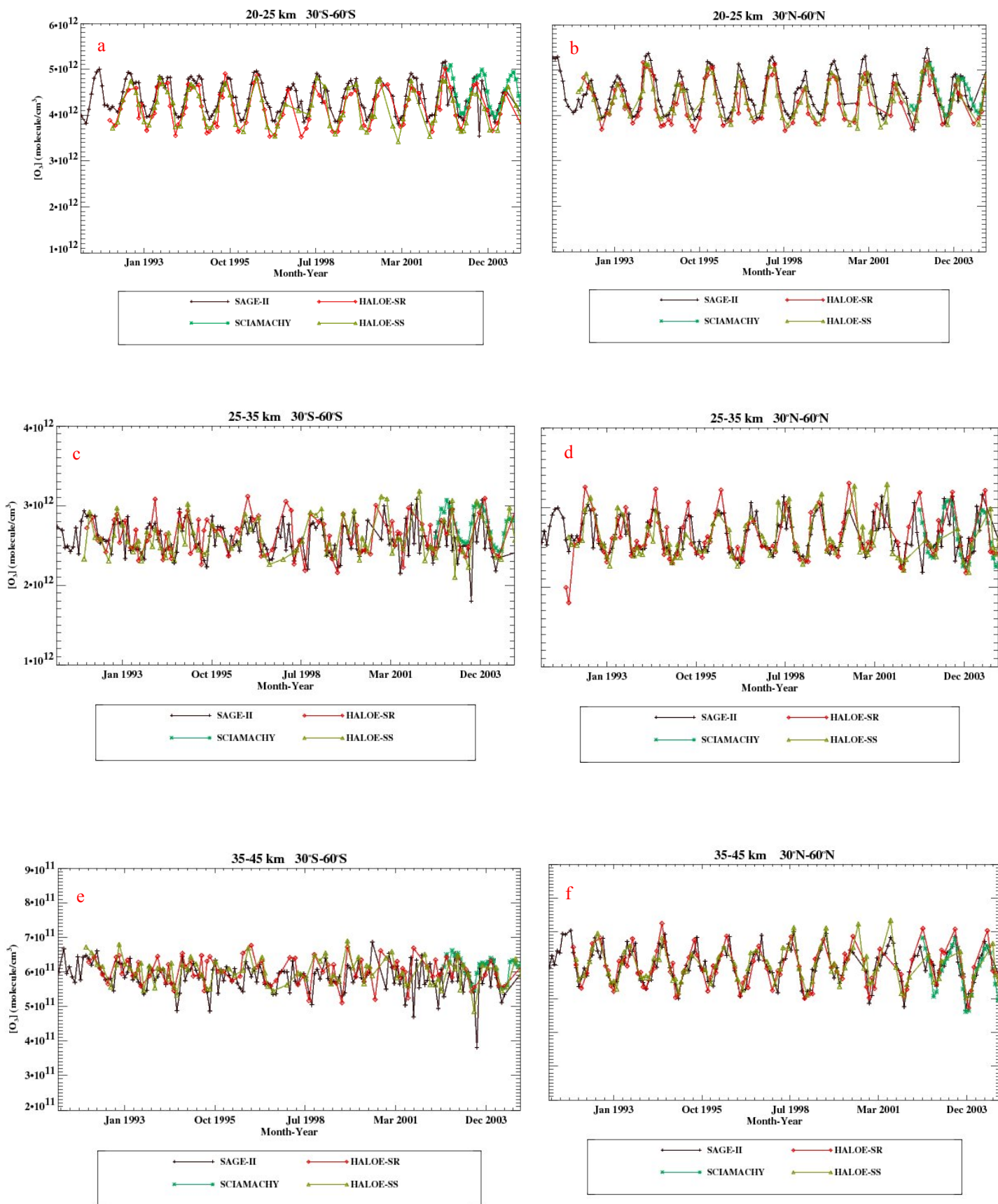
7.1 Determination of the monthly mean

To analyze the trend of ozone, the monthly profiles from each of the satellite instruments were formatted on the same altitude grid and grouped into altitude and latitude bins. The considered altitude bins are 20–25 km, 25–35 km, and 35–45 km, while the considered latitude bins are 60° S–30° S, 30° S–30° N, and 30° N–60° N. The essence of the choice of these latitude and altitude bins was to avoid some uncertainties. For example, below 20 km there are retrieval issues in some data sets due to heavy levels of aerosol loading, atmospheric variability (strong seasonal variation in trends over the northern mid-latitudes during winter and spring) and Rayleigh scattering effects. While above 45 km, much care is needed in order to account for large non negligible diurnal variability in ozone. Also, the choice of latitude bins from 60°N to 60°S was made in order to avoid the use of profiles that may be situated inside the winter polar vortices where the concentration of ozone may be low. To remove unrealistic or erroneous profiles, SAGE II data sets were screened by excluding profiles that were flagged for high aerosol optical depth at 1020 nm (mostly the period after the 1991 Pinatubo eruption) thereby showing unrealistically high ozone values or a failure of the ozone retrieval routine [see Rind *et al.*, 2005]. For the SCIAMACHY and HALOE data sets no additional screening seemed necessary but only unrealistic spikes in the HALOE error estimates were removed. The zonal mean monthly mean profiles for each of the instruments were obtained by averaging all satellite profiles in each of the nine altitude/latitude bins (eqn. 7.0). This was done in order to reduce measurement error or noise from the different instruments and the plots of the resulting profiles are shown in Fig 7.0.

$$M_{(mean)(i,j,k)} = \frac{1}{N_{ijk}} \sum_{n=1}^{N_{i,j,k}} M_n \quad (7.0)$$

Where i, j are the altitude/latitude indices, k is the month index, N is the number of profiles in a given month, and M is the ozone concentration.

CHAPTER 7. RESULTS AND DISCUSSION



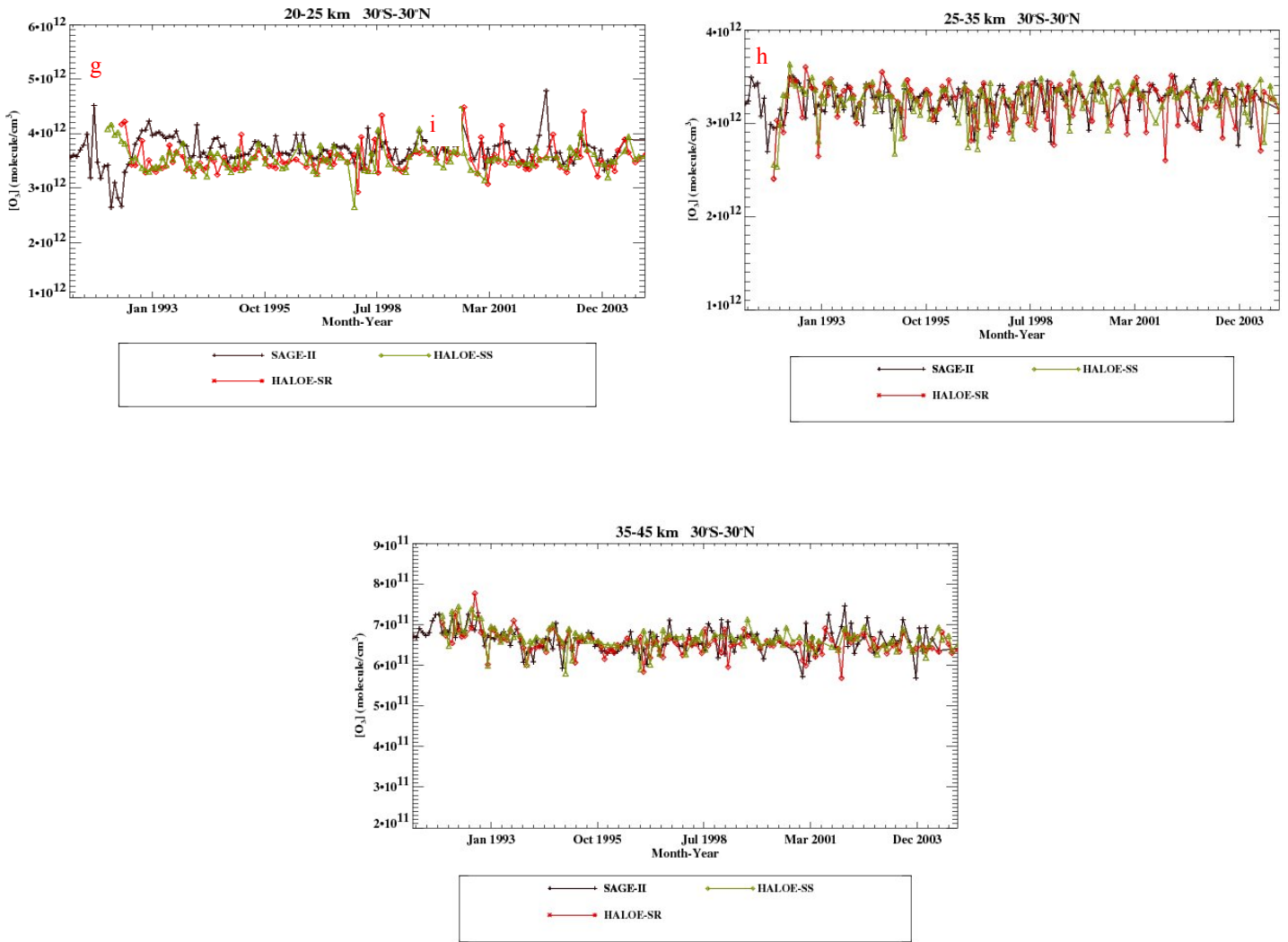


Fig 7.0: The monthly mean ozone concentration averaged over different altitude and latitude bins

The monthly mean plots for all instruments (Fig. 7.0) show the time series of SCIAMACHY in green, HALOE SR in red, HALOE SS in yellow-green and SAGE-II in black. The plots show quite good agreement between all three instruments within the chosen altitude and latitude bins. Although the SCIAMACHY instrument measurements were for a short period of time, the other two instruments show good agreement. When the SAGE II and HALOE data sets were compared at the tropics between October 1991 and March 2004 (Fig 7. 0 (g, h, i)), there was a noticeable decrease of ozone till about 1997 especially at the mid-latitudes from 35-45 km. Although data was filtered for aerosol artifacts, large values of these artifacts still appear to persist in SAGE II data especially in the 20-25 km altitude bin (Fig 7.0g) where there were occasional large mean monthly values, so some of the values that showed unrealistic values for ozone concentration from the instrument mostly between 1991 and 1994 were removed. It is

also observed from the plots that the ozone concentrations in the northern hemisphere are higher than those in the southern hemisphere with each of the individual time series having some variability. Moreover, the seasonal variation in ozone concentrations is more pronounced in the northern hemisphere compared to the southern hemisphere, particularly for the 35–45 km altitude bin. So in summary it has been established that the monthly means from each instrument are generally consistent with each other with low biases during overlapping periods.

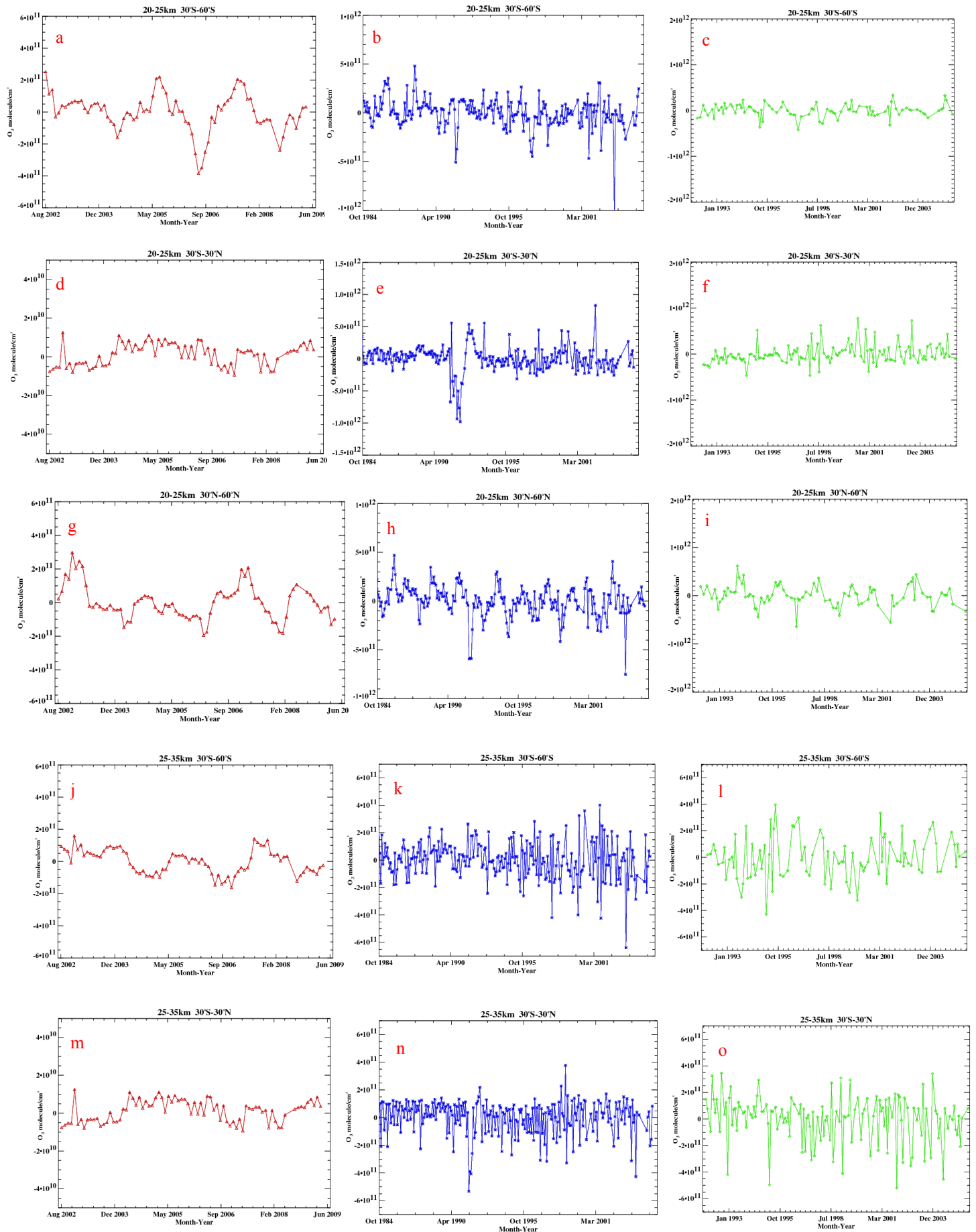
7.6 Determination of ozone anomalies

Some of the variations observed in the individual time series are cyclic in nature associated mainly with the seasonal, QBO and solar cycles, where the main contribution is due to seasonal variation. To remove the seasonal variation from the individual zonal mean monthly mean profiles, a similar approach adopted by *Newchurch et al.* [2003], *Steinbrecht et al.* [2004, 2006, 2009] and *Jones et al.* [2009], was carried out, in which the monthly ozone anomalies were calculated by first removing the annual cycle. This was done for each of the instruments by finding the difference between each monthly mean value from their corresponding average (climatological) annual cycle. For example, in the calculation of the SAGE II anomalies, the annual cycle was first calculated by computing the mean of a particular month (e.g. January mean value calculated from all January from 1984-2005). This computed mean was later subtracted from each individual SAGE II January mean concentrations (eqn. 7.1). Although the anomalies obtained still have some fluctuations associated with the QBO and solar cycles, the contributions of these processes are not so large in the region of interest (35-45 km).

$$M_{(anomaly)_{(i,j,m)}} = M_{(mean)_{(i,j,m)}} - A_{(cycle)_{(i,j)}} \quad (7.1)$$

where $A_{(cycle)}$ is the average annual cycle and i is the particular month within the period (Jan.-Dec.). The anomalies were calculated individually for all the three instruments data sets on all altitude and latitude bins so as to remove systematic biases between individual data sets. The plot of the anomaly from the individual instrument (Fig. 7.2), the grouped all instruments anomalies (Fig. 7.3) and the smoothed anomalies (Fig. 7.4) show a good trend of ozone and instrument agreement.

CHAPTER 7. RESULTS AND DISCUSSION



CHAPTER 7. RESULTS AND DISCUSSION

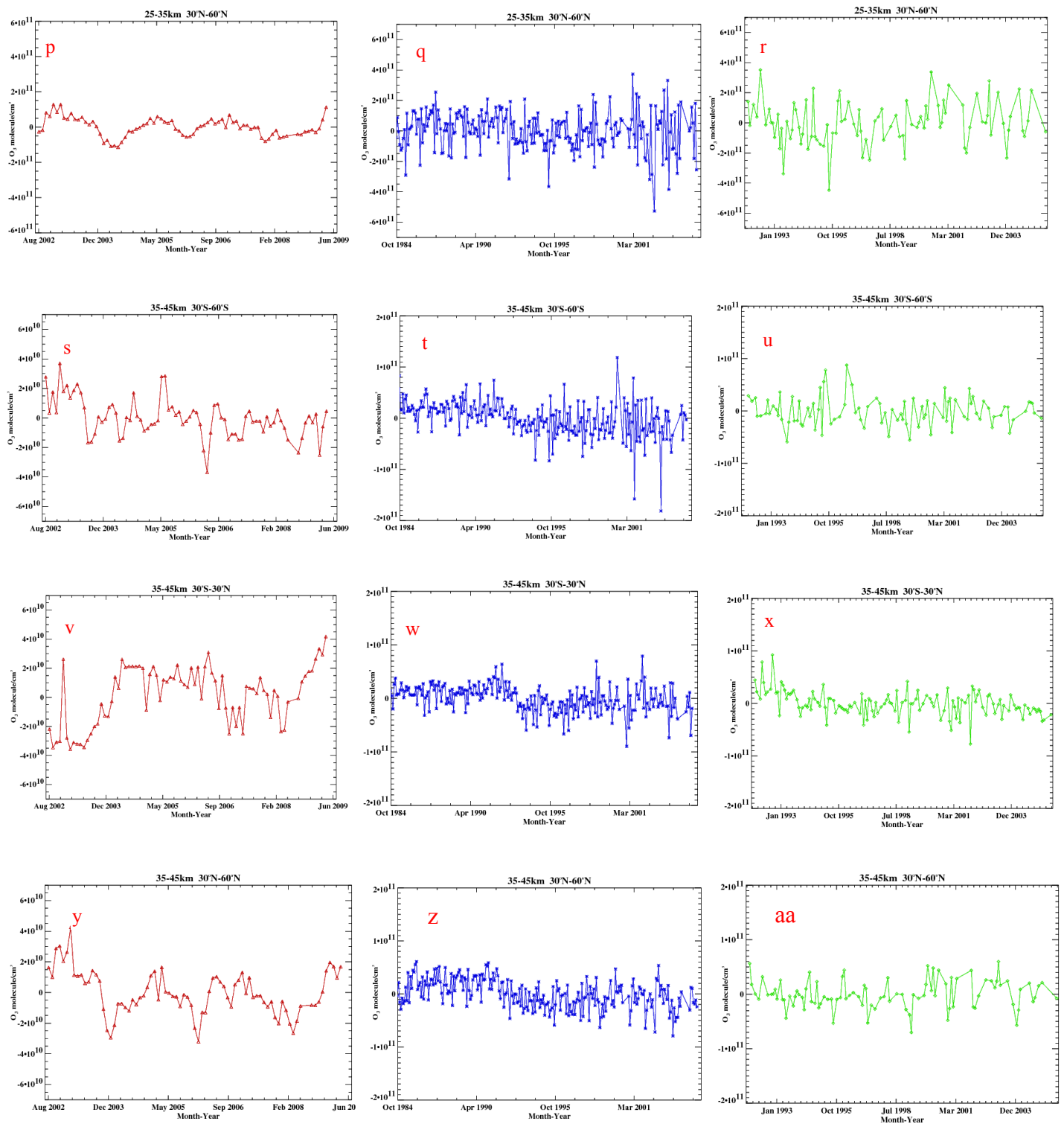


Fig 7.1 Ozone anomaly from the different instruments for different altitude and latitude bins; SCIAMACHY (left panel), SAGE II (middle panel), HALOE (right panel)

Fig 7.1 shows the ozone anomaly from each of the three instruments at the nine altitude/latitude bins. The anomalies from the SAGE II instrument (middle panel in blue) which covers a longer time period than all the three instruments shows a clear variation in the amount of ozone mostly at the 35-45 km altitude bin at all the considered latitude bins (Fig 7.1 t, w, z), such that within this altitude bin we can already identify evidence of recovery or at least stagnation of the decrease of ozone. In the 20-25 km altitude bin for latitudes within 30°S-30°N (Fig 7.1e), there was a sharp decrease in the ozone amount around 1991 after the Mount Pinatubo eruption. The mid-latitudes of the lower stratosphere at both the Northern and Southern hemisphere, measurement from SAGE II also showed declines of up to 10 % by 1995 between 35 and 45 km altitude but this decrease is no longer evident in the last decade [Steinbrecht *et al.*, 2009 , Jones *et al.*, 2009] .

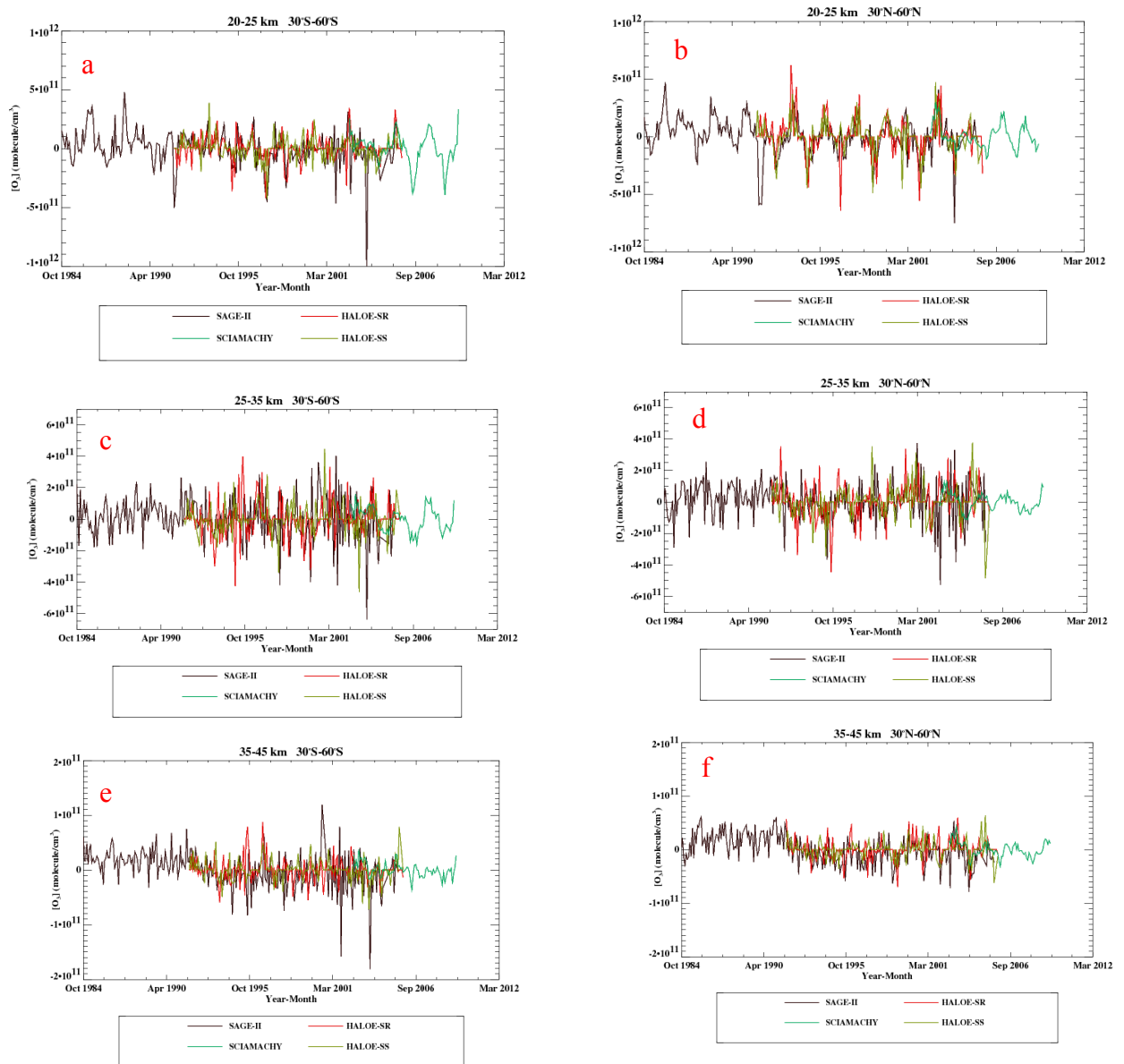
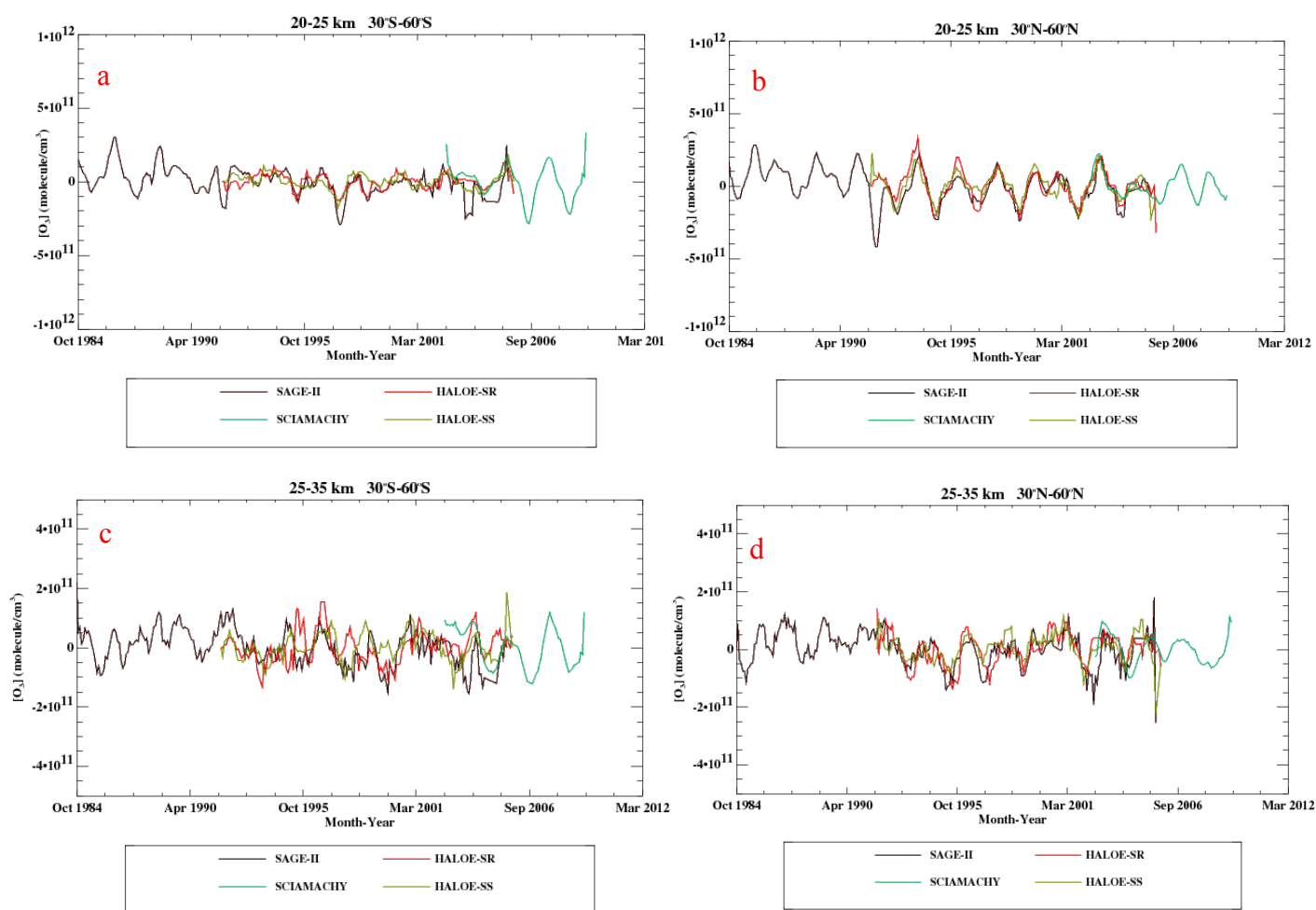


Fig 7.2: Ozone anomaly from all three instruments

CHAPTER 7. RESULTS AND DISCUSSION

When the anomalies from all the three instruments are plotted together (Fig 7.2), quite a good agreement between all instruments at all the altitude/latitude bins is observed, with the downward trend at the 35-45 km recovering or stagnating after 1997. To fully understand and show how the trend analysis depicts the variation of the global stratospheric ozone, the anomalies were smoothed with a five month boxcar (Fig 7.3). The large inter-annual variation in the Southern Hemisphere mid-latitudes and the mid latitude ozone depletion in the Northern Hemisphere in the 1990s, could be due to the dilution of the ozone depleted polar air. Also at the northern hemisphere mid-latitudes the QBO signature is clearly visible basically throughout the entire period investigated.



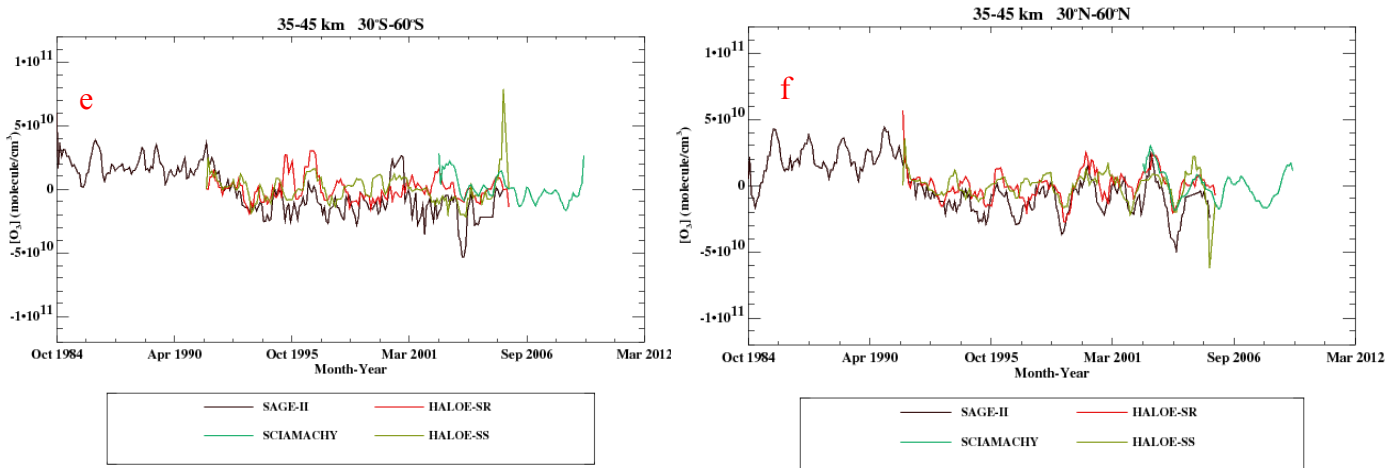


Fig 7.3: Smoothed ozone anomalies from all three instruments

7.2.1 Offset Corrected anomalies

To minimize the difference between the individual anomalies and align those that overlap in time, we performed an offset correction (Fig 7.4). One important factor for the method to work is that each individual data set must overlap with at least one other data set within an overlap period of typically a couple of years. As the primary aim of this thesis is to investigate the trend of stratospheric ozone, special focus was placed on the 35–45 km altitude bin, since it has been confirmed that the largest estimates of ozone loss (6–8%/decade) occurs in the upper stratospheric mid-latitudes, typically between 35–45 km [Newchurch *et al.*, 2003; Steinbrecht *et al.*, 2003, 2004; Cunnold *et al.*, 2004], due to the efficiency of ClO_x catalytic ozone destruction at this altitude bin. So it was considered important first to check the effect of a reduction in the stratospheric chlorine loading on ozone destruction. To correct the offset biases for each of the instruments time series, the mean ozone concentration was determined for the period of January 2003 to August 2005 (for which measurements from all three instruments are available) and the derived differences between SAGE and HALOE, as well as SAGE and SCIAMACHY were used to correct the HALOE and SCIAMACHY time series such that the mean concentration for the period mentioned above were identical for all 3 instruments. The average value (green plot in Fig 7.4) for all observational data sets shows a good correlation with the individual data sets. In addition to the satellite data sets used, the monthly mean ozone profiles from multi-year simulations of twelve state-of-the-art chemistry-climate models were used. These runs which is part of the Chemistry Climate Model Validation initiative [CCMVAL, <http://www.pa.op.dlr.de/CCMVAL/>, Eyring *et al.* 2006, WMO 2007], has all simulations which assumed increasing source gases (CO_2 , N_2O , CH_4 , and CFCs),

realistic sea-surface temperatures, 11-year solar-cycle and QBO. From the CCMVal runs, the zonal mean monthly mean ozone anomalies at the altitude and latitude bins of 35-45 km and 30°-60° respectively on both hemispheres over the period of 1984–2009 were considered. These Anomalies were averaged over all models to form a multi-model mean, which was further smoothed by a 24 month running mean. This running mean, together with the ± 2 standard deviation (gray underlay plot in Fig 7.4c, d) of all modeled monthly mean anomalies over the 24 month window, gave a good representation of the range of upper stratospheric ozone anomalies simulated by the CCMVal models.

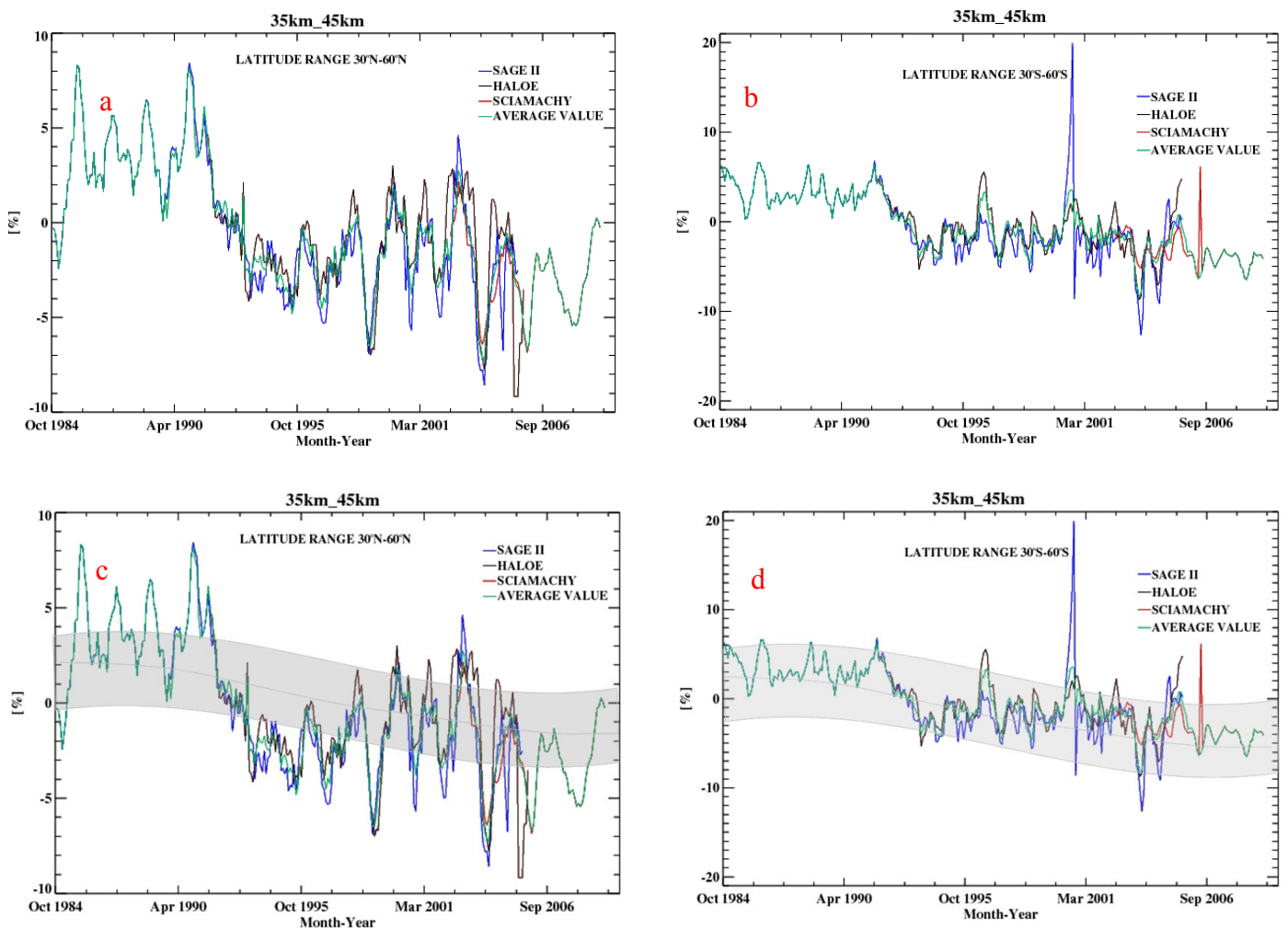


Fig 7.4: Combined and offset corrected anomalies; No CCMVAL model simulations plot (a, b), CCMVAL model simulations plot (c, d)

7.3 Turn around event

Lastly, the ozone trends in each latitude/altitude bin was estimated [Reinsel et al., 2002a, Jones et al., 2009] using the assumption that if there is a change in trend, the trend line will be both linear and continuous Reinsel et al. [2002a]. As it has been suggested that a turn around point for ozone occurred sometime between 1995 and 1997 due to the recorded declines of HCl and HF concentrations, in our analysis we assume that the turn around or break point year in the ozone trend occurred in January 1997 [Steinbrecht et al., 2006, WMO, 2006, Newchurch et al., 2003, Cunnold et al., 2004, Jones et al., 2009]. It is most likely that this turn around point will be firstly seen in the upper stratosphere where halogen compounds responsible for ozone destruction are broken down by strong UV light [Jucks et al., 1996] and should also be later observed in the lower stratosphere as the halogen gases are slowly phased out. This particular date is thought to be the nearest whole year when equivalent effective stratospheric chlorine (EESC) reached its peak before its slow decline in the extra-tropical lower-middle stratosphere based on a 3 year time lag of mean aged air [Newman et al., 2007]. However, an assumption that 1997 is the turn around time for all latitudes and altitudes may not be fully established as there are variations in dynamics and chemistry with time and space thus implying that the turn around time may differ. A careful section of this turn around point is necessary as a shift in the turn around year by just one year or even a few months can give vast differences in trend magnitude both before and after this defining time. Several attempts have been made to accurately define a turn around time using only ozone time series. This includes a linear trend that is continuous [Reinsel et al., 2002a] and a non linear trend using the cumulative sum (CUSUM) method [Reinsel et al. (2002b) as well as Newchurch et al. (2003), and Yang et al. (2006)]. The CUSUM method investigates how the anomalies deviate from the extrapolated trend line while a change in the linear trend characterizes an explicit temporal path. CUSUM studies suggest that the turn around time is typically around the end of 1996 for northern mid-latitudes and from the tropopause up to 45 km. Calculations suggest that a change from a negative trend to a less steep trend or positive trend can take a few years, but does include a linear trend prior to and after the turn around period. So our choice of the linear trend appeared justify although in our analysis we saw that the turn around point occurred earlier than 1997. An easy way to analyze the linear trend method is to use a chi square or maximum likelihood test, which examines the white noise before and after the break date, where the year with smallest χ^2 value indicates the closest time to a possible break in trend. This is justified as we expect smaller stochastic errors when the residuals are closest to the trend model.

7.4 Trend analysis

Fig. 7.5 illustrates the trend line (red line) for the southern and northern mid latitudes at the altitude bin of 35-45 km before and after the turn around point which was calculated from the all instrument average time series (green line). The plot shows a clear decrease in ozone values from 1984 until 1997 as indicated by the all instrument average of $-6.0\%/decade (\pm 0.7)$ in the $30^\circ N - 60^\circ N$ latitude bin and $-5.3 \%/decade (\pm 0.7)$ in the $30^\circ S - 60^\circ S$ latitude bin, which is close to previous findings [Newchurch et al., 2003, Cunnold et al., 2004, Steinbrecht et al., 2008, Jones et al., 2009]. After the turn around point the trend also shows a slowing down of ozone depletion to $-1.4\%/decade \pm 0.7\%$ in the $30^\circ N - 60^\circ N$ latitude bin which is more than the estimates reported by Steinbrecht et al. (~ -2.5 to $0.9\%/decade$). In a paper by Steinbrecht et al. [2006], a significant positive trend after 1997 (at the 2 sigma level) at tropical and southern mid-latitudes between 35 and 45 km was obtained. In our study we obtained a reduced decrease in ozone at a one sigma level ($-2.9\%/decade \pm 0.7\%$), with the sign being different from the one calculated by Steinbrecht et al. [2008] ($3.35\%/decade \pm 2.88\%$) and Jones et al. [2009] ($3.4\%/decade \pm 2.1\%$). The slight difference between the obtained trend value and those of previous findings could be due to the length of period of data used and the different number of instrumental data sets used. For example, the Jones et al. [2008] study also used the Odin/OSIRIS and the Odin/SMR data sets for the period 2001 to present. Moreover, studies show that SUBV shows a more pronounced downward trend before the turn around point as compared to SAGE II, and the SBUV time series was not used in this analysis. The plots also show consistency between HALOE and SAGE II during the overlapping periods.

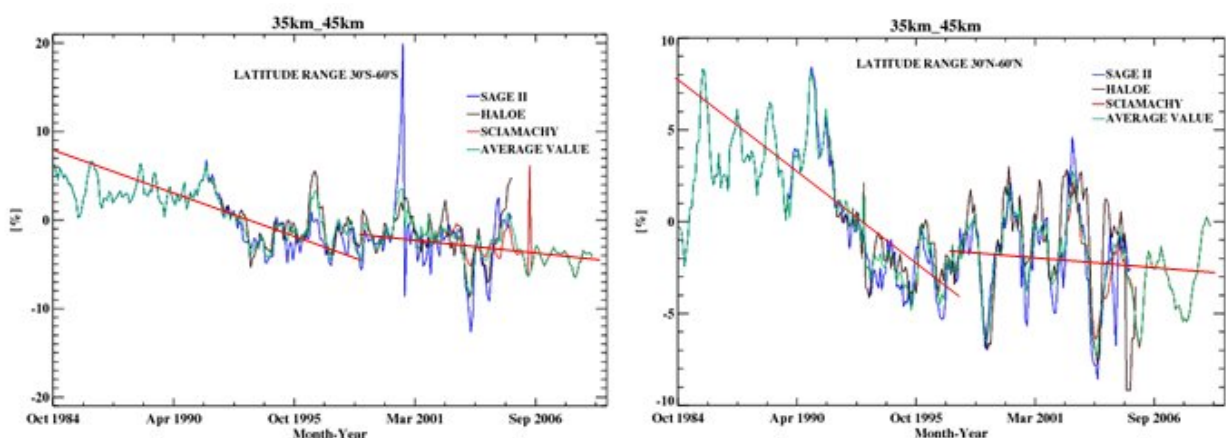


Fig 7.5: Combined and offset corrected anomalies with the best fit trend to all instrument average before and after the 1997 (red line)

7.5 Summary

The long-term evolution of ozone was examined on nine latitude/altitude bins covering 60° S and 60° N and 20-45 km respectively. Seasonal variability was removed from each of the instruments monthly mean time series and the remaining residual from all the individual instrument were combined in order to construct a weighted all instrument mean. Each of the individual satellite monthly mean time series show generally a good agreement with systematic biases typically less than 10% during overlapping periods. For the two latitude bins considered during the assumed turn around point of 1997, significant trend was observed similar to those reported by the WMO [2006]. The decline observed at the southern hemisphere between 35-45 km ($-5.3 \text{ \%/decade} \pm 0.7$) is lower than that observed in the northern hemisphere ($-6.0\text{\%/decade} \pm 0.7$). After 1997, it was found that in both hemispheres considered, the decline has slowed down. If ozone continues to increase at the current rate for these specific bins then pre 1980 values would be reached in approximately 60 years.

Finally, although the all instrument average can provide a more precise estimate of trend as it can combine differing time domains as well as reduce the stochastic noise from individual data sets, a better trend analysis can only be made if the residual time series is long enough and is characterized by low residual noise, and low variability. Shorter time series is also necessary as they have little long-term drift. As current ozone levels are typically 10–12% lower than pre 1980 values in the upper extra-tropical stratosphere, it take quite a long time before it can reach the pre 1980 values as our post 1997 trend gave negative trend on both hemispheres.

REFERENCES

- Anderson, J., J. M. Russell III, S. Solomon, and L. E. Deaver, Halogen Occultation Experiment confirmation of stratospheric chlorine decreases in accordance with the Montreal Protocol, *J. Geophys. Res.*, *105(D4)*, 4483–4490, 2000.
- Angel, I. K., On the relation between atmospheric ozone and sunspot number, *J. Clim.*, *2*, 1404-1416, 1989.
- Baldwin, M. P., Gray, L. J., Dunkerton, T. J., Hamilton, K., Haynes, P. H., Randel, W. J., Holton, J. R., Alexander, M. J., Hirota, I., Horinouchi, T., Jones, D. B. A., Kinnnersley, J. S., Marquardt, C., Sato, K., and Takahashi, M.: The quasi-biennial oscillation, *Rev. Geophys.*, *39*, 179–229, 2001.
- Bates, D., and M. Nicolet, The Photochemistry Of Atmospheric Water Vapor, *J. Geophys. Res.*, *55(3)*, 301-327, 1950.
- Beig, G., N. Saraf and S. Peshin, Evidence of Pinatubo Volcanic Eruption on the Distribution of Ozone over the Tropical Indian Region, *J. Geophys. Res.*, *107*, pp. ACH 3-1 to 3-11, 4674, 2002.
- Bhartia, P., R. McPeters, C. Mateer, L. Flynn, and C. Wellemeyer, Algorithm for the estimation of vertical ozone profiles from the backscattered ultraviolet technique, *J. Geophys. Res.*, *101(D13)*, 18793-18806, 1996.
- Bovensmann, H., J. P. Burrows, M. Buchwitz, J. Frerick, S. Noël, V. V. Rozanov, K.V. Chance, and A. P. H. Goede, SCIAMACHY: Mission objectives and measurement modes, *J. Atmos. Sci.*, *56*, 127-150, 1999.
- Bowman, K. P., Global patterns of the quasi-biennial oscillation in total ozone, *J. Atmos. Sci.*, *46*, 3328-3343, 1989.
- Brasseur, G. and Solomon, S.: Aeronomy of the middle atmosphere, *D. Reidel publishing company, New York*, 2nd edn., 1–472, 1997.
- Brune, W. H., D.W. Toohey, J. G. Anderson, and K. R. Chan, In situ observations of ClO in the Arctic stratosphere: ER-2 aircraft results from 59°N to 80°N latitude, *Geophys. Res. Lett.*, *17(4)*, 505-508, 1990.
- Bruns M. et al., The AMAXDOAS Experiment - Data Retrieval and Sensitivity Studies, *IAMAS*, 2001.
- Burrows, J. et al., SCIAMACHY–A European Proposal for Atmospheric Remote Sensing from the ESA Polar platform, *Max-Planck-Institut für Chemie*, 1988.
- Burrows, J. P., M. Buchwitz, M. Eisinger, V. Rozanov, M. Weber, A. Richter, and A. Ladstätter-Weissenmayer, The Global Ozone Monitoring Experiment (GOME): Mission, Instrument Concept, and First Results (Ozone and NO₂), *J. Atmos. Sci.*, 1997.
- Burrows, J. P., M. Weber, M. Buchwitz, V. V. Rozanov, A. Ladstätter-Weißenmayer, M. Eisinger, and D. Perner, The Global Ozone Monitoring Experiment (GOME): Mission Concept, and First Scientific Results, *J. Atmos. Sci.*, *56*, 151-175, 1999.
- Cabannes, J., and J. Dufay, Mesure de l' altitude de la couche d'ozone dans l'atmosphère. *Comp. Rend.*, *181*, 302-304, 1925.

REFERENCES

- Callis, L. B., and Natarajan M., Ozone and nitrogen dioxide changes in the stratosphere during 1979–84, *Nature* 323, 772 – 777, 1986.
- Chipperfield, M.P., A three-dimensional model study of long-term mid-high latitude lower stratosphere ozone changes, *Atmos. Chem. Phys.*, 3, 1253-1265, 2003.
- Chu, W. P., and M. P. McCormick, Inversion of stratospheric aerosol and gaseous constituents from spacecraft solar extinction data in the 0.38–1.0 μm wavelength region, *J. Appl. Opt.*, 18, 1404–1414, 1979.
- Chu, W. P., M. P. McCormick, J. Lenoble, C. Brogniez, and P. Pruvost, SAGE II inversion algorithm, *J. Geophys. Res.*, 94, 8339–8351, 1989.
- Cicerone, R. J., Stratospheric ozone destruction by man-made chlorofluoromethane, *Science*, 185, 1165–1167, 1974
- Collimore, C. C., D. W. Martin, M. H. Hitchman, A. Huesmann, and D. E. Waliser, On The Relationship between the QBO and Tropical Deep Convection, *J. Clim.* 16, 15 pp. 2552-2568, 2003.
- Cooper, O. R., A. Stohl, G. Hübler, E. Y. Hsie, D. D. Parrish, A. F. Tuck, G. N. Kiladis, S. J. Oltmans, B. J. Johnson, M. Shapiro, J. L. Moody, and A. S. Lefohn, Direct transport of mid-latitude stratospheric ozone into the lower troposphere and marine boundary layer of the tropical Pacific Ocean. *J. Geophys. Res.*, 110, D23310, doi: 10.1029/2005JD005783, 2005.
- Cunnold, D. M., E. S. Yang, M. J. Newchurch, G. C. Reinsel, J. M. Zawodny, and J.M. Russell III.: Comment on “Enhanced upper stratospheric ozone: Sign of recovery or solar cycle effect?”, edited by: Steinbrecht et al., *J. Geophys. Res.*, 109, D14305, 2004.
- Cornu, A., Observation de la limite ultra-violette du spectre solaire a diverses altitudes. C.R. Hebd. Seances Acad. Sci., 89, 808-814, 1879.
- Crutzen, P. J., The influence of nitrogen oxides on the atmospheric ozone content. *Quart. J. Roy. Meteor. Soc.*, 103, 320–327, 1970.
- Crutzen, P. J., Ozone production rates in an oxygen-hydrogen-nitrogen oxide atmosphere, *J. Geophys. Res.*, 76, 7311-7327, 1971.
- Crutzen, P. J., Estimates of possible future ozone reductions from continued use of fluoro-chloro-methanes (CF_2Cl_2 , CFCl_3), *Geophys. Res. Lett.*, 1, 205–208, 1974.
- Crutzen, P. J. and F. Arnold, Nitric acid cloud formation in the cold Antarctic stratosphere: a major cause for the springtime "ozone hole". *Nature*, 324, 651-655, 1986.
- Drdla, K., EGU general assembly in Vienna in 2006
- D’Altorio, A., and G. Visconti, Lidar Observations of Dust Layers Transcience in the Stratosphere Following the El Chichon Volcanic Eruption, *Geophys. Res. Lett.*, 10, 27-30, 1983.
- D’Altorio, A., F. Masci, G. Visconti, V. Rizi and E. Boschi, Simultaneous Stratospheric Aerosol and Ozone Lidar Measurement after the Pinatubo Volcanic Eruption, *Geophys. Res. Lett.*, 10, 393-396, 1992.

REFERENCES

- Dessler, A., M. Burrage, J. U. Grooss, J. Holton, J. Lean, S. Massie, M. Schoeberl, A. Douglass, and C. Jackman, Selected Science Highlights from the First 5 Years of the Upper Atmosphere Research Satellite (UARS) Program, *Rev. Geophys.*, 36(2), 183-210, 1998.
- DeLand M. T. and R. P. Cebula, Solar UV activity at solar cycle 21 and 22 minimum from NOAA-9 SBUV/2 data, *Solar Phys.*, 177, 105–116, 1998.
- Dobson, G. M. B., Annals of the International Geophysical Year V, Part1 (Pergamon, NewYork), pp.46-89, 1957.
- Dobson, G. M. B., The laminated structure of the ozone in the atmosphere, *Quart. J. Roy. Meteor. Soc.*, 99, 599-607, 1973.
- Dobson, G. M. B., Forty Years Research on Atmospheric Ozone at Oxford: a History, *Appl. Opt.*, 7, 387-405, 1968.
- Dutsch, H. U., and J. Staehelin, Results of the new and old Umkehr algorithm compared with ozone soundings. *J. Atmos. Terr. Phys.*, 54(5), 557-569
- Egorova, T. A., E. V. Rozanov, M. E. Schlesinger, N. G. Andronova, S. L. Malyshev, I. L. Karol, and V. A. Zubov, Assessment of the Effect of the Montreal Protocol on Atmospheric Ozone, *Geophys. Res. Lett.*, 28(12), 2389–2392, 2001.
- Eichmann, K.-U., J.W. Kaiser, C. von Savigny, A. Rozanov, V. V. Rozanov, H. Bovensmann, M. von Konig, J. P. Burrows, SCIAMACHY limb measurements in the UV/Vis spectral region: first results, *Adv. Space Res.*, 34(4), 775–779, 2004.
- Eyring, V., et al., Assessment of temperature, trace species, and ozone in chemistry-climate model simulations of the recent past. *J. Geophys. Res.*, 111, D22308, doi: 10.1029/2006JD007327, 2006.
- Fabry, C., H. Buisson, Etude de l'extrémité ultra-violette du spectre solaire. *J. Physique*, 3, 197-226, 1921.
- Farman, J. C., B. G. Gardiner, and J. D. Shanklin, Large Losses of Total Ozone in Antarctica Reveal Seasonal ClO_x/NO_x Interaction, *Nature*, 315, 207-210, 1985.
- Feck T., J. U. Grooss, M. Riese, Sensitivity of Arctic ozone loss to stratospheric H₂O, *Geophys. Res. Lett.*, 35, L01803, 2008.
- Fleming, E. L., C. H. Jackman, J. E. Rosenfield, D. B. Considine, Two dimensional model simulations of the QBO in ozone and tracers in the tropical stratosphere. *J. Geophys. Res.* 107 (D23), 4665, 2002.
- Garcia, R. R. and Solomon, S.: A numerical model of the zonally averaged dynamical and chemical structure of the middle atmosphere, *J. Geophys. Res.*, 88, 1379–1400, 1983.
- Garcia, R. R., and S. Solomon, A new numerical model of the middle atmosphere, Ozone and related species, *J. Geophys. Res.*, 99, 12937 – 12951, 1994.
- Gernandt, H., P. Glode, U. Feister, G. Peters, B. Thees, Vertical distributions of ozone in the lower stratosphere over Antarctica and their relations to the spring depletion. *Planet Space Sci.*, 37(8), 915-933, 1989.

REFERENCES

- Glaccum, W., et al., The polar ozone and aerosol measurement instrument, *J. Geophys. Res.*, *101 (D9)*, 14,479–14,487, 1996.
- Groves, K. S. and Tuck, A. F., Stratospheric O₃-CO₂, coupling in a photochemical-radiative column model, 11: With chlorine chemistry, *Quart. J. R. Met. Soc.*, *106*, 141-157, 1980.
- Gunson, M. R., The atmospheric trace molecule spectroscopy (Atoms) experiment- the atlas 1 mission, *Opt. Meth. Atmos. Chem*, pp. 513–519, SPIES 1715, 1992.
- Haagen-Smit, A. J. and M. M. Fox, Ozone formation in photochemical oxidation of organic substances, *Ind. Eng. Chem.*, *48*, 1484-1487, 1956.
- Hansen, J., A. Lacis, and M. Prather, Greenhouse Effect of Chlorofluorocarbons and Other Trace Gases, *J. Geophys. Res.*, *94(D13)*, 16,417–16,421, 1989.
- Harris, N. R. P., J. C. Farman, D. W. Fahey, Comment on Effects of cosmic rays on atmospheric chlorofluorocarbon dissociation and ozone depletion. *Phys. Rev. Lett.*, *89*, 219801, 2002.
- Hasebe, F., A global analysis of the fluctuations in total ozone, II, Non-stationary annual oscillation, quasi-biennial oscillation, and long-term variations in total ozone, *J. Meteorol. Soc. Jpn.*, *58*, 104-117, 1980.
- Hays, P. B., R. G. Roble, Observation of mesospheric ozone at low latitudes. - *Planet. Space Sci.*, *21(2)*, 273-279, 1973.
- Heath, D. E., A. J. Krueger, H. R. Roeder, and B. D. Henderson, The Solar Backscatter Ultraviolet and Total Mapping Spectrometer (SBUV/TOMS) for Nimbus G, *Opt. Eng.*, 323-331, 1975.
- Herman, J. R., The response of stratospheric constituents to a solar eclipse, sunrise and sunset, *J. Geophys. Res.*, *84*, 3701-3710, 1979.
- Hofmann, D. J., S. J. Oltmans, J. M. Harris, B. J. Johnson, and J. A. Lathrop, Ten years of ozone sonde measurements at the South Pole: Implications for recovery of springtime Antarctic ozone, *J. Geophys. Res.*, *102*, 8931–8943, 1997.
- Hofmann, D. J., S. Solomon, Ozone destruction through heterogeneous chemistry following the eruption of El Chichon. *J. Geophys. Res.*, *94 (D4)*, 5029-5041, 1989.
- Hofmann, D. J., J. W. Harder, S. R. Rolf, and J. M. Rosen, Balloon-borne observations of the development and vertical structure of the Antarctic ozone hole in 1986, *Nature*, *326*, 59–62, 1987.
- Hoinka, K. P., The tropopause: discovery, definition and demarcation. *Meteorol. Z.*, *6(6)*, 281-303, 1997.
- Hood, L. L., and J. P. McCormack, Components of interannual ozone change based on Nimbus 7 TOMS data, *Geophys. Res. Lett.*, *19*, 2309-2312, 1992.
- Iwasaka, Y., Kondoh, Depletion of Antarctic ozone: Height of ozone loss region and its temporal changes. *Geophys. Res. Lett.*, *14(1)*, 87-90, 1987.
- Jensen, E. J, O.B. Toon, H.B. Selkirk, J.D. Spinhirne and M.R. Schoeberl , On the formation and persistence of subvisible cirrus clouds near the tropical tropopause. *J. Geophys. Res.* **101** (1996), pp. 21361–21375, 1996.

REFERENCES

- Johnson, F. S., J. D. Purcell, R. Tousey, Measurements of the vertical distribution of atmospheric ozone from rockets. *J. Geophys. Res.*, 56(4), 583-59, 1951.
- Jones, A., J. Urban, D. P. Murtagh, P. Eriksson, S. Brohede, C. Haley, D. Degenstein, A. Bourassa, C. von Savigny, T. Sonkaew, A. Rozanov, H. Bovensmann, J. Burrows, Evolution of stratospheric ozone and water vapour time series studied with satellite measurements *Atmos Chem and Phys.* 9(1), 2009,
- Jucks, K. W., D. G. Johnson, K. V. Chance, W. A. Traub, R. J. Salawitch, and R. Stachnik, Ozone production and loss rate measurements in the middle stratosphere, *J. Geophys. Res.*, 101, 28785–28792, 1996.
- Komhyr, W. D., R. D. Grass, and R. K. Leonard, Dobson Spectrophotometer 83: A standard for total ozone measurements, 1962-1987, *J. Geophys. Res.*, 94(D7), 9847-9861, 1989.
- Lambert, P., G. Dejardin, D. Chalonge, Sur l'extrémité ultraviolette du spectra solaire et la couche d'ozone de la haute atmosphere. *Comp. Rend. Hebd. Acad. Sci.*, 183, 800-801, 1926.
- Lindemann, F. A., and G. M. B. Dobson, A theory of meteors and the density and temperature of outer atmosphere to which it leads, *Proc. Roy. Soc. London, Series A*, 102, 411, 1923.
- Llewellyn, E. J., D. A. Degenstein, N. D. Lloyd, R. L. Gattinger, S. Petelina, I. C. McDade, C. S. Haley, B. H. Solheim, C. von Savigny, C. Sioris, W. F. J. Evans, K. Strong, D. P. Murtagh, and J. Stegman, First Results from the OSIRIS Instrument on-board Odin, *Sodankyl a Geophys. Obs. Pub.*, 92, 41–47, 2003.
- Lu, Q. B., L. Sanche, Effects of cosmic rays on atmospheric chlorofluorocarbon dissociation and ozone depletion. *Phys. Rev. Lett.*, 87, 078501, 2001.
- Mauldin L. E., N. H. Zaun, M. P. McCormick, J. H. Guy, and W. R. Vaugh, Stratospheric Aerosol and Gas Experiment II instrument: A functional description. *Opt. Eng*, 24, 307–317, 1985.
- McCormick, M. P., P. Hamill, T. J. Pepin, W. P. Chu, T. J. Swissler, and L. R. McMaster, Satellite studies of the stratospheric aerosol, *Bull. Amer. Meteorolo. Soc.*, 60, 1038–1046, 1979.
- McCormick, M. P., Veiga, R. E., Zawodny, J. M., Comparison of SAGE I and SAGE II Stratospheric Ozone Measurements in *Ozone in the Atmosphere*, Edited by Rumun D. Bojkov and Peter Fabian, A. Deepak Publishing, Hampton Virginia, USA, pp. 202-205, 1989.
- McCormick, M. P., R. E. Veiga, and W. P. Chu Stratospheric ozone profile and total ozone trends derived from the SAGE I and SAGE II data, *Geophys. Res. Lett.*, 19(3), 269–272, 1992,
- McCormick, M. P., et al., SAGE III algorithm theoretical basis document: Solar and lunar algorithm, *LARC 475-00-108, Version 2.1*, 2002.
- Mewaldt, R. A., M. D. Looper, C. M. S. Cohen, G. M. Mason, D. K. Haggerty, M. I. Desai, A. W. Labrador, R. A. Leske, J. E. Mazur, Solar-Particle Energy Spectra during the Large Events of October-November 2003 and January 2005, *29th Int. Cosmic Ray Conference Pune*, 00, 101-104, 2005.
- Miller, D. E., P. Ryder, Measurement of the ozone concentration from 55 to 95 km at sunset, *Planet. Space Sci.*, 21, 963-970, 1973.

REFERENCES

- Molina, M. J., T. L. Tso, L. T. Molina, F. C. Y. Wang, Antarctic stratospheric chemistry of chlorine nitrate, hydrogen chloride, and ice: Release of active chlorine. *Science*, 238(4831), 1253-1257, 1987.
- Molina M. J. and F. S. Rowland. Stratospheric sink for chlorofluoromethanes: chlorine atom catalyzed destruction of ozone, *Nature*, 249, 810–814, 1974.
- Müller, R., Comment on: “Resonant dissociative electron transfer of the presolvated electron to CCl₄ in liquid: Direct observation and lifetime of the CCl₄*⁻ transition state” [JCP 128, 041102 (2008)], *J. Chem. Phys.*, 129, 027101, 2008.
- Müller, R., Impact of cosmic rays on stratospheric chlorine chemistry and ozone depletion, *Phys. Rev. Lett.*, 91, 058502, 2003.
- Narayana, R. T., J. Arvelius, S. Kirkwood, and P. von der Gathen, Climatology of ozone in the troposphere and lower stratosphere over the European Arctic, *Adv. Space Res.*, 2003.
- Newchurch, M. J., E. S. Yang, D. M. Cunnold, G. C. Reinsel, J. M. Zawodny, and J. M. Russell III, Evidence for slowdown in stratospheric ozone loss: First stage of ozone recovery, *J. Geophys. Res.*, 108, 4507, 2003.
- Newman, P. A., J. S. Daniel, D. W. Waugh, and E. R. Nash, A new formulation of equivalent effective stratospheric chlorine (EESC), *Atmos. Chem. Phys.*, 7, 4537–4552, 2007.
- Newman, P. A., Nash, E. R., Kawa, S. R., Montzka, S. A. and Schauffler, S. M., When will the Antarctic ozone hole recover? *Geophys. Res. Lett.*, 33, L12814, doi 10.1029/2005GL025232, 2006.
- Newman, P. A., E. R. Nash, and J. E. Rosenfield, What controls the temperature of the Arctic stratosphere during the spring?, *J. Geophys. Res.*, 106, 19999 – 20010, 2001.
- Rowland F. S., "Stratospheric Ozone Depletion", *Annual Rev. in Phys. and Chem.*, 42, 731, 1991.
- Paetzold, H. K., Eine Bestimmung der vertikalen Verteilung des atmosphärischen, Ozons mit Hilfe von Mondfinsternissen, *Z. Naturforsch.*, 5, 661-666, 1950.
- Paetzold, H. K., Die durch die atmosphärische Ozonschicht bewirkte Färbung des Erdschattens auf dem verfinsterten Mond, *Naturwiss.*, 38 (23), 544-545, 1951.
- Paetzold, H. K., E. Regener, Ozon in der Erdatmosphäre. In S. Flugge, editor, *Handbuch der Physik, Springer Vol. XLVIII*, pp 370-426, 1957.
- Pallister R.C., and A. F. Tuck, The diurnal variation of ozone in the upper stratosphere as a test of photochemical theory, *Quart. J. R. Met. Soc.*, 109, pp. 271-284, 1983.
- Randall, C. E., D. W. Rusch, R. M. Bevilacqua, J. Lumpe, T. L. Ainsworth, D. Debrebian, M. Fromm, S. S. Krigman, J. S. Hornstein, E. P. Shettle, J. J. Olivero, and R. T. Clancy, Preliminary results from POAM II: Stratospheric ozone at high northern latitudes, *Geophys. Res. Lett.*, 22, 2733–2736, 1995.
- Reinsel, G. C., E. C. Weatherhead, G. C. Tiao, A. J. Miller, R. M. Nagatani, D. J. Wuebbles, and L. E. Flynn, On detection of turn around and recovery in trend for ozone, *J. Geophys. Res.*, 107(D10), 4078, doi: 10.1029/2001JD000500, 2002a.

REFERENCES

- Reinsel, G. C., Trend analysis of upper stratospheric Umkehr ozone data for evidence of turnaround, *Geophys. Res. Lett.*, 29 (N10), 1451, 10.1029/2002GL014716, 2002b.
- Rind, D., J. Lerner, and J. Zawony, A complementary analysis for SAGE II data profiles, *Geophys. Res. Lett.*, 32, L07812, doi: 10.1029/2005GL022550, 2005,
- Rood, R. B., A. R. Douglass, M. C. Cerniglia, L. C. Sparling, and J. E. Nielsen, Seasonal Variability of Middle Latitude Ozone in the Lowermost Stratosphere Derived from Probability Distribution Functions, *J. Geophys. Res.*, 104, 17793-17805, 2000.
- Rowland F. S., "Chlorofluorocarbons and the depletion of stratospheric ozone", *Amer. scientist*, 77, 36, 1989.
- Rozañov, A., H. Bovensmann, A. Bracher, S. Hrechanyy, V. Rozañov, M. Sinnhuber, F. Strohh, and J. Burrows, NO₂ and BrO vertical profile retrieval from SCIAMACHY limb measurements: Sensitivity studies, *Adv. Space Res.*, 36, 846-854, 2005.
- Rubin, M. B., The History of ozone. The Schönbein Period, 1839-1868, *Bull. Hist. Chem.*, 26(1), 2001.
- Russell III, J. M., Gordley, L. L., Park, J. H., Drayson, S. R., Hesketh, D. H., Cicerone, R. J., Tuck, A. F., Frederick, J. E., Harries, J. E., and Crutzen P.: The Halogen Occultation Experiment, *J. Geophys. Res.*, 98, 10777–10797, 1993.
- Schaeler B., D. OffermannV. Kuell and M. Jarisch, Global water vapour distribution in the upper troposphere and lower stratosphere during CRISTA 2, *Adv Space Res* 43, 1, Pp 65-73, 2009
- Singleton, C. S. , C. E. Randall, M. P. Chipperfield, S. Davies, W. Feng, R. M. Bevilacqua, K. W. Hoppel, M. D. Fromm, G. L. Manney, and V. L. Harvey, 2002–2003 Arctic ozone loss deduced from POAM III satellite observations and the SLIMCAT chemical transport model, *Atmos. Chem. Phys.*, 5, 597– 609, 2005.
- Schiller, C., A. Wahner, U. Platt, H. P. Dorn, J. Callies, D. Ehhalt, Near UV atmospheric absorption measurements of column abundances during Airborne Arctic Stratospheric Expedition, January-February 1989 2. OCIO observations. *Geophys. Res. Lett.*, 17(4), 501-504, 1990.
- Schönbein, C. F., On the Odour Accompanying Electricity and on the Probability of its Dependence on the Presence of a New Substance, *Phil. Mag*, 17, 293-294, 1840.
- Schwab, J., R. J. Pan, and J. Zhang, What constitutes a valid intercomparison of satellite and in situ stratospheric H₂O measurements? *J. Geophys. Res.*, 101(D1), 1517-1528, 1996.
- Shindell, D. T., D. Rind, and P. Lonergan, Climate change and the middle atmosphere, Part IV: Ozone response to doubled CO₂. *J. Clim.*, 11, 895-918, 1998.
- Shiotani, M., Annual, quasi-biennial, and El Nino-Southern Oscillation (ENSO) timescale variations in equatorial total ozone, *J. Geophys. Res.*, 97, 7625-7633, 1992.
- Showstack, R., Montreal Protocol Benefits Cited, *Eos Trans. AGU*, 84(39), 2003.
- Solomon, S., G. H. Mount, R. W. Sanders, R. O. Jakoubek, A. L. Schmeltekopf, Observations of the nighttime abundance of OCIO in the winter stratosphere above Thule, Greenland. *Science*, 242(4878), 550-555, 1988.

REFERENCES

- Solomon, S., R. R. Garcia, F. S. Rowland, D. J. Wuebbles, On the depletion of Antarctic zone, *Nature*, 321, 755-758, 1986.
- Sonkaew, T., V. V. Rozanov, C. von Savigny, A. Rozanov, H. Bovensmann, and J. P. Burrows, Cloud sensitivity studies for stratospheric and lower mesospheric ozone profile retrievals from measurements of limb scattered solar radiation, *Atmos. Meas. Tech., revised*, 2008
- Steinbrecht W., Claude, H., and Winkler P.: Enhanced stratospheric ozone: Sign of recovery or solar cycle? *J. Geophys. Res.*, 109, D2308, doi: 10.1029/2004JD004284, 2003.
- Steinbrecht W., et al., Long-term evolution of upper stratospheric ozone as seen by NDSC lidars, SAGE and HALOE, *Extended Abstracts, QOS, Kos*, 2004.
- Steinbrecht W., et al., Long-term evolution of upper stratospheric ozone at selected stations of the Network for the Detection of Stratospheric Change (NDSC). *J. Geophys. Res.*, 111, D10308, doi: 10.1029/2005JD006454, 2006.
- Steinbrecht, W., H. Claude, F. Schöenborn, I. S. McDermid, T. Leblanc, S. Godin-Beekmann, P. Keckhut, A. Hauchecorne, J. A. E. Van Gijssel, D. P. J. Swart, G. E. Bodeker, A. Parrish, I. S. Boyd, N. Kämpfer, K. Hocke, R. S. Stolarski, S. M. Frith, L. W. Thomason, E. E. Remsberg, C. von Savigny, A. Rozanov, J. Burrows, Ozone and temperature trends in the upper stratosphere at five stations of the Network for the Detection of Atmospheric Composition Change. *Int. J. of remote sensing*, 30(15), 3875-3886, 2009.
- Stenchikov, G., A. Robock, V. Ramaswamy, M. D. Schwarzkopf, K. Hamilton, and S. Ramachandran, Arctic Oscillation response to the 1991 Mount Pinatubo eruption: Effects of volcanic aerosols and ozone depletion, *J. Geophys. Res.*, 107, (D24), 4803, 2002.
- Stolarski, R. S. and Cicerone, R. J., Stratospheric chlorine: A possible sink for ozone. *Canadian J. Chem.*, 52, pp. 1610-1615, 1974.
- Tilmes, S., R. Müller, R. J. Salawitch, The sensitivity of polar ozone depletion to proposed geoengineering schemes, *Science*, 320, 1201-1204, 2008.
- Thomason, L. W., S. P. Burton, N. Iyer, J. M. Zawodny, and J. Anderson, A revised water vapor product for the Stratospheric Aerosol and Gas (SAGE) II version 6.2 data set, *J. Geophys. Res.*, 109, D06312, doi:10.1029/2003JD004465, 2004.
- Tilmes, S., D. Kinnisen, R. Müller, F. Sassi, D. Marsh, B. Boville, R. Garcia, Evaluation of heterogeneous processes in the polar lower stratosphere in the whole Atmosphere Community climate model, *J. Geophys. Res.*, 112, D24301, 2007.
- Tilmes, S., R. Müller, J. U. Grooss, J. M. Russell, Ozone loss and Chlorine activation in the Arctic winters 1991-2003 derived with the tracer-tracer correlations. *Atmos. Chem. Phys.*, 4(8), 2181-2213., 2004.
- Toon, Owen B., Hamill, Patrick, Turco, P. Richard, Pinto, and Joseph, Condensation of nitric acid and hydrochloric acid in the winter polar stratospheres, *Geophys. Res. Lett.*, 13, 1284-1287, 1986.
- Thomas, G. E., Solar Mesosphere Explorer measurements of polar mesospheric clouds (noctilucent clouds), *J. Atmos. and Terr. Phys. vol. 46*, pp. 819-824, 1984.

REFERENCES

- Trepte, C.R., R. E. Veiga and M.P. McCormick, The poleward dispersal of Mount Pinatubo volcanic aerosol. *J. Geophys. Res.* 98, 18563-73, 1993.
- Tuck, A. F., Numerical model studies of the effect of injected nitrogen oxides on stratospheric ozone, *Proc. Roy. Soc.*, A355, 267-299, 1977.
- Tuck, A. F., Synoptic and chemical evolution of the Antarctic vortex in late winter and early spring, *J. Geophys. Res.*, 94, 11687-11737, 1989.
- Tung, K. K., M. K. W. Ko, J. M. Rodriguez, and N. D. Sze, Are Antarctic ozone variations a manifestation of dynamics or chemistry? *Nature*, 333, 811-814, 1986.
- Vaughan, G., Diurnal variation of mesospheric ozone, *Nature*, 296, 133-135, 1982.
- Vaughan, G., Mesospheric ozone theory and observation, *Q. J. R. Meteorol. Soc.*, 110(463), 239-260, 1984.
- Venkateswaran, S. V., J. G. Moore, and A. J. Krueger, Vertical distribution of ozone by satellite photometry, *J. Geophys. Res.*, 66(6), 1751-1771, 1961.
- von Savigny, C., J. W. Kaiser, H. Bovensmann, J. P. Burrows, I. S. McDermid, and T. Leblanc, Spatial and temporal characterization of SCIAMACHY limb pointing errors during the first three years of the mission, *Atmos. Chem. Phys.*, 5, 2593-2602, 2005a.
- von Savigny, C., A. Rozanov, H. Bovensmann, K. U. Eichmann, S. Noël, V. V. Rozanov, B. M. Sinnhuber, M. Weber, J. P. Burrows, and J. W. Kaiser, The ozone hole break-up in September 2002 as seen by SCIAMACHY on ENVISAT, *J. Atm. Sci.*, 62, 721-734, 2005b.
- Wallace, J. M., and P. V. Hobbs, Atmospheric Science: An Introductory Survey, *Academic Press*, 2006.
- Wang, C. R., K. Drew, T. Luo, M. J. Lu, Q. B. Lu, Resonant dissociative electron transfer of the presolvated electron to CCl₄ in liquid: Direct observation and lifetime of the CCl₄*⁻ transition state, *J. Chem. Phys.* 128, 041102, 2008.
- Wang, J, R. C. Flagan, J. H. Seinfeld, H. H. Jonsson, D. R. Collins, P. B. Russell, B. Schmid, J. Redemann, J. M. Livingston, S. Gao, D. A. Hegg, E. J. Welton, and D. Bates, Clear-column radiative closure during ACE-Asia: Comparison of multiwavelength extinction derived from particle size and composition with results from sunphotometry, *J. Geophys. Res.*, 107(D23), 4688, 2002.
- Warneck, P., Chemistry of the natural atmosphere, *International Geophysics Series, Volume 41*, *Academic Press, San Diego*, 1988.
- Wayne, R. P., The Photochemistry of Ozone, *Atmosp. Env.*, 21, 1683-1694, 1987.
- Wayne, R. P., Chemistry of Atmospheres, chap. Ozone in Earth's stratosphere, 155-320, 3rd ed., *Oxford university Press Oxford*, 2000
- Weatherhead, E. C., G. C. Reinsel, G. C. Tiao, C. H. Jackman, L. Bishop, S. M. H. Firth, J. DeLuisi, T. Keller, S. J. Oltmans, E. L. Fleming, D. J. Wuebbles, J. B. Kerr, A. J. Miller, J. Herman, R. McPeters, R. M. Nagatani, and J. E. Frederick, Detecting the recovery of total column ozone, *J. Geophys. Res.*, 105, 22,201-22,210, 2000.

REFERENCES

William J., J. W. Randel, R. S. Stolarski, D. M. Cunnold, J. A. Logan, M. J. Newchurch, J. M. Zawodny, Trends in the Vertical Distribution of Ozone, doi: 10.1126/science.285.5434.1689, 285(5434), pp. 1689 – 1692, 1999.

WMO (World Meteorological Organization), *Scientific Assessment of ozone Depletion: 1994*, Global Ozone Research and Monitoring Project, Report No. 37, Geneva, Switzerland, 1995.

WMO (World Meteorological Organization), *Scientific Assessment of ozone Depletion: 1998*, Global Ozone Research and Monitoring Project, Report No. 44, Geneva, Switzerland, 1999.

WMO (World Meteorological Organization), *Scientific Assessment of ozone Depletion: 2002*, Global Ozone Research and Monitoring Project, Report No. 47, Geneva, Switzerland, 2003.

WMO (World Meteorological Organization), United Nations Environment Programme, *Scientific Assessment of ozone Depletion: 2006*. Global Ozone Research and Monitoring Project, Report No. 50, Geneva, Switzerland: WMO/UNEP, 2007.

Yang, E.S., D. M. Cunnold, R. J. Salawitch, M. P. McCormick, J. Russell III, J. M. Zawodny, S. Oltmans, M. J. Newchurch, Attribution of recovery in lower-stratospheric ozone, *J. Geophys. Res.*, 111, D17309, doi: 10.1029/2005JD006371, 2006.

Zanis, P., E. Maillard, J. Staehelin, C. Zerefos, E. Kosmidis, K. Tourpali, and I. Wohltmann.: On the turnaround of stratospheric ozone trends deduced from reevaluated Umkehr record of Arosa, Switzerland. *J. Geophys. Res.*, 111, D22307, doi:10.1029/2005JD006886, 2006.

Zerefos, C. S., A. F. Bais, I. C. Ziomas, and R. D. Bojkov.: On the relative importance of quasi-biennial oscillation and El Nino/Southern Oscillation in the revised Dobson total ozone records, *J. Geophys. Res.*, 97, 10,135-10,144, 1992.